AD704616

ON THE THEORY OF BULK CAVITATION
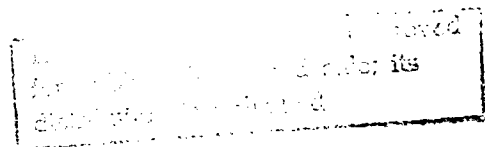
Final Report

By Vincent J. Cushing

Prepared for

OFFICE OF NAVAL RESEARCH
Washington, D. C. 20360
Contract Nonr-3709 (00)

Sponsored by

DEFENSE ATOMIC SUPPORT AGENCY
Washington, D. C. 20305

December 1969

EPCO **ENGINEERING-PHYSICS COMPANY**

12721 TWINBROOK PARKWAY. / ROCKVILLE, MARYLAND 20852

ENGINEERING-PHYSICS COMPANY
12721 Twinbrook Parkway
Rockville, Maryland   20852

ON THE THEORY OF BULK CAVITATION

Final Report

By Vincent J. Cushing

Prepared For

Office of Naval Research
Washington, D. C.   20360
Contract   Nonr-3709(00)

Sponsored By

Defense Atomic Support Agency
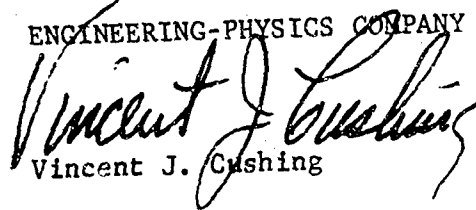Washington, D.C.   20305

December 1969

FOREWORD

This final report, entitled "On the Theory of Bulk Cavitation," presents the results of a study by the writer for the Office of Naval Research under Contract NONR 3709(00)--EPCO Project 106.

The author's approach to the problem benefited from many helpful technical discussions, especially with Hans A. Snay and E. Swift, Jr. of the Naval Ordnance Laboratory, and William Murray, Heinrich Schauer, and R.R. Walker of the Naval Ship Research and Development Center. The support, understanding, and generously given assistance by the project officer, Jacob Warner, is gratefully acknowledged.

Respectfully submitted,

ENGINEERING-PHYSICS COMPANY

Vincent J. Cushing

Preceding Page Blank

ABSTRACT

When the compressive shock from an underwater explosion intercepts the free water surface, part of the shockwave energy is propagated into the overlying air and part is reflected back into the water. Early acoustic theories failed to describe the transmitted and reflected waves because acoustic theory implies a linear stress/strain relationship for the water--including the ability of water to withstand considerable tension. The analysis provided in this report assumes that the water can withstand no substantial amount of tension, so that an incident shockwave causes a surface layer of the water to rupture and spall upward. The region between the spall and the underlying (relatively) quiescent water has long been termed the cavitated region, and the entire process has been termed bulk cavitation.

The energy contained in the incident compressive shockwave is temporarily stored in the kinetic and gravitational potential energy of the spall. When the spall falls back and impacts (water hammers) the underlying water this stored energy is re-emitted. The spalled interface behavior is essentially different from the earlier acoustic interface picture, and the magnitude and shape of the pressure waves in the overlying air and those generated in the water at the time of spall impact are essentially different from that derived from the acoustic interface assumption.

This report studies the mechanism of water rupture, cavitation, and spall formation; studies the dynamics of this spall and cavitated region; studies the dynamics of spall impact and generation of secondary waves under water. The study concludes with a discussion of the air blast wave shape to be expected when the water surface moves in accord with the spallation and cavitation picture.

Preceding Page Blank

Preceding Page Blank

TABLE OF CONTENTS

ON THE THEORY OF BULK CAVITATION

I. INTRODUCTION

When the pressure wave from an underwater explosion arrives at the water surface, a reflected wave is generated which is rarefactive. It is easily shown[1] that, when the strong rarefactive front progresses into the waning portions of the incoming compression wave, the net stress in the medium is a tension. Meticulously clean water is able to withstand a considerable amount of tensile stress; but seawater, because of the abundance of impurities, can withstand very little tension. Consequently, the above described tensile wave cannot propagate as such; rather, the water ruptures and the pressure in the ruptured water falls to the vapor pressure of water--zero for all practical purposes when we are dealing with pressures produced by underwater explosions.

When such a rupture process takes place, a layer of water near the surface spalls upward. It no longer has any tensile stresses at its lower boundary tending to return the water particles to their original, pre-shockwave position; the motion of the spalled water layer is determined by the pressure in the atmosphere overlying the spall, and by the acceleration of gravity. The motion of such a spalled water surface is essentially different from what one obtains by simple acoustic analysis, where it is implicitly assumed that the water can sustain tensile as well as compressive stresses. This spall-type motion of the water surface will accordingly produce pressure waves in the overlying air that are essentially different from what one would expect from acoustic surface behavior.

---

[1] Cole, Robert H., _Underwater Explosions_ (Princeton University Press, Princeton, N. J., 1948), p. 261

The spalled water layer is driven back downward so that ultimately it must impact the underlying water; the dynamics of this process produces a traveling source of secondary pressure waves in the water. This traveling source is tantamount to a generator of "sonic boom"; because of focusing effects, there are certain locations underwater where the secondary pressures become intense. The significant role that spalled surface behavior plays in the production of air blast waves and in the production of underwater secondary pressure waves has prompted this investigation.

The intervening region between the upward traveling spalled water layer and the underlying (relatively quiescent) water necessarily has an average specific volume greater than that of seawater. This intervening region is termed the cavitated region; and the entire process has for some time been termed Bulk Cavitation.

A large fraction of the total explosion hydrodynamic yield becomes temporarily stored in the bulk cavitation process; and the stored energy is later re-emitted when the cavitation closes. For an underwater explosion one-half of the shockwave energy intercepts the water surface and thus becomes involved in phenomena, such as bulk cavitation, at the surface. Even after discounting that portion of the shockwave energy which intercepts the surface at grazing angles (large distances from surface-zero) where bulk cavitation phenomena are relatively insignificant, the fraction of shockwave energy emitted by the explosion and significantly involved in surface effects is still large; hence, pressure waves in the air and in the water have their character largely influenced by the bulk cavitation process.

Bulk cavitation was analyzed by Kennard[2] approximately 25 years ago. It plays a role not only in connection with a free surface--as we are studying here-- but also plays a role when an underwater shockwave interacts with a compliant, inertially loaded surface, such as a hull plate; Kennard also investigated this aspect[3]. In 1961, the writer investigated in detail the mechanisms of water rupture[4], and the dynamics of cavity growth and closure and consequent water hammer. Equations of motion were set up; results were obtained by machine computation. In 1962, there was further investigation of the extent of the cavitated region for a spherical explosion and investigation of the "sonic boom" effects due to the dynamics of cavitation closure[5]. In 1965, the bulk cavitation phenomena associated with a compliant plate were studied[6].

Section III of this report sets up the equations of motion and obtains closed form solutions describing as functions of time: (1) spall thickness, (2) spall surface position, (3) spall surface velocity, (4) spall surface acceleration; and in particular, determines the depth at which closure occurs and the impact velocity with which the spall hammers the underlying water.

[2] E. H. Kennard, Phys. Rev., 63, 172 (1943).

[3] E. H. Kennard, "Explosive Load on Underwater Structures as Modified by Bulk Cavitation," Report 511, David Taylor Model Basin (1943).

[4] Vincent Cushing, "Study of Bulk Cavitation and Consequent Water Hammer," Final Report for Office of Naval Research under Contract Nonr-3389(00), October 31, 1961.

[5] Vincent Cushing, George Bowden, and Dean Reily, "Three-Dimensional Analysis of Bulk Cavitation," Report for Office of Naval Research under Contract Nonr-3709(00), September 24, 1962.

[6] Vincent Cushing and William Losaw, "Hull Plate Deformation from Underwater Shockwaves," Report prepared for Underwater Explosions Research Division of DTMB under Contract N189(181)-56855A(X), July 30, 1965.

4

In Section IV we make a change of variable so that the general solutions obtained in Section III can be used to obtain results for underwater shockwaves that strike the free water surface at arbitrary angles of incidence. We solve the equations for the condition where the underwater shockwave consists of a shock rise with exponential tail-off typical of underwater explosions. The Appendix provides tabulations of the solutions to these equations as a function of wave length for exponential waves.

In Section V, we study the spallation and reloading dynamics, including the generation of secondary pressure waves in the water for a spherically symmetric explosion, and compare analytical results with the experiments reported by Walker[7]. In Section VI, we indicate the implications to the air blast pressure signature.

---

[7]R. R. Walker and J. D. Gordon, "A Study of the Bulk Cavitation Caused by Underwater Explosions," DTMB Report 1896, September, 1966.

II.   FORMATION OF CAVITATION

A detailed description of the mechanics of cavitation and the extent of the cavitated region is provided in references 3 and 4. Here we will review briefly the shockwave motion toward the water (free) surface, and the motion of the reflected rarefaction. We will set up an expression for the pressure that would exist at the rarefaction front if one permits sizeable tensile stresses in the water, and from this we can determine the depth--the onset depth--where rupture of the water or cavitation first takes place. We will then set up an expression for the velocity of the water particles in the cavitated region, and from this we can determine the depth--the termination depth--beyond which cavitation or rupture can no longer take place. Finally, we will see that the cavitated region exists for a very long duration compared with the time it takes the causative rarefaction front to traverse the entire cavitated region; hence, as an approximation we will be justified in later analyses in assuming that the entire cavitated region is formed instantaneously.

To keep the discussion simple at the outset, we will discuss a one-dimensional shockwave traveling vertically upward and incident normally at the free water surface. In Section IV we show how the results--with simple redefinition of the variables--are applicable to shockwaves with arbitrary angle of incidence.

A.   Wave Propagation

At a time before the incident shockwave strikes the water surface, the pressure p as a function of water depth z is as indicated in figure 1. The pressure p is indicated by the solid curve: it is the superposition of atmospheric pressure, hydrostatic pressure, and shockwave pressure.

When the incident compression wave is reflected from the free water surface, a reflected rarefaction wave must be generated such that the pressure at

Figure 1. Total pressure p--the superposition of atmospheric pressure, hydrostatic pressure, and shockwave pressure--as a function of water depth z just before the incident shockwave reaches the water surface.

the water surface is atmospheric pressure p_a. A portion of the pressure wave is also propagated out into the air; however, since the specific acoustic impedance of water and air differ by a factor of 3,600, we can for the moment neglect the airwave pressure and simply require that the pressure at the surface be atmospheric pressure p_a. The front of the rarefaction wave must have a strength of the same magnitude as the incoming shockwave, and as this strong rarefaction front progresses into the waning portions of the incident shockwave, the total pressure p is as depicted by the solid curve in figure 2.

If the incident shock peak pressure p_o is sufficiently large, then it is possible, as shown in figure 2, that the total pressure p becomes negative beyond a certain onset depth z_o.

If water could withstand substantial tensile stress, these pressure waves would propagate in acoustic fashion. Negative pressure in water is an unstable condition; the stable condition is that the water will rupture so that its specific volume increases by vaporization, and the stable pressure is the vapor pressure--effectively zero on the scale of pressures of interest in underwater shockwaves. The unstable condition of large tension has been observed in very pure water contained in capillaries; but in seawater, where there is numerous foreign matter which serves as the nucleus for vaporization, we can expect that the water is unable to sustain tensile stress, and we will henceforth assume that the pressure in the cavitated region is zero. This assumption seems to be borne out by the experimental results shown in reference 7.

B. Pressure at Rarefaction Front

As indicated in figure 2, the minimum pressure at any instant in time occurs at the front of the reflected rarefaction wave. If rupture of the water is to take place, the total pressure p at this front must at some depth reach
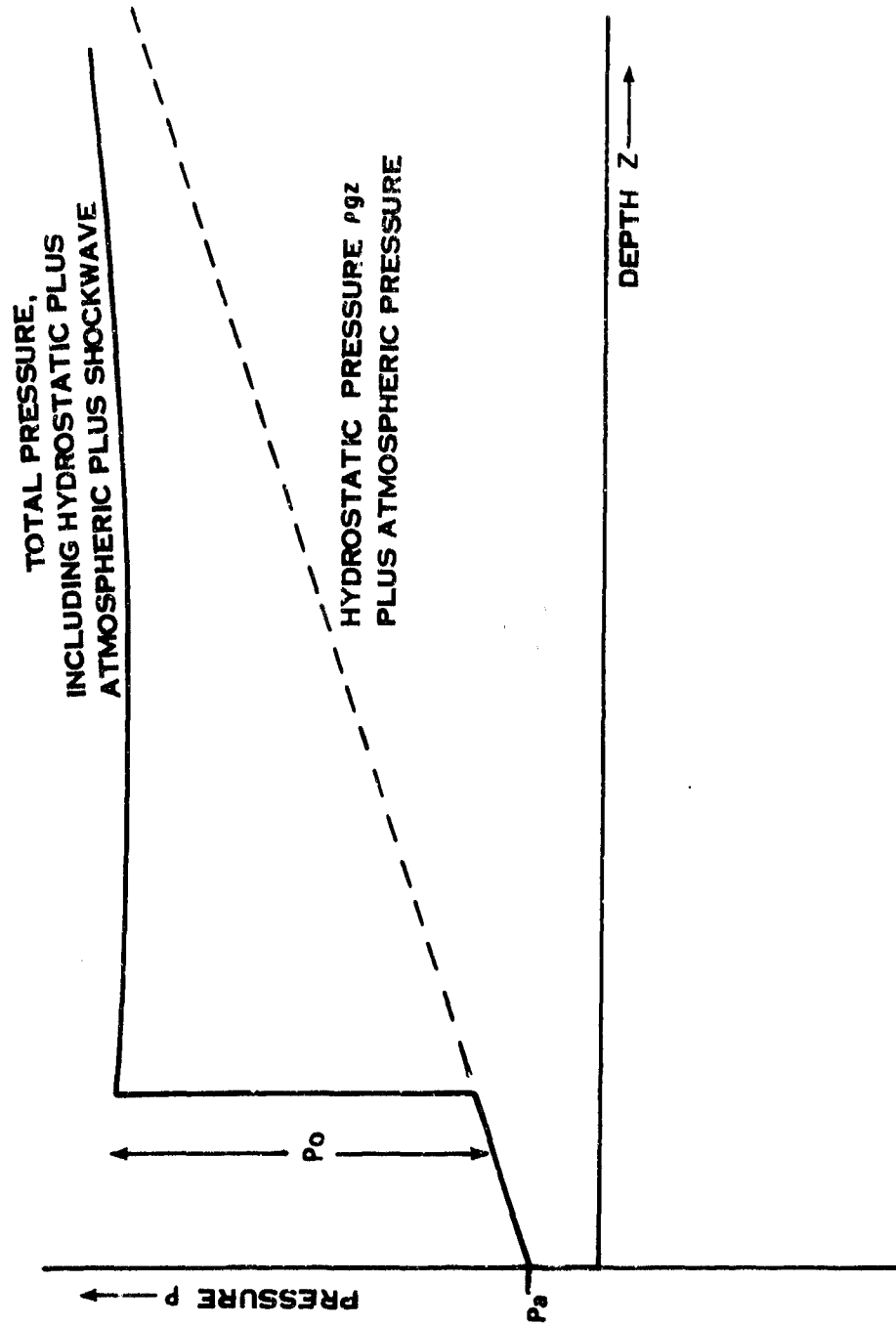
8
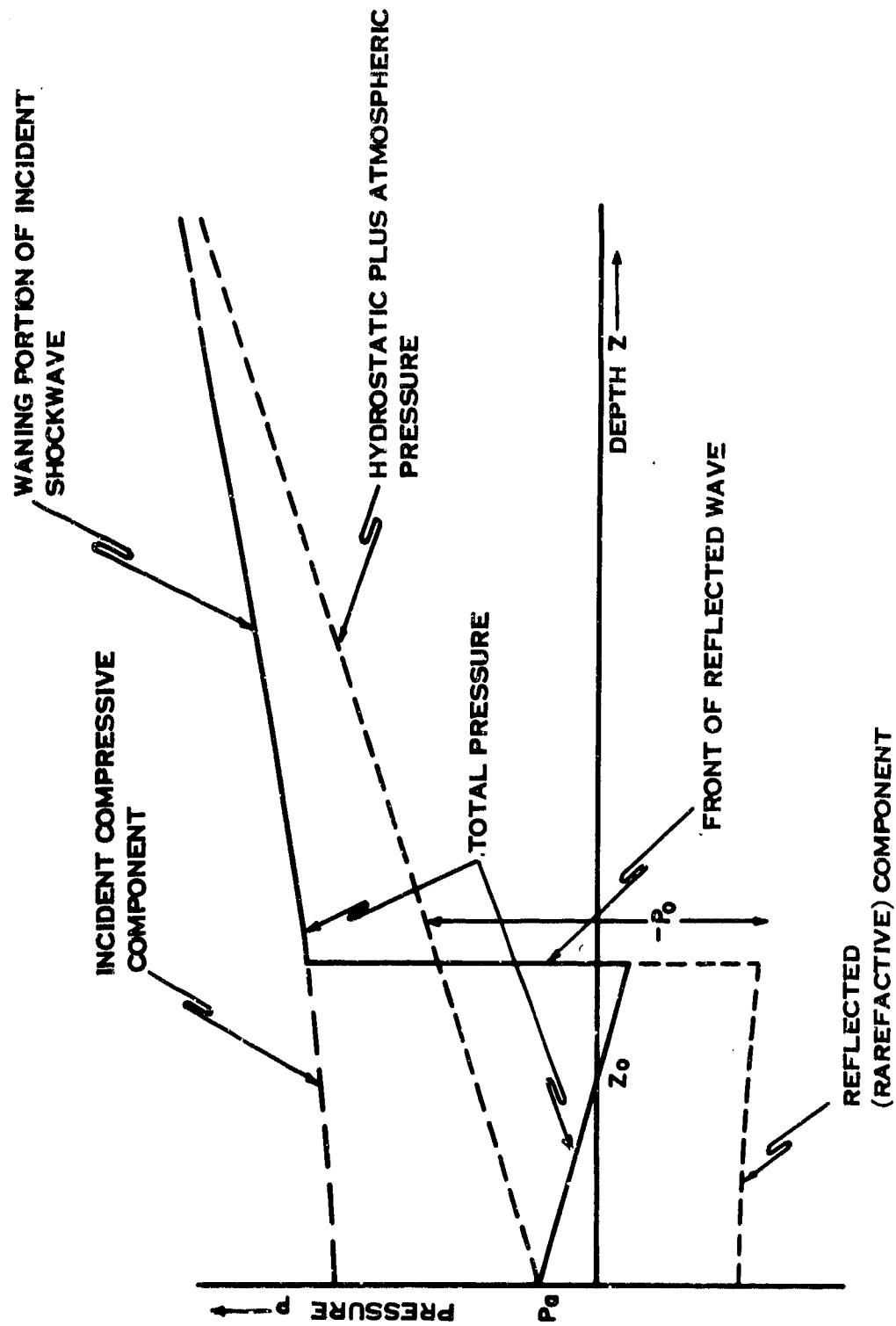
Figure 2. Total pressure p--the superposition of atmospheric pressure, hydrostatic pressure, incident shockwave pressure, and reflected rarefaction wave pressure--as a function of depth z after the incident shockwave has reflected from the free water surface.

zero. For example, if the incident shockwave consists of a shock rise to peak pressure p_o and with exponential tail-off of wave length λ, i.e., if it is of the form $p_o e^{-(t+z/c)/\lambda}$, then it has been shown that the total pressure p as a function of depth z--neglecting cavitation--is described by

$$p = p_a + \rho gz - p_o(1 - e^{-2z/\lambda}) ,$$ (1)

where p_a is atmospheric pressure; ρgz is hydrostatic pressure; and $-p_o(1 - e^{-2z/\lambda})$ is the pressure contribution due to the peak rarefaction pressure plus the waning portions of the incoming compressive shockwave.

In figure 3 we show as pressure curve III one that does not have any minimum value in the water; and at the surface its value--in common with all three pressure curves--is equal to the atmospheric pressure p_a. With a pressure expression as described by equation (1) such a type III curve can occur if p_o is too small and/or if the shockwave wavelength λ is too long. Such a wave cannot produce cavitation.

Curve II in figure 3 satisfies the requirement that the minimum pressure occurs in the water, i.e., at positive values of depth z. However, we have the additional requirement--if cavitation is to occur--that the total pressure reaches a minimum value which is negative for some positive value of depth z.

C. Onset Depth

From figure 3 we see that the total pressure p first reaches zero--and cavitation commences--at the onset depth z_o; from equation (1) for exponential type waves, this onset depth z_o must satisfy the transcendental equation

$$0 = p_a + \rho gz_o - p_o(1 - e^{-2z_o/\lambda}) .$$ (2)
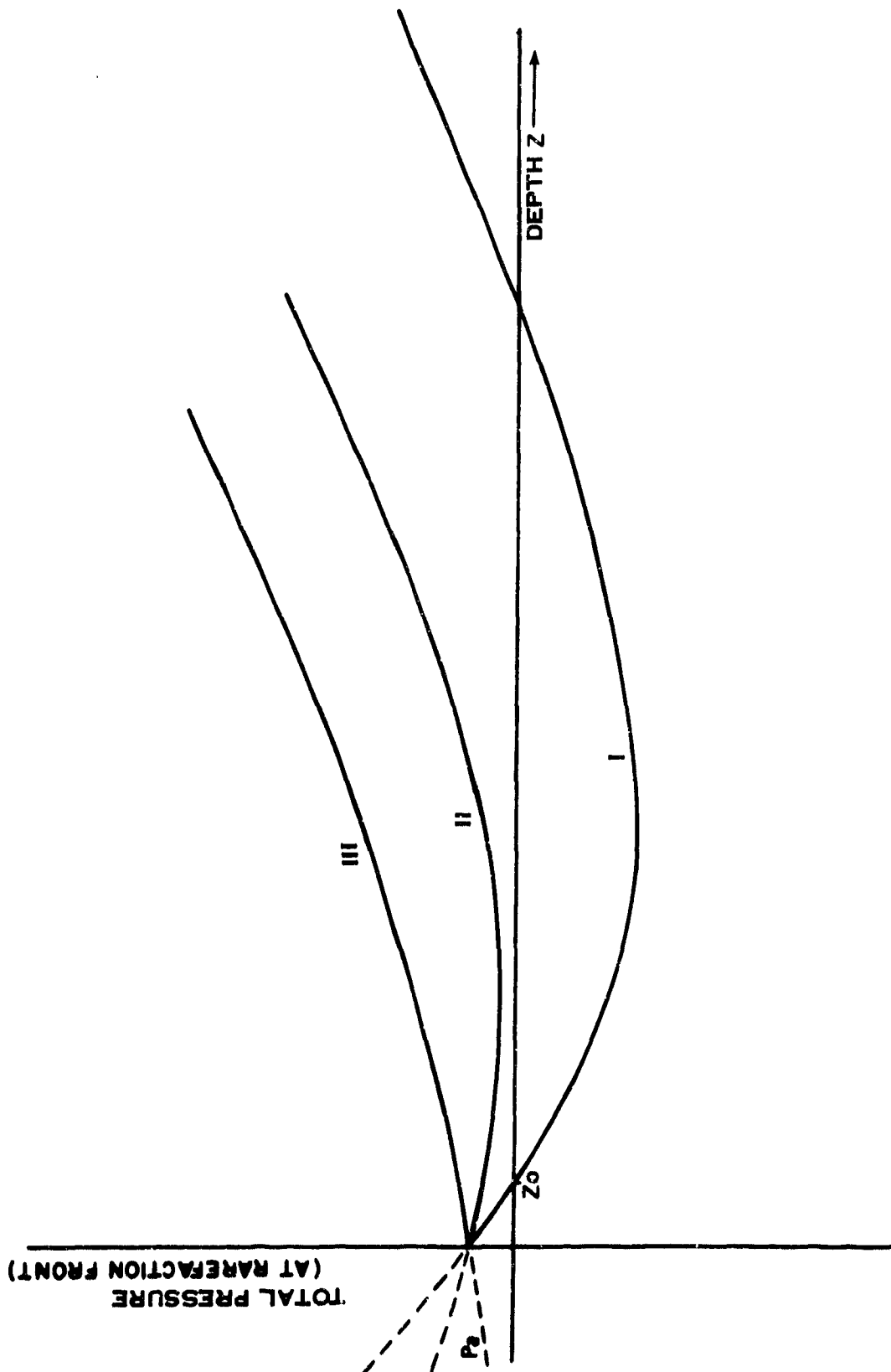
Figure 3. Total pressure at reflected rarefaction front as a function of depth z.

If z_o/λ is sufficiently small, the solution to equation (2) is approximated by

$$z_o/\lambda = \frac{p_a}{2p_o - \rho g \lambda}$$
(3)

The term $\rho g \lambda$ is the hydrostatic pressure at depth λ--it is an expression that will show up repeatedly in bulk cavitation analysis.

D. **Particle Velocity History**

Figure 4 shows the motion of water particles at various initial depths. In figure 4 water depth z is measured vertically downward; and time t is the abscissa. In that figure we see the trajectory of the incoming shock front and also the trajectory for the reflected rarefaction front. All water particles are quiescent prior to arrival of the incoming shock front. Immediately after arrival of the shock front, the water particle is traveling upward with particle velocity computed in the usual fashion--for the pressure levels of interest we generally compute this particle velocity in accord with the acoustic approximation.

When the incoming shock front strikes the free surface, a rarefaction wave is reflected back down into the water; the trajectory of the reflected rarefaction front is also shown in figure 4. The rarefaction wave causes a further increase in upward velocity of the water particles. As indicated earlier, the total pressure p in the water remains positive until a certain depth z_o, as indicated in figure 4; to this depth we can compute water particle velocity by the acoustic approximation. According to such a computation, the particle velocity in the neighborhood of the surface z_s is given by the usual expression $2p_o/\rho c$ where ρc is the specific acoustic impedance for water. Thus, the water surface initially takes off with a surface rate as depicted in figure 4.

Let us now compute the upward particle velocity of the water immediately after passage of the reflected rarefaction front. When the reflected rarefaction
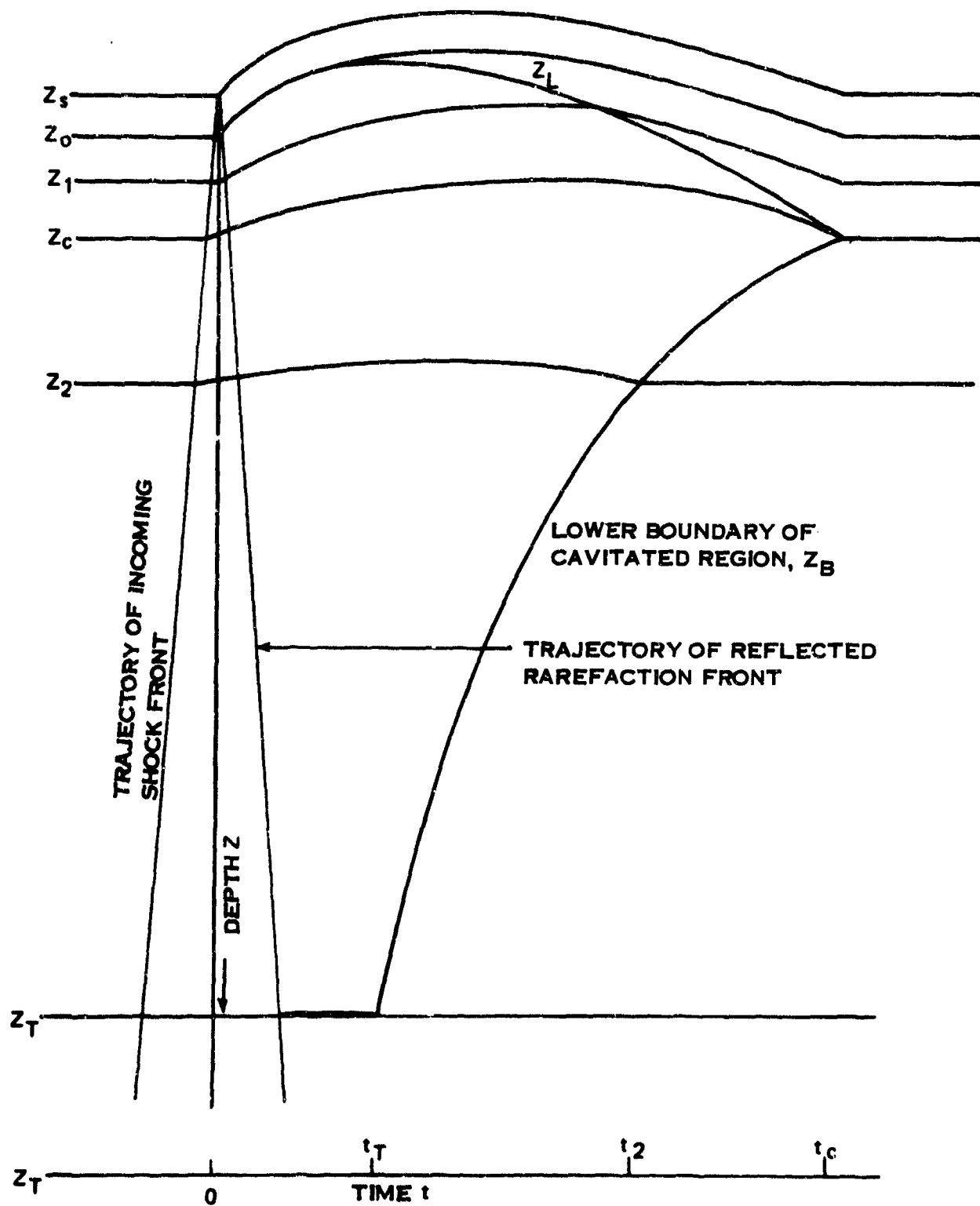
Figure 4. Motion of water particles at various depths, ranging from z_s (the water surface) to z_o (the depth of cavitation onset), z_c (the depth of cavitation closure), and z_T (the terminal depth beyond which there is no cavitation). The particle originally at depth z_1 is typical of the water particle which is accreted to the lower boundary z_L of the spall. The water particle of depth Z_2 follows a ballistic trajectory till it falls back to its original depth.

front has reached a depth z, the particle velocity u_i just below the front--due to the waning portion of the incoming compression wave--is vertically upward (i.e. negative in our coordinate system) and computed in the acoustic approximation to be (see reference 3)

$$u_i = \frac{-p_o e^{-2z/\lambda}}{\rho c} \quad . \tag{4}$$

If the water behaves acoustically, i.e., can withstand any required extent of tensile or compressive strength, the reflected rarefaction front drops the pressure by an amount p_o; in the acoustic approximation, the upward velocity increment u_r due to this pressure change is described by

$$u_r = - p_o/\rho c \quad , \tag{5}$$

For an acoustic medium, the upward particle velocity after passage of the reflected rarefaction front would be the sum of u_i and u_r expressed in equations (4) and (5).

However, seawater cannot withstand the required tensions, and therefore for depths greater than the onset depth z_o, the reflected rarefaction front can do no more than drop the pressure to zero (more precisely, the vapor pressure of water). The pressure p_p in the water immediately below the rarefaction front is expressed by

$$p_p = p_a + \rho g z + p_o e^{-2z/\lambda} \quad , \tag{6}$$

where p_a is atmospheric pressure, $\rho g z$ is hydrostatic pressure, and $p_o e^{-2z/\lambda}$ is the pressure remaining in the waning portions of the incoming shockwave. The reflected rarefaction front drops the pressure in the water by the amount p_p expressed by equation (6). The process of dropping this pressure takes place before the water has actually ruptured; hence, the increment in particle velocity u_p due to this pressure drop can be computed in the acoustic approximation. The pressure drop

from p_p to zero by the rarefaction front causes an upward increment in particle velocity u_p described by

$$u_p = - p_p/\rho c \qquad . \qquad (7)$$

The total particle velocity immediately after passage of the reflected rarefaction front is the sum of: (1) the velocity u_i, i.e., the particle velocity in the water just prior to arrival of the reflected rarefaction front; plus (2) the increment in particle velocity u_p due to the pressure change p_p caused by the rarefaction front. Therefore, the particle velocity $u(z)$ at depth z in the water immediately after passage of the reflected rarefaction front is the sum of equations (4) and (7)

$$u(z) = -(p_a + \rho gz + 2p_o e^{-2z/\lambda})/\rho c \qquad . \qquad (8)$$

We use a minus sign in front of the expression in equation (8) because, in our analysis, we are measuring z vertically downward; the "launch velocity" $u(z)$ immediately after passage of the reflected rarefaction front is upward.

E.   Instant Cavitation Approximation

The reflected rarefaction front travels at the speed of sound in water c. Therefore, the particle at depth z is launched at a time z/c. As suggested in figure 4, we find that the motions of the particles in the cavitated region and the motion of the overlying spall take place during times which are very large compared with z/c; and so we will henceforth simplify the analysis by neglecting the time z/c, i.e., by assuming that at all depths z the water particles are launched at time t equal to zero, as shown in figure 5. With this instant cavitation approximation, we assume that all water particles beyond the onset depth z_o are launched simultaneously at time zero, and that the "launch velocity" with the particle at depth z is expressed by equation (8).
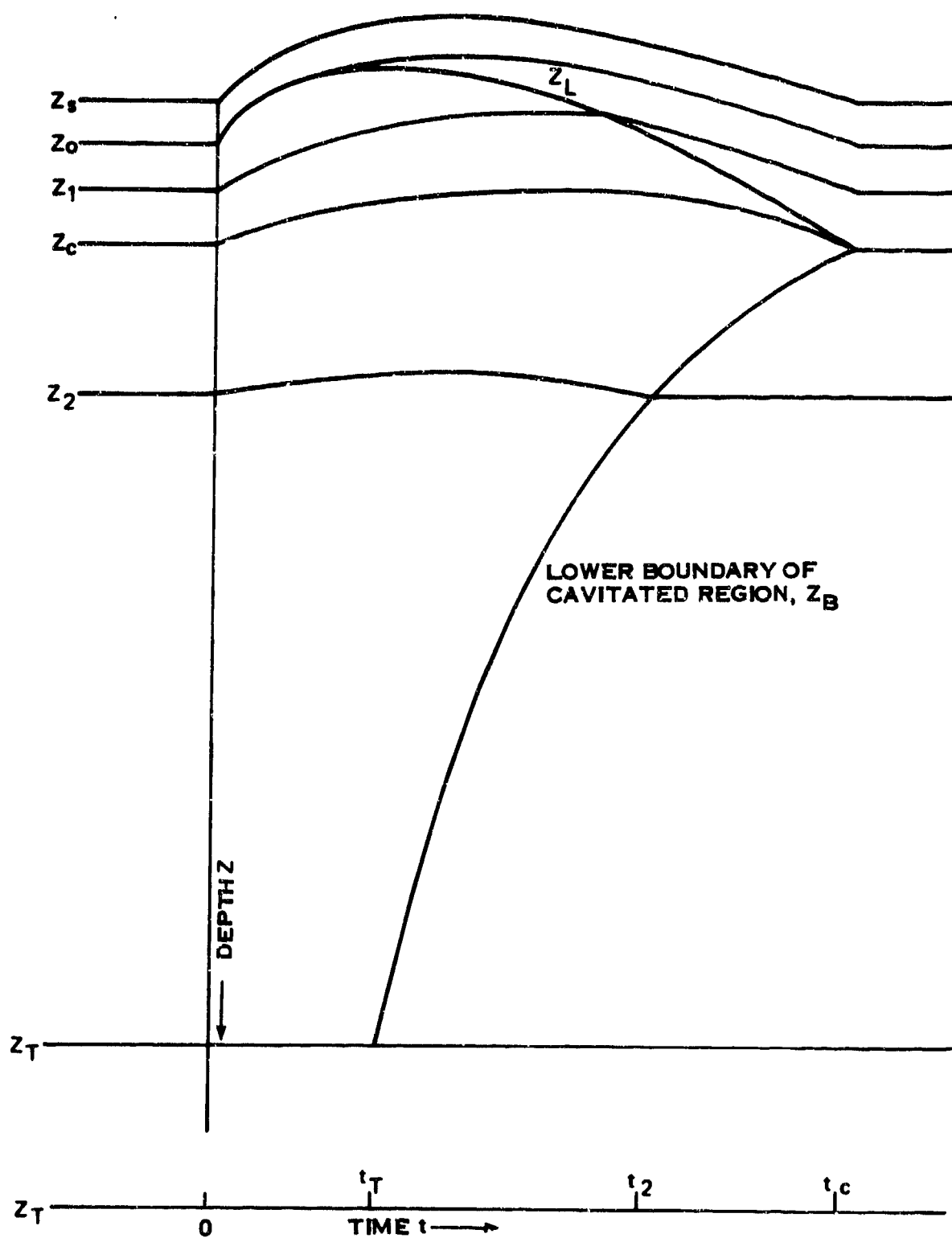
Figure 5. Water particle trajectories under the approximation that the transit time of the rupturing rarefaction front is negligible compared with the trajectory times of the cavitated water.

We will see later that, depending on the shockwave peak pressure p_o, there is a certain depth z_T--as depicted in figures 4 and 5--beyond which the cavitation process cannot take place. For depths less than the onset depth z_o and greater than the termination depth z_T, the specific volume of the water is that of liquid water, with only slight variations in specific volume which are in accord with the acoustic approximation.

Between the onset depth z_o and the termination depth z_T the water has ruptured or cavitated; it has vaporized to the extent necessary. Macroscopically, the specific volume can increase considerably beyond that of ambient seawater; to achieve this macroscopic increase in specific volume, we can imagine the cavitated region to consist mostly of liquid water with numerous water vapor bubbles dispersed throughout the volume, or we may alternately envision it as numerous liquid water droplets dispersed throughout a volume of water vapor.

Since the pressure throughout the cavitated region is virtually zero (the vapor pressure of water at standard temperature), there is no pressure gradient throughout the cavitated region. Therefore, only the body force of gravity acts on the cavitated water particles, and hence, each water particle, once launched by the reflected rarefaction front, follows a ballistic trajectory. Conservation of matter considerations indicate that a water particle can follow this "cavitated trajectory" only while it is at a depth less than its quiescent depth. For example, in figures 4 and 5 we show a water particle initially at depth z_2. It can exist in a cavitation condition during the parabolic trajectory indicated, but when this parabolic trajectory falls back to the pre-shockwave depth, the cavitated condition is terminated. If after flow is taken into account, the water particle initially at depth z_2 will complete its trajectory when it returns to a depth somewhat less than the initial depth.

F.   Closure From the Bottom

Figures 4 and 5 depict the locus of the lower boundary of the cavitated region. At the terminal depth z_T the water is launched into ballistic trajectory with velocity $u(z_T)$. The equations which allow one to solve for the termination depth z_T are discussed later. Since this water travels under the action of gravity alone, the water particle at this termination depth will fall back to its ambient depth at a time t_T described by

$$t_T = -\frac{2}{g} u(z_T) \qquad (9)$$

(again we recall that, in our system of coordinates, the launch velocity $u(z)$ is negative--vertically upward). In other words, the cavitated region commences to close from the bottom at the time t_T. In general, a water particle at depth z will fall back on the underlying water--i.e., will fall back to its original depth --at a time t described by

$$t = -\frac{2}{g} u(z) \qquad . \qquad (10)$$

If the incident shockwave has a shock-rise with exponential tail-off so that the launch velocity is as described by equation (8), cavitation closure from the bottom--i.e., the t versus z curve--has the general shape of the curve labelled "Lower Boundary of Cavitated Region" shown in figures 4 and 5.

G.   Closure From the Top

The liquid layer or spall is contained between the curves labelled z_s and z_L as depicted in figures 4 and 5. At any instant of time, this liquid layer is forced downward by: (1) the body force of gravity, and (2) atmospheric pressure acting on the upper surface of the spall. Hence, the spalled liquid layer is accelerating downward more rapidly than if it were acted upon by the force of grav-

18

ity alone. If we now follow a water particle at depth z_1 as shown in figure 4,
we know that, once launched in its cavitated trajectory, it follows a ballistic
trajectory. It follows that the more rapidly accelerating liquid spall layer
"overtakes" a particle that was launched from the depth z_1. In other words, the
mass and momentum of the water particle originating at depth z_1 is at some time
accreted to the lower boundary z_L of the spall. In Section III we will take this
accretion of mass and momentum into account in setting up the equations of motion
of the spall.

Because of this continuing accretion process, the thickness of the spall
grows. When the z_L curve intersects the z_B curve shown in figures 4 and 5, cavi-
tation is finally concluded. The depth at which this closure or conclusion takes
place is the depth z_c as shown in figures 4 and 5. The time of closure is equal
to the ballistic trajectory time of the water particle launched from depth z_c.

At the time of closure, the liquid spall contained between z_B and z_c has
a vertically downward momentum; this momentum is suddenly arrested by impacting
on the underlying water, and this impact or "water hammer" is a source of second-
ary pressure waves. These will be studied in more detail in Section V of this re-
port.

H.   Termination Depth

Once cavitation is initiated, the reflected rarefaction front can con-
tinue to cavitate water as it progresses to deeper depths provided the launch
velocity gradient $du(z)/dz \equiv u'(z)$ is favorable. The lower bound of the cavitated
region z_T is determined by noting when the launch velocity gradient becomes un-
favorable, i.e., the termination depth is determined by

$$u'(z_T) = 0 \qquad \qquad . \qquad \qquad (11)$$

For the shock-rise and exponential tail-off incident wave where the launch velocity $u(z)$ is as described by equation (8) we find the following relationship for the termination depth z_T,

$$z_T/\lambda = \tfrac{1}{2} \ln (4p_0/\rho g\lambda)$$ (12)

III.   **ANALYSIS**

In earlier sections we described the cavitated region as one where the water had ruptured and where the (macroscopic) specific volume could increase considerably beyond that of liquid water. Overlying this cavitated region is a liquid layer of water--the spall--which is driven downward by gravity and the overlying air pressure acting at its surface. The spall is thus driven down into the cavitated region, accreting momentum and mass from the cavitated water particles; the spall thus grows in thickness during its trajectory.

From figure 6 we note that the water particle originally at depth z becomes accreted to the spall at a time when the spall has reached a thickness of z. This simply says that the liquid water making up the spall of thickness z must have derived from the liquid water which originally was contained between the water surface and depth z.

At the time that the spall has achieved a thickness of z, its surface is at the position z_s. From figure 6 we see that the cavitated water particle originating from depth z has risen--in ballistic trajectory--to the height z_s at the instant that it accretes to the spall.

A.   **Equations of Motion**

In the following analysis, the time t is the independent variable; $z(t)$ is the thickness of the spall; $z_s(t)$ is the position of the spall surface.

Conservation of momentum requires the following equation be satisfied (we will discuss each term following the equation)

$$\rho z \dot{z}_s - \rho \int_0^z u(z)dz = \rho g z t + p_a t \qquad . \qquad (13)$$

The first term on the left of equation (13) is the momentum of the spall at time t; the second term on the left of the equation represents the total momentum in
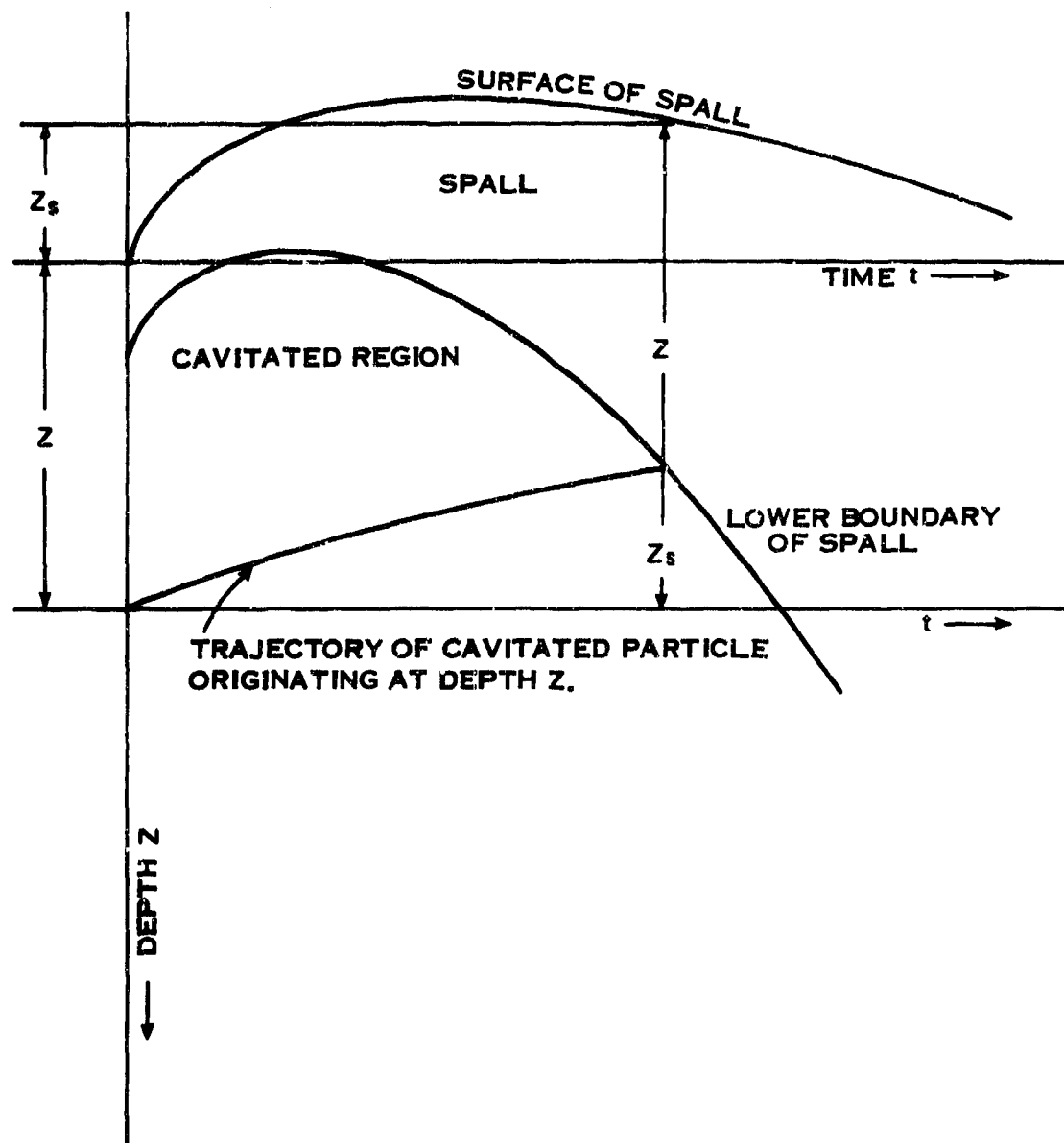
Figure 6. Relationship between spall surface position z_s and spall thickness z.

the water to depth z at the onset of cavitation. The left hand side of the equation therefore is the change in momentum of all the water originally contained between the water surface and depth z. The first term on the right hand side of equation (13) is the gravitational body force--acting through time t--applied to all of the water contained between the surface and depth z; the second term on the right is the atmospheric pressure--acting through time t--applied on the upper surface of the spall. Since the cavitated region under the spall is at vapor pressure--virtually zero--there is no surface force on the under side of the spall. The two terms on the right hand side of equation (13) therefore represent the impulse applied during the time t to all of the water contained between the water surface and depth z.

We have already indicated in our discussion of figure 6 that the water particle launched from depth z rises in a ballistic trajectory by an amount z_s at the time it accretes to the spall. We therefore have the following relationship (recall that z is measured vertically downward, and u(z) is a negative number since the cavitated water is launched vertically upward)

$$z_s = t \, u(z) + \frac{g}{2} \, t^2 \qquad . \qquad (14)$$

If we differentiate equation (14) with respect to time and substitute $\dot{z}_s$ into equation (13) we obtain, after some manipulation,

$$z\dot{z}u'(z) + \frac{d}{dt} \left[tz\dot{z}u'(z) \right] = p_a/\rho \qquad , \qquad (15)$$

where $\dot{z}$ denotes the time derivative of z; and $u'(z)$ denotes du/dz. Equation (15) allows one to solve the spall thickness z as a function of time t. It is interesting to note that spall growth depends only on the form of u(z) and on the overlying air pressure p_a which drives the spall downward, accreting the

24

mass and momentum of the underlying cavitated water. As one would expect from dynamics in a uniformly accelerating coordinate system, $z(t)$ should not depend on the gravitational acceleration g.

B. Solutions

The solution to equation (15) is

$$z\dot{z}u'(z) = p_a/2\rho \qquad . \qquad (16)$$

If we separate variables in equation (16) and integrate, we obtain

$$t = \frac{2\rho}{p_a} \int_0^z zu'(z)dz \qquad . \qquad (17)$$

This can be alternatively written as

$$t = \frac{2\rho}{p_a} \left[zu(z) - \int_0^z u(z)dz \right] \qquad . \qquad (18)$$

The launch velocity $u(z)$ depends on the wave shape of the incident shock-wave; for a shock-rise to peak pressure p_o with exponential tail-off with wave length λ, $u(z)$ has the form of equation (8). Once $u(z)$ is established, equation (17) or (18) becomes a relationship implicitly giving spall thickness z as a function of time t. If equation (17) or (18) is substituted into equation (14) we then also can describe the position of the spall surface z_s as a function of time. In Section IV of this report, we carry out solutions of these equations for exponential waves.

We reiterate that we have simplified the analysis by making the "instant cavitation approximation" described earlier. Thus equations (14) and (15) are valid only when $z(t) \ll ct$. This inequality holds for most explosion configurations of interest after cavitation has commenced, i.e., for $t \geq z_o/c$, where z_o is the cavitation onset depth described in Section IIC.

IV. SPALL DYNAMICS WITH EXPONENTIAL WAVES

Pressure waves from underwater explosions are generally depicted as having a shock-rise to a pressure p_o followed by an exponential fall-off in pressure with a wave length λ, where λ is the distance behind the shock front where the peak pressure has fallen to $1/e$ of its value. In this section, we will obtain solutions to the equations already developed for such exponential waves--further taking into account that the shock wave can make an angle of incidence α with the free surface, as shown in figure 7.

Analytically, the incident pressure wave p_i is of the form

$$p_i = p_o \, e^{-(t + az/c)/\tau} \qquad\qquad t + az/c \geq 0 \quad , \qquad (19)$$

$$= 0 \qquad\qquad t + az/c < 0 \quad , \qquad (20)$$

where $a \equiv \cos \alpha$; z is depth measured from the surface ; $\tau = \lambda/c$.
Similarly, the reflected rarefaction wave p_r is described by

$$p_r = -p_o \, e^{-(t - az/c)/\tau} \qquad\qquad t - az/c \geq 0 \quad , \qquad (21)$$

$$= 0 \qquad\qquad t - az/c < 0 \quad . \qquad (22)$$

Our objective is to find the vertical component of the water particle velocity immediately after passage of the reflected rarefaction front, i.e., our objective is to ascertain the cavitation launch velocity $u(z)$. Following the discussion in Section II of this report, and observing the geometry of figure 7, we note that the vertical component of particle velocity in the incident wave just prior to arrival of the reflected rarefaction front is u_i described by
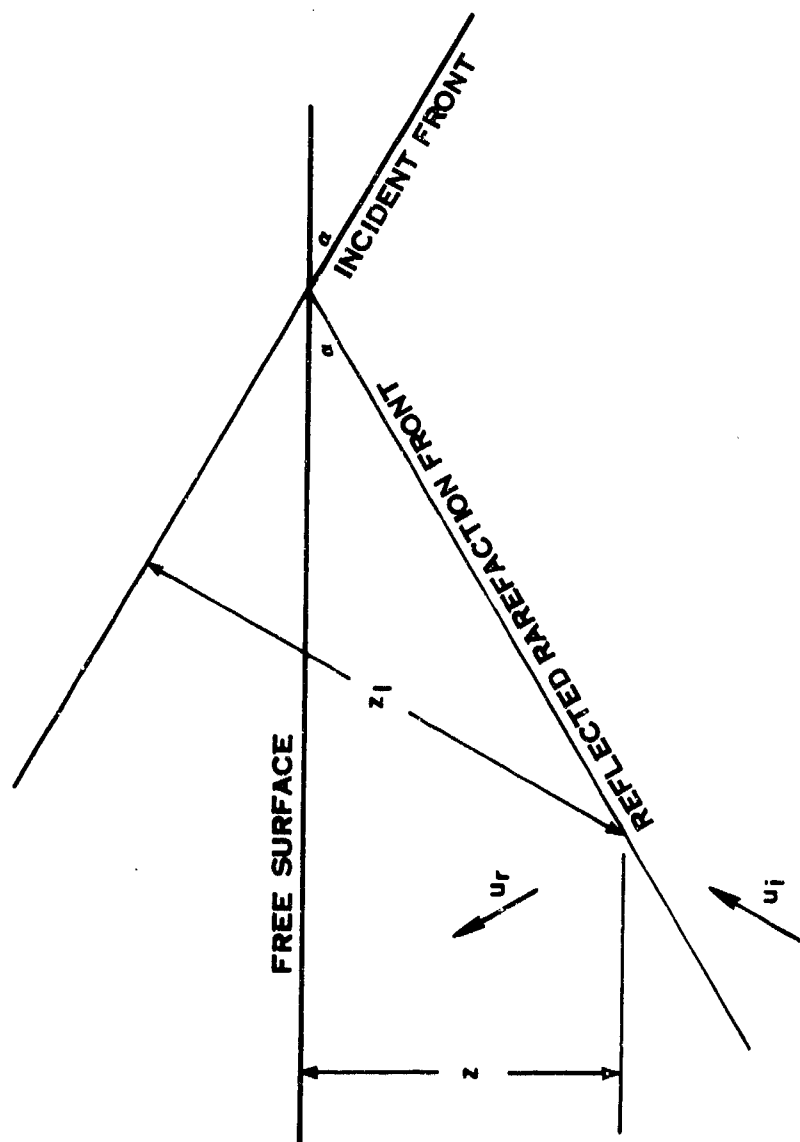
Figure 7. Geometry of cavitation producing shockwave incident obliquely at the free water surface.

$$u_1 = - \frac{ap_o \, e^{-2az/\lambda}}{\rho c} \qquad . \tag{23}$$

The pressure p_p [analogous to that discussed in equation (6) on page 13 of this report] in the water just prior to arrival of the rarefaction front is

$$p_p = p_a + \rho gz + p_o \, e^{-2az/\lambda} \qquad . \tag{24}$$

When cavitation takes place, this pressure p_p is dropped to zero, and this pressure reduction imparts a particle velocity component u_r normal to the rarefaction front (see figure 7); the vertical component of particle velocity is u_p described by

$$u_p = - ap_p/\rho c \qquad . \tag{25}$$

The launch velocity $u(z)$ of the cavitated water is the sum of u_i and u_p described by equations (23) and (25) taking into account equation (24), we obtain finally

$$u(z) = - a \, (p_a + \rho gz + 2 \, p_o \, e^{-2az/\lambda})/\rho c \qquad , \tag{26}$$

where again we note that the minus sign occurs in equation (26) because we measure z vertically downward, whereas the cavitation launch velocity $u(z)$ is vertically upward. Equation (26) is valid in the cavitated region, i.e., where $z_o \leq z \leq z_T$ (z_o is the depth of cavitation onset; z_T is the depth of cavitation termination).

We now make the following definitions of variables:

$$L = \lambda/a \qquad ; \tag{27}$$

$$Z = z/L \qquad ; \tag{28}$$

$$\tau = \lambda/c \qquad ; \tag{29}$$

$$P_L = \rho g L / p_a \qquad\qquad ; \qquad\qquad (30)$$

$$P_o = p_o / p_a \qquad\qquad . \qquad\qquad (31)$$

L is the modified wave length of the incident shock wave, taking into account the angle of incidence α; τ is the characteristic time of the incident shock wave; Z is the dimensionless depth (taking into account the angle of incidence α); P_L is the hydrostatic pressure at depth L, expressed in atmospheres; P_o is the peak pressure of the incident shock wave, expressed in atmospheres. In terms of these new variables, equation (26) can be rewritten as

$$u(Z) = \frac{-a p_o}{\rho c} \left[\frac{1}{P_o} + \frac{P_L}{P_o} Z + 2 e^{-2Z} \right] \quad . \qquad (32)$$

A. Spall Thickness Versus Time

If we make the necessary change in variables in equation (18), use equation (32) and carry out the indicated integration, we obtain the following expression for the real time t

$$t = 2 \tau P_o T \qquad\qquad \text{seconds} , \qquad\qquad (33)$$

where the dimensionless time T is defined as

$$T = 1 - (1 + 2Z) e^{-2Z} - \frac{P_L}{2 P_o} Z^2 \quad . \qquad (34)$$

The real time t is largely proportional to the shock strength p_o--especially so when p_o is large; we therefore find it convenient for computational tabulations in the Appendix to employ a reduced time t_p defined by

$$t_p = t / a p_o \qquad\qquad \text{seconds per unit-pressure} \qquad . \qquad (35)$$

This can be written for computational purposes as

$$t_p = \frac{2L}{p_a c} T \qquad \text{seconds per unit-pressure} \qquad . \tag{36}$$

If atmospheric pressure p_a is expressed in psi (14.7 psi) and the speed of sound in water is taken as 5 feet per millisecond, equation (36) for computational purposes can be written as

$$t_p = LT/36.75 \qquad \begin{array}{l} \text{milliseconds per psi, or} \\ \text{seconds per thousand psi} \end{array} \qquad . \tag{37}$$

The results of computer runs employing equation (37) are tabulated in the Appendix.

B. Spall Surface Position Versus Time

Since we now have an expression for real time t as a function of spall thickness z, we can substitute into equation (14) to find surface position z_s as a function of time; we obtain

$$z_s = \frac{2(ap_o)^2}{\rho c^2 p_a} LZ_s \qquad , \tag{38}$$

where the dimensionless surface position Z_s is defined by

$$Z_s = -2 \left[\frac{1}{2P_o} + \frac{P_L}{P_o} Z + e^{-2Z} - \frac{P_L}{2} T \right] T \qquad . \tag{39}$$

Since the surface position z_s is largely proportional to the square of the incident shock wave pressure p_o (more specifically, proportional to the square of the "vertical component of pressure" ap_o), we find it convenient to define a

reduced surface position z_{sp} defined by

$$z_{sp} = z_s / (ap_o)^2 \qquad .$$

(40)

For computational purposes, this is

$$z_{sp} = \frac{576}{1470} LZ_s \qquad \text{feet per thousand psi squared.}$$

(41)

To determine the coefficient of LZ_s in equation (41) we have taken the density of seawater ρ to be equal to 2 slugs per cubic foot; and noted that we must allow for the conversion factor from psi to pounds per square foot if we want to express equation (41) in terms of feet per thousand psi squared. Results of computer runs with equation (41) are tabulated in the Appendix.

C. Spall Velocity Versus Time

To find an expression for the surface velocity $\dot{z}_s$, we differentiate equation (14) and obtain

$$\dot{z}_s = \frac{ap_o}{\rho} U_s \qquad ,$$

(42)

where U_s is the dimensionless surface velocity defined by

$$U_s = -2\left[\frac{1}{2P_o} + \frac{P_L}{2P_o} Z + e^{-2Z} - \left\{P_L + \frac{1}{2Z}\right\} T\right] \qquad .$$

(43)

The dimensionless velocity U_s is in a form useful for computation purposes; it is already normalized to the vertical component of particle velocity in the incident shockwave. Results of computer runs using equation (43) for the dimensionless or scaled velocity are tabulated in the Appendix.

D. Spall Acceleration Versus Time

To find the surface acceleration $\ddot{z}_s$, we differentiate equation (42) and obtain

$$\ddot{z}_s = \frac{g}{2P_L} \, dU_s/dT \qquad , \qquad (44)$$

where

$$dU_s/dT = 2P_L G_s \qquad , \qquad (45)$$

and where

$$G_s = 1 + \frac{1}{P_L Z} - \frac{Te^{2Z}}{8P_L Z^3} \qquad . \qquad (46)$$

G_s is equal to $\ddot{z}_s/g$, i.e., it is the surface acceleration expressed in "gees." Results of computer runs employing equation (46) are tabulated in the Appendix.

E. Onset Depth

By following an analysis similar to that leading to equations (2) and (3) in Section II, we find that the onset depth Z_o must satisfy the relationship

$$0 = \frac{1}{P_o} + \frac{P_L}{P_o} Z_o - \left(1 - e^{-2Z_o} \right) \qquad . \qquad (47)$$

If Z_o is sufficiently small, the solution to this equation is approximately

$$Z_o \simeq \frac{1}{2P_o - P_L} \qquad . \qquad (48)$$

F. Termination Depth

Following the analysis leading to equation (12) in Section II, we find

that cavitation terminates at the dimensionless depth Z_T expressed by

$$Z_T = \frac{1}{2} \ln (4P_o/P_L) \qquad (49)$$

G. Closure Depth

The dimensionless closure depth Z_c occurs when the expression in the brackets of equation (39) reaches zero, i.e., when the surface position returns to zero. This zero can be found by numerical methods on a digital computer, as is done in the Appendix. In the strong shock approximation where P_o is very large compared with P_L, the zero of equation (39) is found by solving the following simpler, although still transcendental, relationship

$$e^{2Z_c} - 2Z_c - 1 + \frac{2}{P_L} = 0 \quad . \qquad (50)$$

The relationship indicated in equation (50) is shown in figure 8, where Z_c is plotted as a function of P_L.

Inspection of equation (50) discloses that when P_L is very small (i.e., very short wave length exponential waves), then Z_c is large and expressed approximately by

$$Z_c \simeq \frac{1}{2} \ln (2/P_L) \qquad \text{for } P_L \ll 1 \quad ; \qquad (51)$$

whereas when P_L is large (i.e., long wave length exponential waves), Z_c is small, expressed approximately by

$$Z_c \simeq P_L^{-\frac{1}{2}} \qquad \text{for } P_L \gg 1 \quad . \qquad (52)$$
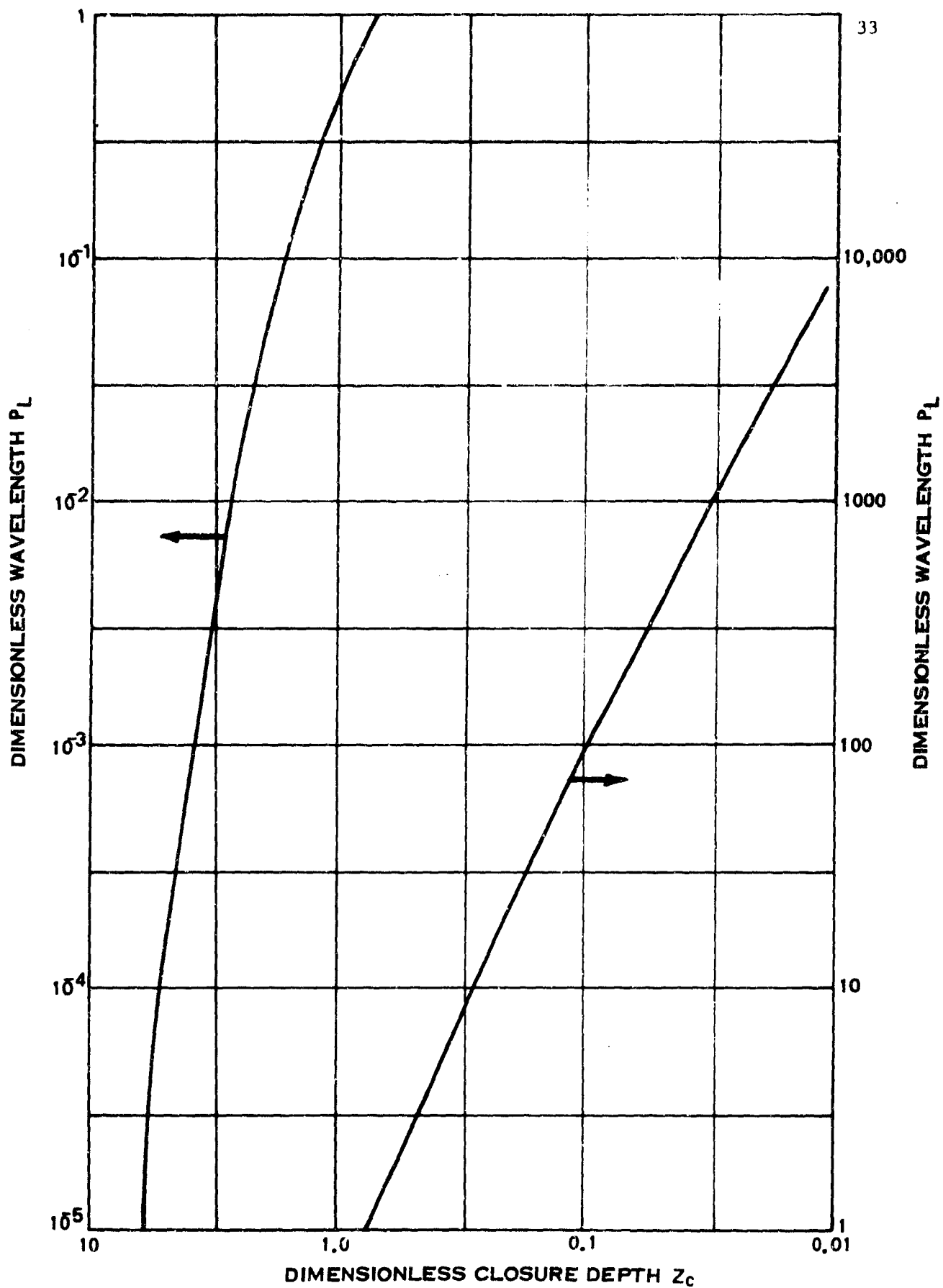
Figure 8.

Equations (51) and (52) are approximations in terms of the dimensionless varia-
bles Z_c and P_L. Using equations (27) through (31), we can rewrite equations (51)
and (52) in terms of the real closure depth z_c and the real wave length λ as

$$z_c \simeq \frac{\lambda}{2a} \ln (2ap_a/\rho g\lambda) \qquad \text{for } \rho g\lambda \ll ap_a \quad , \qquad (53)$$

and

$$z_c \simeq (\lambda p_a/\rho g a)^{\frac{1}{2}} \qquad \text{for } \rho g\lambda \gg ap_a \quad , \qquad (54)$$

where ρ is the ambient density of seawater; g is the acceleration of gravity; p_a
is atmospheric pressure; and $a = \cos \alpha$ where α is the incident shockwave's angle
of incidence with the free water surface.

H.   Closure Time (Strong Shock)

After the closure depth Z_c has been found from the foregoing equations,
the closure time T_c can be found by substitution into equation (34). In the strong
shock approximation where P_o is very large compared with P_L, we have

$$T_c = 1 - (1 + 2Z_c) e^{-2Z_c} \quad , \qquad (55)$$

or, making use of the relationship of equation (50) which holds at the time of
closure

$$T_c = \frac{1}{1+P_L/2+P_L Z_c} \quad . \qquad (56)$$

In the approximation that Z_c is small (i.e., that P_L is large), we have

$$T_c \simeq \frac{2}{P_L} \left[1 - 2P_L^{-\frac{1}{2}} \right] \qquad \text{for } P_L \gg 1 \quad . \qquad (57)$$

In terms of real time, the time of closure t_c from equation (33) can be written

$$t_c \simeq \frac{2ap_o}{\rho c}\left(\frac{2}{g}\right)\left[1 - 2P_L^{-\frac{1}{2}}\right] \quad \text{for } P_L \gg 1 \quad , \tag{58}$$

or

$$t_c \simeq \frac{2u_s}{g}\left[1 - 2P_L^{-\frac{1}{2}}\right] \quad \text{for } P_L \gg 1 \quad , \tag{59}$$

where u_s is the peak water velocity at the free surface due to reflection of the incident shockwave (i.e., u_s is twice the vertical component of the particle velocity of the incident shockwave), described by

$$u_s = 2ap_o/\rho c \quad , \tag{60}$$

where $p_o/\rho c$ is the peak particle velocity in the incident shockwave, and a is the cosine of the angle of incidence of the incident shockwave. We note in equation (59) that $2u_s/g$ is the time of flight, under the action of gravity alone, of a particle launched with velocity u_s. Hence, when P_L is very large--when we have a long wavelength incident shockwave and/or when the angle of incidence with the free surface is very large--a good approximation for the time of flight of the spall (i.e., the time at which cavitation closure occurs) is that it is launched with velocity u_s and is acted upon by gravity alone; that is, we can neglect the additional acceleration due to the atmospheric pressure p_a acting on the top side of the spall. We will make use of this fact in Section VI, which is a discussion of the effects of spall surface motion in the generation of air blast associated with an underwater explosion.

When the scaled closure depth Z_c is large (i.e., when the dimensionless

wave length P_L is very small), we can substitute the approximation indicated by equation (51) into equation (56) and find for the dimensionless time of closure T_c

$$T_c = 1 - \frac{P_L}{2}\left[1 + \ln(2/P_L)\right] \qquad \text{for } P_L \ll 1 \quad . \tag{61}$$

In terms of real closure time t_c, this can be rewritten

$$t_c \simeq u_s\left(\frac{\lambda\rho}{ap_a}\right)\left[1 - \frac{P_L}{2}\left\{1 + \ln(2/P_L)\right\}\right] \quad \text{for } P_L \ll 1 \quad , \tag{62}$$

where u_s is the peak surface velocity as defined by equation (60). From equation (62) we note that for very short wave length incident shockwaves the pertinent acceleration which determines the closing time is that due to atmospheric pressure acting on the top side of the spall, i.e., the effective average acceleration is $2ap_a/\lambda\rho$.

I. Spall Velocity at Closure Time (Strong Shock)

By substituting from equation (56) into equation (43), we find the dimensionless spall velocity U_c at the time of cavitation closure

$$U_c = 2\left[\frac{P_L/2 + 1/2Z_c}{1 + P_L/2 + P_L Z_c}\right] \quad . \tag{63}$$

If the dimensionless wave length P_L is very large, we have approximately

$$U_c \simeq 2\left[1 - P_L^{-\frac{1}{2}}\right] \qquad \text{for } P_L \gg 1 \quad . \tag{64}$$

The real impact velocity u_c for this long wave length approximation is therefore

$$u_c \simeq u_s\left[1 - P_L^{-\frac{1}{2}}\right] \qquad \text{for } P_L \gg 1 \quad . \tag{65}$$

From equation (65) we see that when the wave length of the incident shockwave is very large and/or the angle of incidence with the surface is large, the spall velocity at the time of impact u_c is approximately equal to the vertical component of the peak surface velocity due to the incident shockwave, i.e., approximately equal to u_s as defined by equation (60).

When the wave length of the incident shockwave is very small, we have the approximation

$$U_c \simeq \frac{2}{\ln(2/P_L)} \qquad P_L \ll 1 \quad , \tag{66}$$

or, in terms of the real velocity u_c

$$u_c \simeq \frac{u_s}{\ln(2/P_L)} \qquad P_L \ll 1 \quad . \tag{67}$$

J. Spherical Explosions

The foregoing analysis has been carried out using a plane wave incident obliquely at angle α against a free surface. Of central importance in the analysis has been the form of $u(z)$, i.e., the "launch velocity" of a particle which is cavitated at depth z. For spherical explosions, one might expect that the foregoing analysis would be applicable provided the closure depth z_c were small compared with the burst depth--that is, provided the phenomena took place in a region such that the curvature were negligible.

It is perhaps surprising that the formulas derived with the foregoing plane wave analysis agree quite well with experimental data even when the closure depth z_c is at or well below the burst depth d. To see why this is so, we make reference to figure 9: a charge of weight W is burst at a depth d. The origin of coordinates is surface-zero. We are interested in the form of $u(z)$ as a
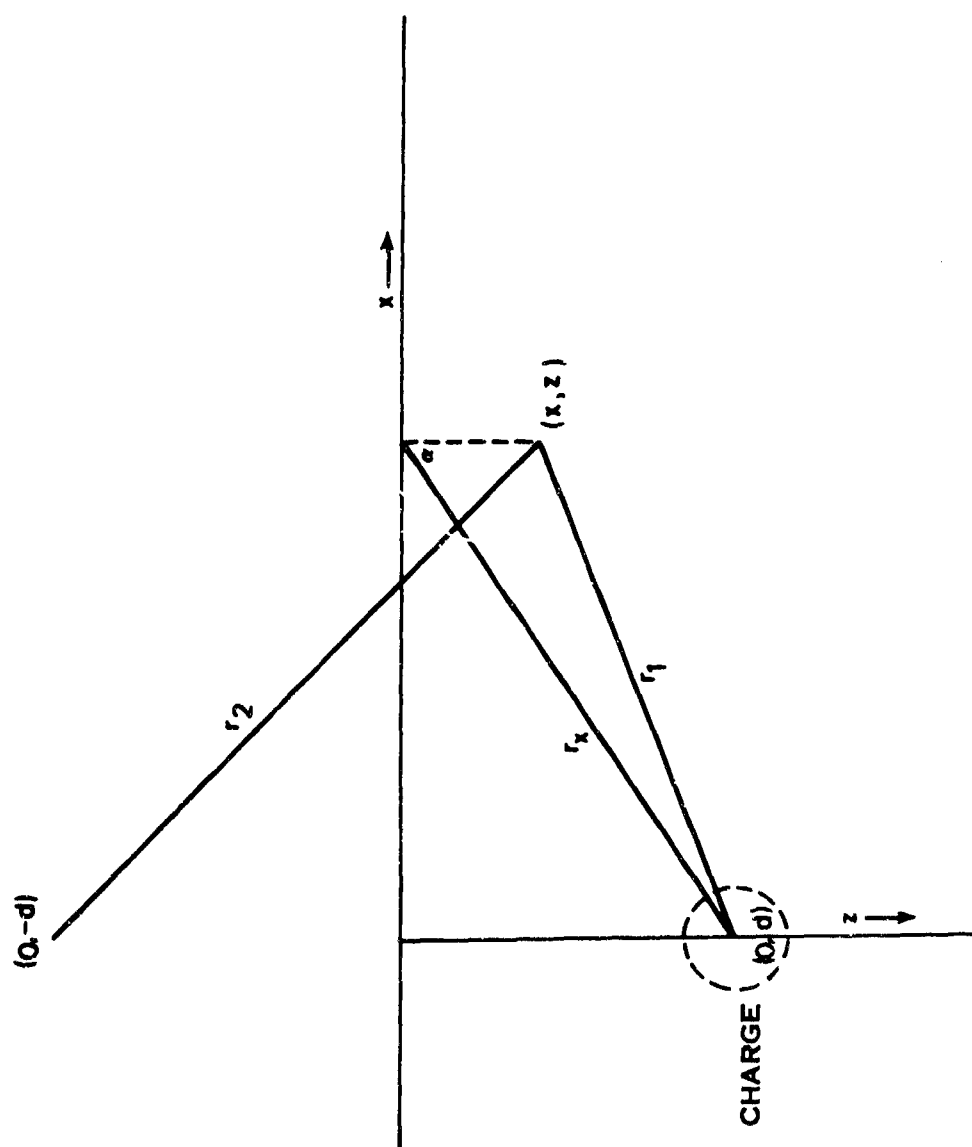
Figure 9. Geometry for analysis of spherical explosions.

function of the horizontal distance x.

In the usual fashion for the acoustic approximation, we use the image source at the altitude d in order to account for surface reflection of the explosion. Following the approach earlier in this section, we must first find the pressure and particle velocity in the main shockwave at the point (x,z) just prior to arrival of the rarefaction front. The rarefaction front then drops this pressure to zero, causing an additional increment in particle velocity in the direction of the image source (which is at altitude d). Then, u(z) is the vertical component of velocity of this now-cavitated particle.

We have the following geometric relationships

$$r_1^2 = x^2 + (d-z)^2 = r_x^2 + z(z-2d) \quad , \tag{68}$$

$$r_2^2 = x^2 + (d+z)^2 = r_x^2 + z(z+2d) \quad . \tag{69}$$

The pressure in the compression wave at (x,z) at the instant just prior to arrival of the rarefaction front is p_o

$$p_o = \frac{KW^{1/3}}{r_1} e^{-\left(r_2 - r_1\right)/\lambda} \quad , \tag{70}$$

where W is the weight of the explosive charge, and K is a constant of proportionality.

The vertical component of particle velocity u_{1v} in the compression wave at this instant is

$$u_{1v} = -\frac{KW^{1/3}(d-z)}{\rho c \, r_1^2} e^{-(r_2 - r_1)/\lambda} \tag{71}$$

The rarefaction fr··· drops the pressure p_o in the compression wave to zero, and in the process, imparts an increment of particle velocity normal to the rarefaction front. The vertical component of this increment due to cavitation is

$$u_{2v} = - \frac{KW^{1/3}(d+z)}{cc \; r_1 r_2} e^{-(r_2 - r_1)/\lambda} . \qquad (72)$$

Again we assume that cavitation takes place instantly that is, that the propagation time of the cavitating rarefaction front is negligible compared with the times of interest in the spall motion. The cavitation launch velocity function $u(z)$--which we hereafter will write in the form $u(x,z)$ to indicate that it is a function of horizontal distance from surface-zero--is the sum of equations (71) and (72)

$$u(x,z) = - \frac{Kv^{1/3}}{\rho c r_1} e^{-(r_2 - r_1)/\lambda} \left[\frac{d-z}{r_1} + \frac{d+z}{r_2} \right] . \qquad (73)$$

Using equations (68) and (69), the exponential in equation (73) can be written approximately

$$e^{-(r_2 - r_1)/\lambda} \simeq e^{-2zd/r_x \lambda} \left[1 \pm \frac{zd}{r_x^2} \left(\frac{z}{r_x} \right)^2 \right] , \qquad (74a)$$

and the remainder of the geometric terms in equation (73) can be written approximately

$$\left[\frac{d-z}{r_1} + \frac{d+z}{r_2} \right] / r_1 \simeq \left[1 - (z/r_x)^2 \right]^2 \left[1 + zd/r_x^2 \right] / r_x^2 . \qquad (74b)$$

In terms of these approximations, equation (73) can be rewritten as

$$u(x,z) \simeq u(x,o) e^{-2zd/\lambda r_x} \left[1 + \frac{zd}{r_x^2} \left(\frac{z}{r_x} \right)^2 \right] \left[1 - (z/r_x)^2 \right]^2 \left[1 + zd/r_x^2 \right] / r_x^2 \qquad (75)$$

where

$$u(x,0) = \frac{-2dKW^{1/3}}{\rho c r_x^2} \qquad . \qquad (75)$$

In equation (76), $u(x,0)$ is recognized as the surface velocity at distance x from surface-zero when the peak pressure relationship is as described by equation (70). From figure 9 we recognize that

$$d/r_x = \cos \alpha \qquad , \qquad (77)$$

so that the dimensionless depth Z, as defined in equation (28), is

$$zd/\lambda r_x = Z \qquad . \qquad (78)$$

Equation (75), then, indicates that the earlier derived equations for spall dynamics may give approximately reasonable answers at depth z for spherical explosions provided that the burst depth d and the closure depth z satisfy the inequalities

$$\left(z/r_x \right)^2 \ll 1 \qquad , \qquad (79a)$$

and

$$\left(zd/r_x \right)^2 \ll 1 \qquad . \qquad (79b)$$

K. Comparison With Experiment

R. R. Walker[8] reported on a series of explosion tests conducted in Chesapeake Bay during 1962 by the Underwater Explosions Research Division of the David Taylor Model Basin. The tests were specifically designed to gain experimental information concerning bulk cavitation from underwater explosions. All of the

---

[8] loc. cit.

analytical results presented here were not yet available at the time Walker reduced his data. However, a preliminary, simplified analysis had been carried out so that there were available at that time: (1) equation (50) above, which defines the dimensionless closure depth Z_c as a function of dimensionless wave length P_L; (2) equation (56) above, which defines the dimensionless closure time T_c as a function of dimensionless wave length P_L and dimensionless closure depth Z_c; and (3) equations (47), (48), and (49) above, which describe the boundaries of the cavitated region.

The UERD Chesapeake Bay series consisted of seven explosion tests. The charge weight in each test was 10,000 pounds HBX-1. Four of the charges were detonated at a depth of 50 feet, three at a depth of 100 feet; the water depth was approximately 150 feet.

Walker reports that the foregoing equations provided good agreement with his experimental data; and further, that spot checks with other data indicated the relationships were valid for a wide range of charge sizes and geometries. The predicted time of closure was generally slightly larger than the value measured; this is ascribed to the fact that the foregoing analysis neglects afterflow, which raises slightly the level of the underlying water so that the spall completes its trajectory and impacts slightly earlier than it would if the underlying water had not been raised by such afterflow.

The data included in Walker's report also shows agreement with some of the wave shapes of the secondary pressure waves generated under water when the spalled water layer impacts with the underlying water. These facets are discussed in Section V of this report.

V. SECONDARY PRESSURE WAVES UNDER WATER

So far in this report, we have studied the aspects of bulk cavitation and motion and growth of the overlying spall which results when an underwater shock-wave is incident and "reflected" from the free water surface. Just prior to the instant of closure, the overlying spall has downward momentum; at the instant of closure this momentum is arrested, i. e., there is a water hammer--generation of secondary pressure waves. In this section we will examine the character of these secondary pressure waves under water.

When a spherically symmetric explosion takes place under water, the main shockwave is incident first at surface-zero; and the incidence of the shock front with the water surface progressively moves outward thereafter from surface-zero. At surface-zero, the main shock is most intense and is incident normal to the surface, so that the vertical surface velocity is correspondingly large. At greater distances from surface-zero, the intensity of the shockwave is less because of the greater distance from the burst point, and also the angle of incidence progressively increases, with the consequence that the initial vertical surface velocity is less as we recede from surface-zero.

In this section we are interested in the time of cavitation closure as a function of horizontal distance from surface-zero. When we take into account: (1) the time of arrival of the main shockwave as a function of horizontal distance from surface-zero; (2) the variation in initial surface velocity as a function of distance from surface-zero--then it is clear that cavitation closure does not occur simultaneously everywhere. Rather, we will find that the cavitation closes, that is, the water hammer occurs, at different times depending on the distance we are from surface-zero.

44

We can carry out a fairly complete analysis, employing the relationships for closure depth and time of closure as a function of shock wavelength and peak pressure which have already been developed in earlier sections of this report. The tedium and complication of such an analysis does not lend itself to generalization for a report such as this. Consequently, we will be satisfied here with making certain simplifying approximations in order to achieve a generalized analysis that at the same time will more clearly show the major considerations. The simplified analysis presented here turns out to be fairly accurate for larger scale explosions or when the angle of incidence is large--specifically, good agreement with experiment may be expected where

$$\frac{\rho_w g \lambda}{p_a \cos \alpha} \gg 1 \qquad , \qquad (80)$$

where ρ_w is the density of seawater, g is the acceleration of gravity, λ is the wave length of the shockwave incident at the free water surface, p_a is atmospheric pressure, and α is the angle of incidence that the incident shockwave makes with the free water surface (see figure 7).

A. Assumptions

In this section, we assume that: (1) the pressure disturbance in the water consists of a shock rise with exponential tail-off, and that this disturbance propagates with the speed of sound in water c_w; (2) the peak pressure disturbance p_o at the shock front is of the form $KW^{1/3}/r$; and, (3) once the spall is separated from the underlying water, the force of gravity is the only significant force.

The first assumption above provides

$$p = p_o \exp \left[- (t + r/c_w)/\tau \right] \qquad , \qquad (81)$$

where r is the radius from the burst point, and where τ is the characteristic time of the exponential wave. In the acoustic approximation, the wave length λ of the exponential wave is related to the characteristic time by

$$\lambda = c_w \tau \qquad . \qquad (82)$$

The second assumption above indicates that we are neglecting the super-sonic effects of the shockwave close-in to the underwater explosion. The second assumption provides

$$P_o = KW^{1/3}/r \qquad . \qquad (83)$$

where K is a constant of proportionality and W is the weight of the explosive charge. For the value of K, we use here[*]

$$K = 2.28 \times 10^6 \qquad . \qquad (84)$$

The third assumption above is valid, as we saw from the considerations in Section V, provided the inequality (80) holds.

Figure 10 shows the geometry for the analysis in this section. The origin of the cylindrical coordinates (x,z) is at surface-zero. The coordinate x is the horizontal distance from the vertical axis; the coordinate z is measured verti-cally downward from surface-zero. The explosive charge of weight W is burst at a

---

[*] This corresponds with the assumption that a one pound charge of HE produ es--in the acoustic approximation--a pressure of 2.28×10^6 pounds per square foot at a distance one foot from the source.

46
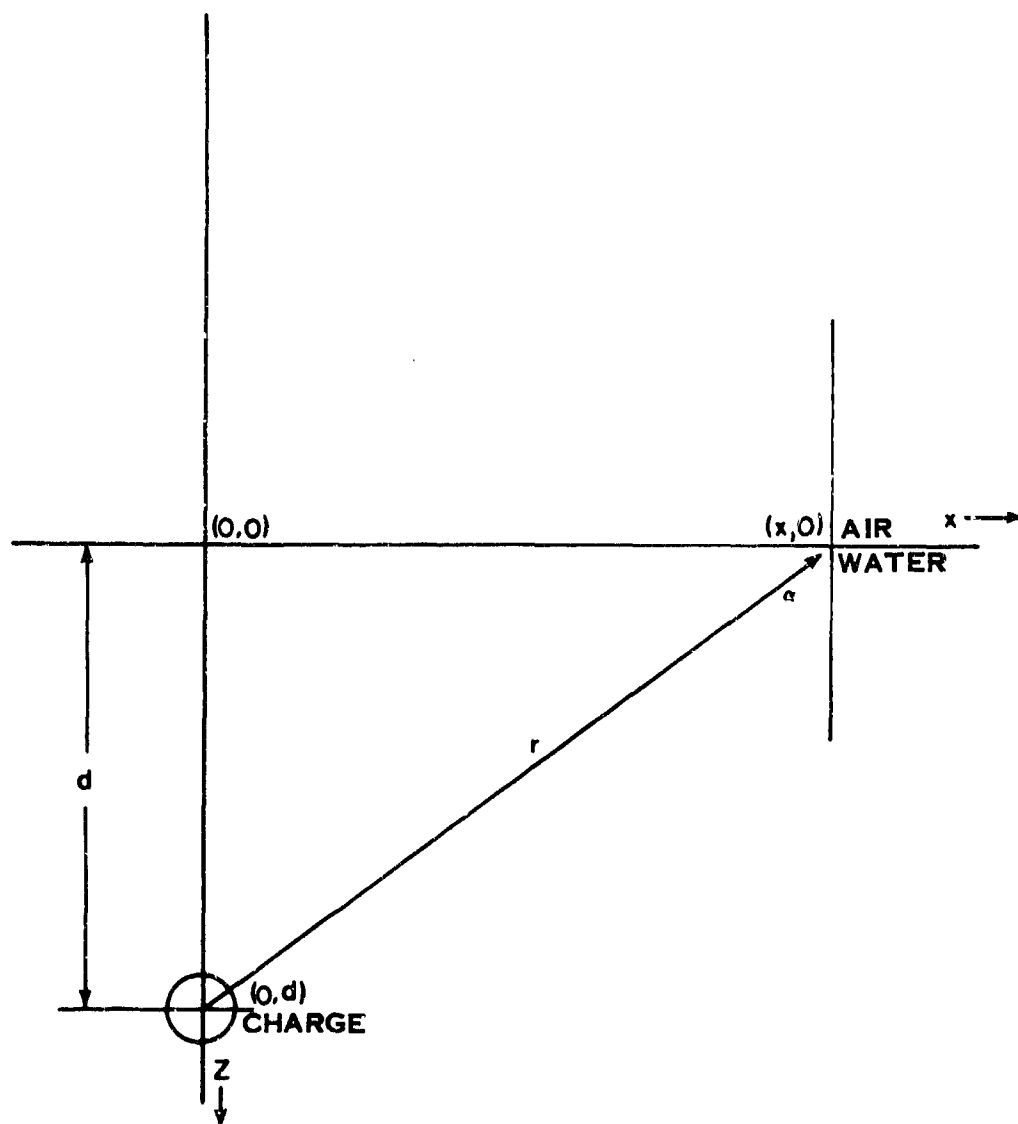
Figure 10. Geometry for analysis of secondary shockwaves under water.

depth d. At the point[*] at surface-zero described by $(x,0)$ the main shockwave from the underwater explosion makes an angle of incidence α.

B. Main Shock Arrival Time

The main shock front from the underwater explosion arrives at the surface at the radius x at the time t_1 expressed by

$$t_1 = r/c_w \tag{85}$$

This can be rewritten in terms of the dimensionless time T and the dimensionless distance X as

$$T_1 \equiv (1 + X^2)^{\frac{1}{2}} \quad ; \tag{86}$$

$$X \equiv x/d \quad ; \tag{87}$$

where

$$T_1 \equiv t_1/t_o \quad ; \tag{88}$$

$$t_o \equiv d/c_w \quad . \tag{89}$$

From equation (87) we see that we are normalizing distances relative to the explosion's depth of burst d; and from equations (88) and (89) we are normalizing times relative to t_o, which is the time at which the explosion's shock front first reaches (in the acoustic approximation) surface-zero. The shock front arrival time T_1 is plotted as a function of the dimensionless horizontal distance X in figure 11.

We emphasize that the dimensionless time T as used in this 3-dimensional analysis is normalized differently from the dimensionless time T employed in Section IV.

---

[*]Actually, because of circular symmetry, this is a circular ring.

48

Figure 11. Dimensionless time of arrival T_1 of main shockwave, and dimensionless time of closure T_c of cavitation--as a function of dimensionless distance X from surface-zero. Time of closure is plotted for two charge weights--10 pounds and 10 kilotons--each burst at the cube-root-scaled depth λ_d of 0.5.
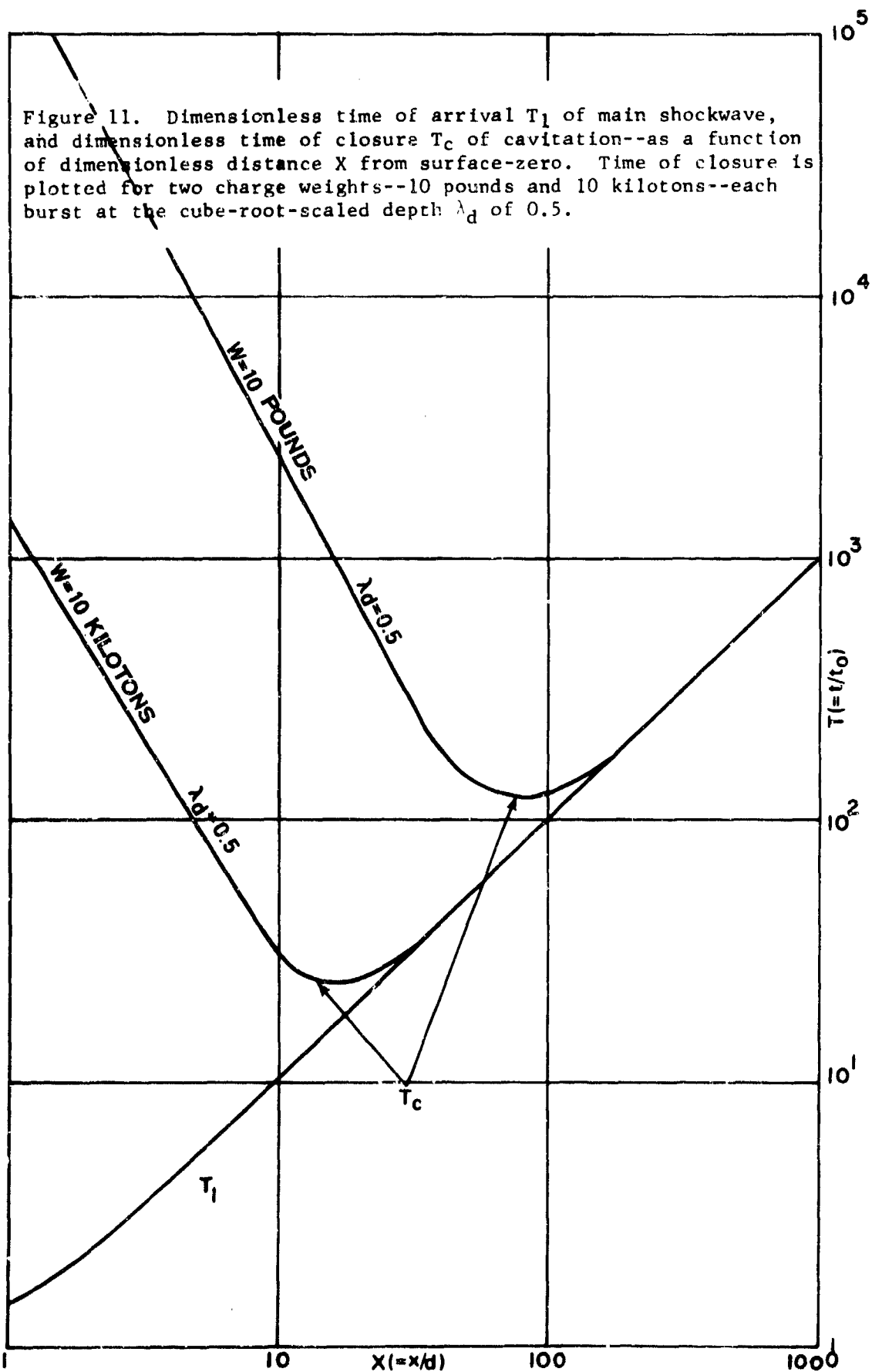
C.   Spall Launch Velocity

When the underwater shock front arrives at the water surface, a spall is formed and is launched upward with a velocity twice the vertical component of the particle velocity in the incident shockwave [(see the discussion leading to equation (60) in Section IV)], that is, the water spall is launched upward with a velocity u_s described by

$$u_s = 2KW^{1/3}d/\rho_w c_w r^2 \qquad , \qquad (90)$$

where $\rho_w c_w$ is the specific acoustic impedance for water, and where we have made use of equation (83).

D.   Spall Flight Duration

Under our assumption of a ballistic trajectory for the water spall (and, ignoring the column or blow-out due to the bubble, which may be significant near surface-zero), the spall will return to its original position (i.e., the spall will close) after a time interval t_s expressed by

$$t_s = t_{so}/(1 + X^2) \qquad (91)$$

where

$$t_{so} = 2u_o/g \qquad (92)$$

and where

$$u_o = 2KW^{1/3}/\rho_w c_w d \qquad . \qquad (93)$$

In the above expressions, u_o is the initial spall velocity at surface-zero, and t_{so} is the spall flight time at surface-zero. If we normalize equation (91) rela-

tive to t_o [in the same manner as we did in equation (88)] we obtain

$$T_s = T_{so}/ (1 + X^2) \qquad , \qquad (94)$$

where

$$T_{so} = t_{so}/t_o \qquad , \qquad (95)$$

or

$$T_{so} = 4KW^{1/3}/g\rho_w d^2 \qquad . \qquad (96)$$

In terms of scaled depth of burst λ_d, this can be written

$$T_{so} = \frac{4K}{g\rho_w W^{1/3}\lambda_d^2} \qquad , \qquad (97)$$

Where

$$\lambda_d \equiv d/W^{1/3} \qquad . \qquad (98)$$

Equation (97) is plotted in figure 12 for charge weights of 1 pound and 1 kiloton.

E. Spall Closure Time

The spall returns to its original position (i.e., the cavitation closes) at a time t_c expressed by

$$t_c = t_1 + t_s \qquad . \qquad (99)$$

If we define the dimensionless closure time T_c by

$$T_c = t_c/t_o \qquad , \qquad (100)$$

Figure 12. Dimensionless characteristic time T_{so} as a function of cube-root-scaled burst depth λ_d.
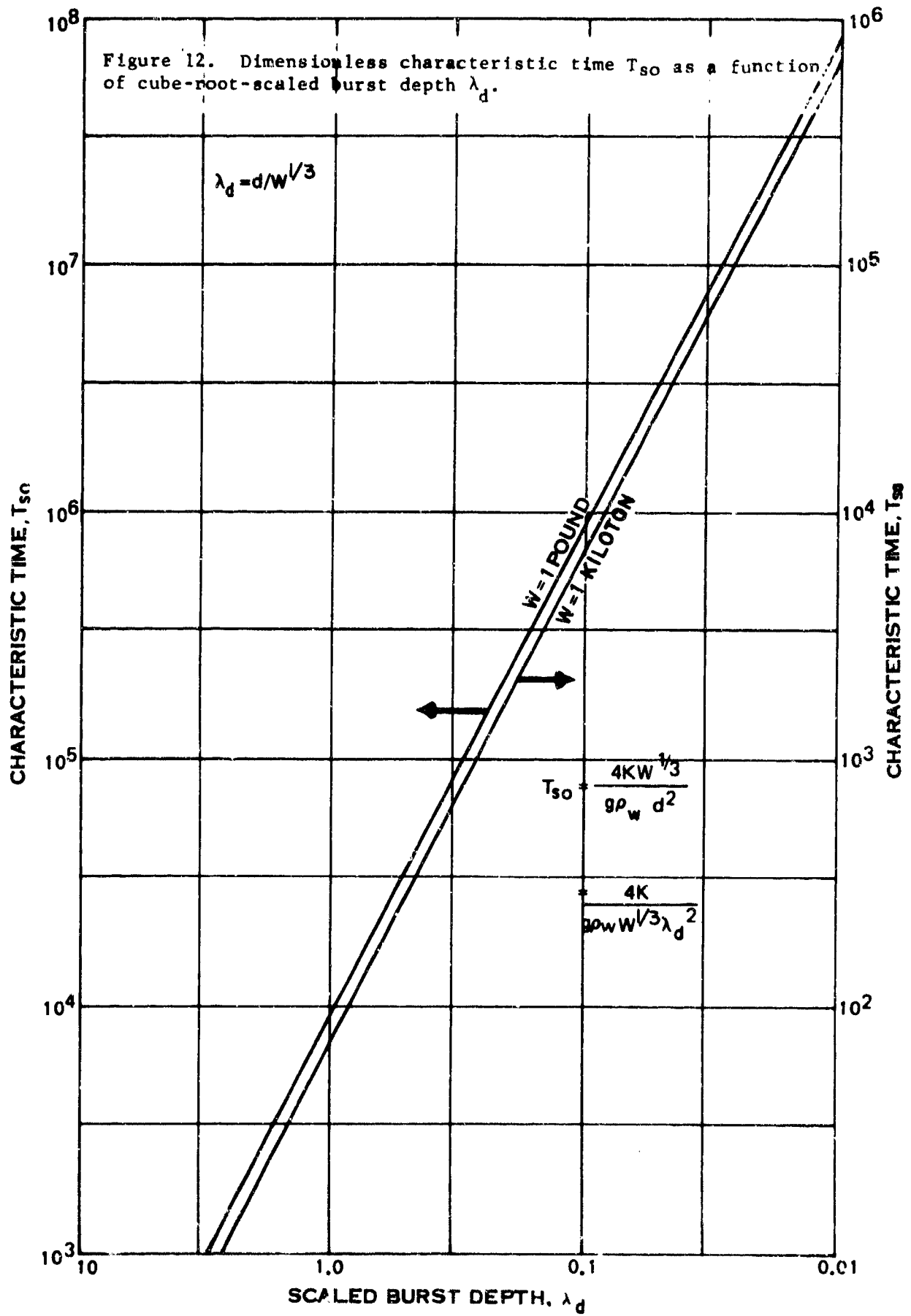
we obtain

$$T_c = (1 + X^2)^{\frac{1}{2}} + T_{so}/(1 + X^2) \quad . \tag{101}$$

F.   Radius and Time of First Closure

The spall does not close (i.e., return to its original position) simultan-
eously for all values of horizontal distance X.   To find the dimensionless dis-
tance X_{cl} where the spall first closes, we set the derivative of T_c equal to zero
in equation (101) and find

$$X_{cl} = \left[(2\ T_{so})^{2/3} - 1 \right]^{1/2} \quad . \tag{102}$$

The time T_{cl} of first spall closure is

$$T_{cl} = \frac{3}{2}\ (2\ T_{so})^{1/3} \quad . \tag{103}$$

For explosion geometries of interest, equations (102) and (103) are excellently
approximated by

$$X_{cl} \quad \simeq \quad (2\ T_{so})^{1/3} \quad ; \tag{104}$$

$$T_{cl} \quad \simeq \quad \frac{3}{2}\ X_{cl} \quad . \tag{105}$$

The radius of first closure X_{cl} is plotted as a function of dimensionless
time T_{so} in figure 13.   We see that cavitation closure first occurs at surface-
zero geometries typified by a T_{so} less than or equal to 0.5.   In figure 11, T_c is
plotted as a function of x for charge weights of 10 pounds and 10 kilotons--each
burst at the scaled depth λ_d of 0.5.   In that graph we see that, in terms of cube
root scaling, the small charge takes considerably longer for its spall, or cavitation,

to close than does the very large charge.[*]

Table I.			
$\lambda_d = 0.5$			
Charge Weight	T_{so}	X_{c1}	T_{c1}
10 pounds	260,000	80	120
10 kilotons	2,080	16	24

Table I provides examples of the values of the characteristic time T_{so}, and the radius and time of first cavitation clo... , X_{c1} and T_{c1}

---

[*]Since both the time and distance are cube root scaled in the same fashion, the dimensionless variables plotted in figure 10 show the correct relationship.

G.   Travelling Closure Point

The cavitation first closes at the radius X_{cl} at time T_{cl}, as described above. Thereafter, as described by equation (101), for each value of dimension-less closure time T_c there are two values of dimensionless distance X. In other words, for each T_c greater than T_{cl}, the cavitation is just closing at two dif-ferent values of horizontal distance X--and as shown in figure 14, one of the X values is greater than X_{cl}, while the second value of X is less than X_{cl}.

As described by equation (101), then, the closure points X are a function of the time T_c. The dimensionless velocity M_c with which these two closure points move--one moves radially inward while the other moves radially outward--are given by

$$M_c \equiv dX/dT_c \qquad , \qquad (106)$$

$$= \frac{(1 + X^2)}{X \left[(1 + X^2)^{3/2} - 2 T_{so} \right]} \quad . \qquad (107)$$

The dimensionless velocity M_c defined by equation (106) is, it turns out, equal to the mach number at which the closure point is moving, i.e., it is the velocity at which the closure point is moving divided by the speed of sound in water. In-spection of equation (107) shows that the outward traveling closure point is al-ways traveling supersonically and asymptotically approaches mach 1. The inward traveling closure point is traveling at a very large mach number (a negative mach number in equation (107) implies that the closure point is the inward traveling

Figure 13. Dimensionless radius of first cavitation closure X_{c1} and radius of Mach 1 closure rate X_{-1} as a function of dimensionless time T_{so}.
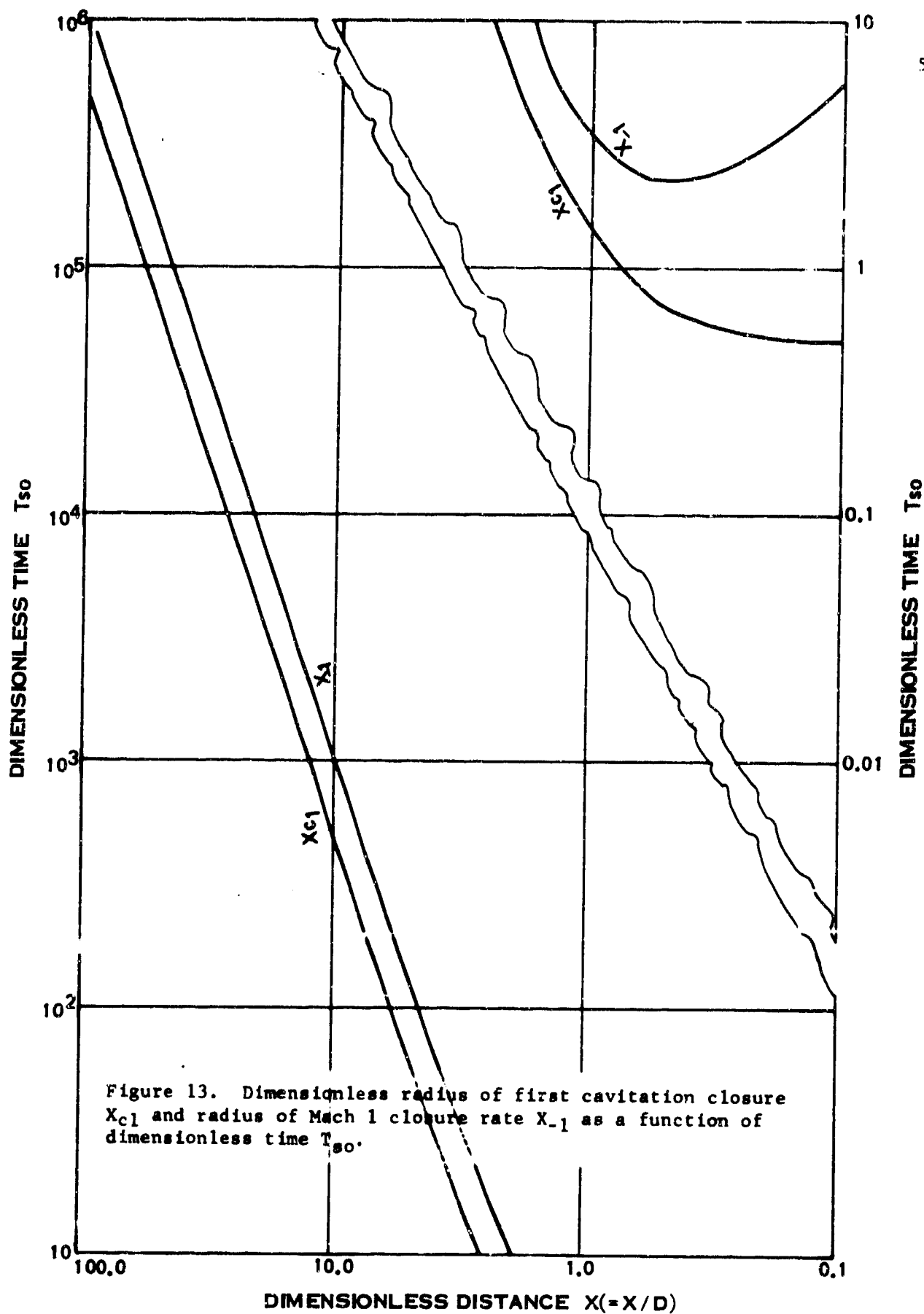
one) at or near the point of first closure X_{c1} and progressively decreases in magnitude.

For certain explosion configurations--that is, for certain values of the dimensionless time T_{so} defined by equation (96)--this closure mach number M_c can fall to a magnitude of unity and less.

For later discussion in this section, we will find that the horizontal distance X where the closure mach number M_c reaches the value -1 is the place where the secondary water hammer waves due to closure are extremely intense. In figure 13, we plot the values of X_{-1} as a function of the dimensionless time T_{so} where the inward traveling closure mach number has a magnitude of 1. From that curve, it is evident that for each burst configuration, for which T_{so} is typified by a value of 2 or greater, there is a mach 1 closure: (1) very close to surface-zero; and, (2) at a distance somewhat less than X_{c1}, the radius of first closure. For most explosion configurations of interest the second mach 1 closure radius is approximately eighty percent of the radius of first closure.

H.   Generation of Secondary Pressure Waves Underwater

With reference to figure 15 we can investigate the character of the secondary pressure wave or water hammer wave generated by the progressive impacting of the spall, i.e., by the progressive closure of the cavitation. We assume that closure takes place at a depth z_c, and that the impact velocity of the spall is u_c. When the spall impacts the underlying quiescent water, the required matching of particle velocity at the interface indicates that the particle velocity in the spall falls to $u_c/2$, as indicated in figure 15. The pressure front of the secondary wave generated by this progressive point of closure is the mach wave. If the velocity of the progressive closure point is v (and we will henceforth neglect the minus sign for the velocity, since we are principally concerned with the
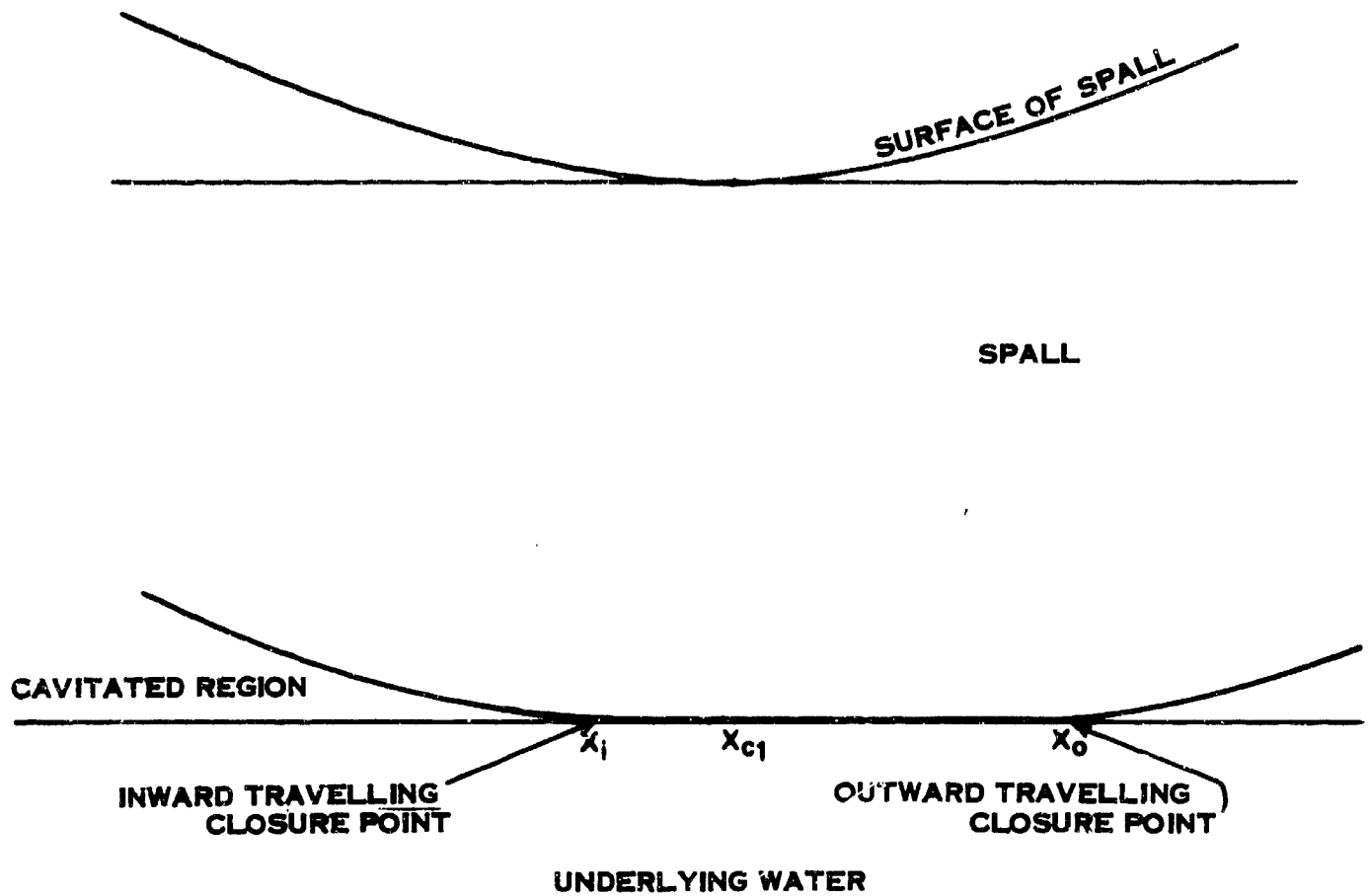
Figure 14. Geometry showing surface spall that has closed along the line extending from X_i to X_o. The spall first impacted at the radius X_{c1}; thereafter, the spall closure point travels in both directions--radially outward and radially inward.
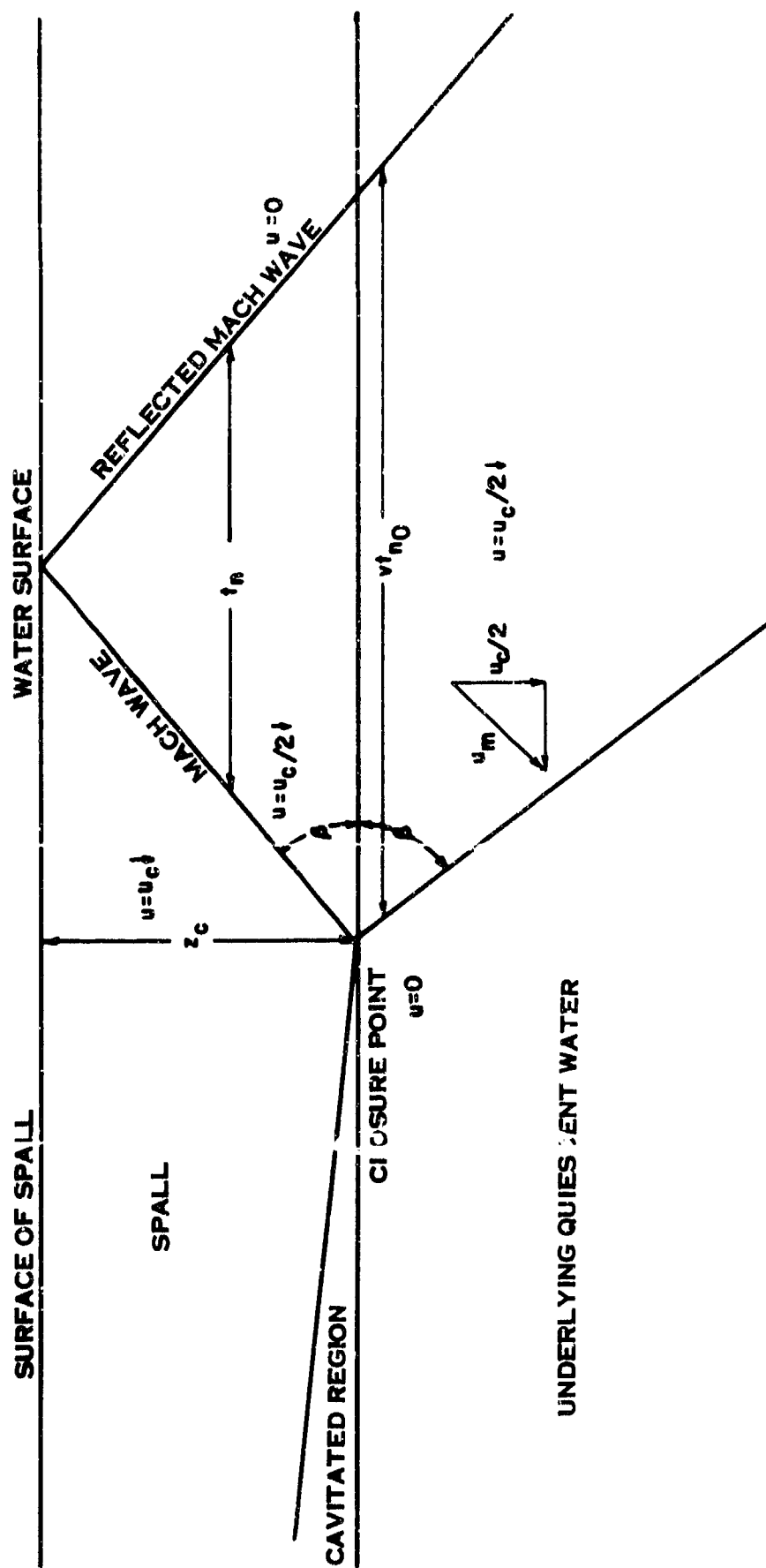
Figure 15. Water-hammer Mach wave due to the inward traveling closure point.

inward traveling closure point), and if the speed of sound in water is c_w, then the mach number of the closure point is described by

$$M_c = v/c_w \qquad . \qquad (108)$$

The angle β of the mach wave, as indicated in figure 15, is given by

$$\sin \beta = M_c^{-1} \qquad . \qquad (109)$$

The change in vertical component of particle velocity across this mach wave is $u_c/2$; hence, the normal component of particle velocity change, u_n, across the mach wave is expressed by

$$u_n = \frac{M_c u_c}{2(1 - M_c^2)^{\frac{1}{2}}} \qquad . \qquad (110)$$

I.   Secondary Wave Pressure

The pressure rise p_n across the mach front is, in the acoustic approximation,

$$p_n = \rho_w c_w u_n \qquad , \qquad (111)$$

$$= \frac{M_c \rho_w c_w u_c}{2(1 - M_c^2)^{\frac{1}{2}}} \qquad . \qquad (112)$$

From equation (112) we see that at the point of first closure, where the mach number is indefinitely large, the hammer pressure p_n generated at the time of cavitation closure has the magnitude $\rho_w c_w u_c/2$, where u_c (see Section IV, equation 63 et seq) is the velocity of the spall at the time of cavitation closure. We also see that the hammer pressure p_n becomes indefinitely large at the radius X_{-1} where the mach number M_c of the closure point falls to a magnitude of unity.

60

J. Secondary Wave Duration

From figure 15 we see that the upward traveling mach wave reflects from the free surface. After this reflection, the vertical component of particle velocity of the (erstwhile) spall is finally reduced to zero. The surface reflected wave will reach the closure depth z_c at a time after closure expressed by

$$t_{no} = \frac{2z_c \, (M_c^2 - 1)^{\frac{1}{2}}}{c_w M_c} \qquad . \qquad (113)$$

If a pressure sensor is located at a depth z_c or greater, the duration of the (flat topped) water hammer pressure p_n is equal to t_{no}. If the sensor is at a depth less than z_c, the duration is proportional to depth. In other words, the water hammer pressure duration t_n is

$$t_n = \frac{2z_c \, (M_c^2 - 1)^{\frac{1}{2}}}{c_w M_c} \qquad \text{for } z \geq z_c \qquad (114)$$

$$= \frac{2z \, (M_c^2 - 1)^{\frac{1}{2}}}{c_w M_c} \qquad \text{for } z \leq z_c \qquad . \qquad (115)$$

In an experimental situation, gages are placed along a string at various depths z. Observing among these gages the relative times of first arrival of the secondary pressure wave, and also observing the duration of the secondary pressure pulse, offers a means of establishing the depth z_c at which cavitation closure occurs. Such variable duration, flat-topped pressure pulses can be seen in the bulk cavitation experimental data included in Walker's[9] report.

---

[9] loc. cit

K.   Secondary Wave Impulse

The impulse I_n in the secondary pressure wave is given by

$$I_n = P_n t_n \qquad . \tag{116}$$

The value of the impulse is

$$I_n = \rho z_c u_c \qquad \text{for } z \geq z_c \tag{117}$$

$$= \rho z u_c \qquad \text{for } z \leq z_c \qquad . \tag{118}$$

For depths below the closure depth z_c, the impulse I is seen from equation (117) to be simply the impacting spall's momentum per unit area.

The region most important for the generation of intense secondary pressure waves is the region contained within the radius of first impact X_{c1}, that is, the radius at which cavitation first closes. The reason for this is twofold: (1) the spall closure velocity u_c can be quite large within this region; and (2) the closure mach number M_c can, with explosions configurations of interest, reach a magnitude of 1 with the consequent pressure "amplification" described by equation (112). Beyond the radius of first cavitation closure, the closure point asymptotically approaches a mach number of 1, that is, this pressure "amplification" is achieved only at very large distances from surface-zero. But, at these very large distances the spall closure velocity u_c is quite small.

L.   Example

To demonstrate the use of information developed in Sections IV and V, let us consider a 10 kiloton explosion burst at a depth of 150 feet. We seek to determine:

(1)   The radius x_{c1} where cavitation closure first takes place;

(2)   The time t_{c1} when cavitation first closes;

(3) The radius x_{-1} where the closure velocity reaches mach 1, i.e.,

where the pressure wave due to cavitation closure is most intense.

Using equation (89), we find that, in the acoustic approximation, the shock front first reaches surface-zero at the time t_o given by

$$t_o = 150/5000 = 0.030 \text{ seconds}.$$

To compute the dimensionless time T_{so} in equation (96) when the charge weight W is expressed in kilotons, the constant K [see equation (84)] is

$$K = 2.88 \times 10^8 \qquad .$$

We then find from equation (96) that the dimensionless time T_{so} is

$$T_{so} = 1700 \qquad .$$

From equation (102) we find that the cavitation first closes at the dimensionless radius X_{c1} given by

$$X_{c1} = \lfloor (3400)^{2/3} - 1 \rfloor^{1/2} = 15 \qquad ,$$

and from equation (103) we find that the spall first closes at the dimensionless time T_{c1}

$$T_{c1} = 22.5 \qquad .$$

The actual radius of first cavitation closure, x_{c1}, is

$$x_{c1} = (150)(15) = 2,250 \text{ feet} \qquad ,$$

and the actual time of first cavitation closure, t_{c1}, is

$$t_{c1} = (0.030)(22.5) = 0.675 \text{ seconds} \qquad .$$

These values of closure radius and time have been determined under the assumption that atmospheric pressure is negligible compared with the gravitational

body force acting on the spall. In the language of Section IV, this approximation
is good provided the dimensionless wavelength P_L is very large compared with unity.
In the present example, we shall see in a moment that P_L is 50 at the above-
computed radius x_{c1}. From equation (59), we see that our above-computed value of
T_{so}, as a second approximation, should be multiplied by $(1 - 2P_L^{-\frac{1}{2}})$; in this
instance, our above-computed value of T_{so} should therefore be multiplied by 0.72.
Thus, as second approximations, we have

$$T_{so} = 1230 \qquad ;$$

$$x_{c1} = 2000 \text{ feet} \qquad ;$$

$$t_{c1} = 0.6 \text{ seconds} \qquad .$$

The radius x_{-1} at which the cavitation is closing at mach 1, and where the
secondary pressure due to closure is a maximum is, for this size explosion, about
80 percent of the radius of first closure, i.e., we have

$$X_{-1} = 1600 \text{ feet} \qquad .$$

At the radius of 2,000 feet from surface-zero, the angle of incidence α is

$$\alpha = \arccos (0.07) \qquad .$$

The wavelength λ for the exponential wave is approximately expressed by

$$\lambda = 53.5 \ W^{1/3} = 115 \text{ feet} \qquad ,$$

so that the modified wavelength L, employing equation (27), is

$$L = \lambda/\cos \alpha = 1,650 \text{ feet} \qquad ,$$

and the dimensionless wavelength P_L, using equation (30), is

$$P_L = 50 \qquad .$$

To find the dimensionless closure depth Z_c, we employ equation (50), which is
plotted in figure 8. We find Z_c to be

$$Z_c = 0.12? \qquad .$$

64

The actual depth of closure z_c is

$$z_c = (1,650)(0.135) = 220 \text{ feet} \quad .$$

From equation (83) we find the peak pressure p_o in the incident shockwave at the 2,000 foot radius is

$$p_o = 2,000 \text{ psi} \quad ,$$

and the peak surface velocity is

$$u(x_{c1},0) = \frac{2p_o}{\rho c} \cos \alpha = 4 \text{ feet/second} \quad .$$

The dimensionless depth of onset Z_o is, using equation (48)

$$Z_o = 0.0045 \quad ,$$

so that the actual depth of cavitation onset z_o is

$$z_o = 7.43 \text{ feet} \quad .$$

If we are interested in the dynamics of the spall motion, we can use the results tabulated in the Appendix. On page 45 of the Appendix, the pertinent variables have been tabulated for a wavelength of 1,333 feet; on page 46, they have been tabulated for a wavelength of 1,778 feet. The modified wavelength L for our situation at 2,000 feet from surface-zero has been seen above to be $L = 1,650$ feet. As an approximation, let us use the data on page 46 of the Appendix. The peak pressure, as we have computed above, is 2,000 psi. In order to use the tables in the Appendix, we must compute [see equations (35), (38), (42)] the "vertical component of pressure," i.e. we need to know p_v

$$p_v = p_o \cos \alpha = 140 \text{ psi} = 0.14 \text{ Kpsi} \quad .$$

From page 46 of the Appendix, we see that the maximum surface excursion z_{max} is

$$z_{max} = 8.94 \ (0.14)^2 = 0.175 \text{ feet} \quad .$$

Also from page 46 of the Appendix, we note that the closure depth is 231 feet, in good agreement with the value we have computed above--recalling that our actual modified wavelength is 1,650, whereas the table we are using has a modified

wavelength of 1,778 feet. Next, from the information on page 46 of the Appendix, we find that closure takes place t_c seconds after arrival of the incident shock-wave, where t_c is

$$t_c = (1.38)(0.14) = 0.19 \text{ seconds.}$$

Since the incident shockwave arrives at the 2,000 foot horizontal distance at about 0.4 seconds after initiation of the explosion, we see that our above-described value of $t_c = 0.19$ seconds is in agreement with the value of t_{cl} of 0.6 seconds computed earlier.

It is to be noted that a spall which is launched at 4 feet per second will complete its trajectory at approximately 0.25 seconds if it is acted upon by gravity alone. The above computed value for flight time of 0.19 seconds indicates that, at this modified wavelength of 1778 feet, the average acceleration acting on the spall is somewhat greater than one g. In our earlier calculation of spall closure time-- including the transit time for the incident shockwave, we corrected for this increased average effective acceleration when we multiplied by the factor $(1 - 2P_L^{-\frac{1}{2}})$.

In the remainder of the table on page 46 of the Appendix, we see that the time in the first column has been normalized relative to the closure time--computed above to be 190 milliseconds. The spall thickness as a function of time, shown in the second column, is normalized to the closure depth of 231 feet. The surface position as a function of time, shown in the third column, is normalized relative to the maximum surface excursion--computed above to be 0.175 feet. The surface velocity as a function of time, shown in the fourth column, is normalized to the vertical component of particle velocity in the incident shockwave--computed above to be 2 feet/second (note: 4 feet/second is the initial surface velocity--equal to twice the vertical component of particle velocity in the incident shockwave). The surface acceleration as a function of time, shown in the fifth column, has

been normalized relative to the acceleration of gravity, 32.2 feet per second. The lower cavity boundary as a function of time, shown in the sixth column, has been normalized relative to the closure depth of 231 feet.

The computations tabulated in the Appendix have been carried out in the high pressure limit analysis--that is, we have assumed that the peak pressure in the incident shockwave is large compared with $\rho g \lambda$, and large compared with atmospheric pressure. With these assumptions, the onset of cavitation takes place at zero depth. During these initial stages, the spall is of infinitesimal thickness so that the body force due to gravity acting on it is negligible compared with the finite atmospheric pressure acting on the topside. Accordingly, when the spall thickness is virtually zero, the acceleration of the spall is unbounded, as indicated in the fifth column.

We have already calculated in our example that cavitation sets in at a depth of 7.43 feet. The dimensionless depth of onset, normalized to the closure depth of 220 feet is 0.0338. Hence, the data contained on page 46 of the Appendix would be considered credible only after the spall thickness has achieved this value. For example, from page 46 of the Appendix, we would expect surface acceleration initially observed to be in the neighborhood of 4 gees.

At this very early time, the final column on page 46 of the Appendix would indicate that the lower cavity boundary is at a normalized depth of 26, or an actual depth of about 6,000 feet. Since the radius from the burst point is 2,000 feet, the indicated lower cavity boundary of 6,000 feet would assuredly not satisfy the requirement that [see equation (79)] the quantity $(z/r_x)^2$ be small compared with unity. Hence, at these early times the plane wave spall dynamic analysis cannot be used as an approximation in describing the dynamics of the lower cavity boundary.

VI. EFFECTS ON AIR BLAST

Pittman[10] describes the air blast from underwater explosions in a set of experimental programs where the explosive yield ranged from 8.6 to 10,000 pounds. He further compares these HBX shots with data from nuclear underwater shots Baker (Operation Crossroads) and Umbrella (Operation Hardtack).

The indication is that cube root scaling holds over the range of HE charge weights used; however, attempts to extend cube root scaling into the kiloton range were not successful: Umbrella produced lower than predicted air blast pressures, while Baker yielded higher than predicted air blast pressures.

Pittman has identified three principal air blast pulses (see figures 22 and 23): (1) the direct, ray-acoustic pulse, denoted as the P_1 pulse; (2) a pressure pulse diffracted into the air from the neighborhood of surface-zero, denoted as the P_2 pulse; and (3) a pressure pulse generated in the neighborhood of surface-zero by the water column or blow-out of the bubble, denoted as the P_3 pulse. The first two pulses would appear to arise from a common mechanism, namely, motion of the boundary, i.e., motion of the water surface. In this section, we will concentrate on blast waves in the air due to this mechanism, that is, we shall concentrate on the mechanisms for production of the P_1 and P_2 pulses.

These two pulses in many ways are similar to the two air-pressure pulses shown in the work of Towne and Arons[11]. The magnitude and arrival time of the P_1 pulse in the air is correctly described by their acoustic analysis; however, the

---

[10] J. F. Pittman, "Air Blast from Shallow Underwater HBX-1 Explosions (U)," Naval Ordnance Laboratory Report 68-45, April 3, 1968.

[11] D. H. Towne and A. B. Arons, "On the Acoustical Theory of Transmission of a Spherical Blast Wave from Water to Air," Woods Hole Oceanographic Institution Reference No. 56-61, August, 1956.

68

size (i.e., the impulse) of the P_2 pulse in their acoustic analysis is decidedly

too small (perhaps by as much as 1 or 2 orders of magnitude) for most explosion

configurations of interest. The analysis in this section would seem to indicate

that the acoustic boundary conditions used by Towne and Arons are responsible for

the unrealistically small size of the P_2 pulse which they obtain.

The acoustic boundary condition implies a linear stress-strain relationship

in the water. For shockwave profiles typical of underwater explosions, the acoustic

boundary condition consequently requires the production of unrealistically large

tensile stresses beneath the water surface. From the foregoing sections, we know

that the air/water interface does not move in accord with the acoustic boundary

conditions when forced by an underwater explosion; rather, a layer of the water

surface spalls upward, leaving a low density or cavitated region underneath.

A thorough analysis of the air blast wave produced by motion of the water

surface requires a diffraction analysis, which is beyond the scope of this bulk

cavitation endeavor. However, if for the present we limit ourselves to air blast

waves at or very near to the water surface, we are able to obtain results--taking

bulk cavitation into account--that agree with the air blast signatures at low

altitude, as described in Pittman's report.

In describing air blast from an underwater explosion using the acoustic

approximation, Towne and Arons[12]:

(1) used the classical wave equation in the water and also in the
    overlying air;

(2) at the interface--that is, the water surface--required that the wave
    equation solutions in the air and in the water match in pressure and
    in normal component of particle velocity; and

---

[12]ibid

(3) assumed a wave shape from an underwater explosion which consists of a shock rise to peak pressure p_o followed by an exponential tailoff with time constant τ (or wavelength $\lambda = c_w\tau$, where c_w is the speed of sound in water).

A. Spalled Interface

Since the solution to the wave equation in the air is determined completely by the boundary conditions, it is instructive to notice the difference in boundary motion for (1) the already analyzed acoustic interface assumption, and (2) the spalled interface assumption. Figures 16 and 17 show the characteristic velocity-time behavior for the acoustic interface and for the spalled interface. Figure 16 shows that in the acoustic interface the peak surface velocity is u_s, where u_s is twice the vertical component of particle velocity at the front of the underwater shockwave as it reaches the point in question on the surface. The time constant (i.e., the time it takes for the peak surface velocity to fall to $1/e$ of its peak value) is equal to τ.

Spalled water surface motion is shown in figure 17. The initial surface velocity is again u_s; but now it takes much more time for the surface position to return to zero. As we have discussed, a good approximation (especially when inequality (80) is satisfied) is that the spalled water surface falls back to its starting point under the action of gravity alone; under this assumption, the duration of the surface motion is the order of $2u_s/g$. A somewhat better approximation is that the spalled water surface is forced back downward additionally by the overlying atmospheric pressure. With this taken into account, the spalled surface decelerates initially at a value greater than g (see the tabulations for short wavelength in the Appendix). This is shown by the dotted curve in figure 17.
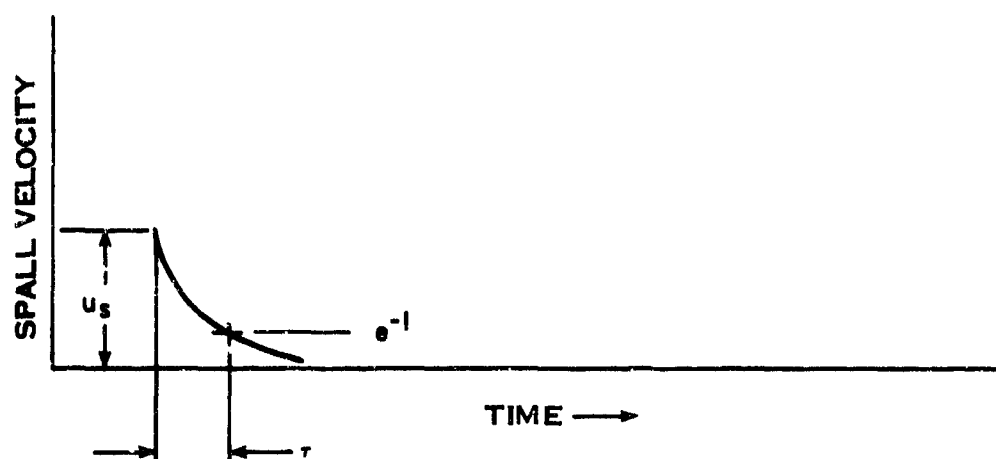
Figure 16. Velocity-time behavior for an acoustic interface.
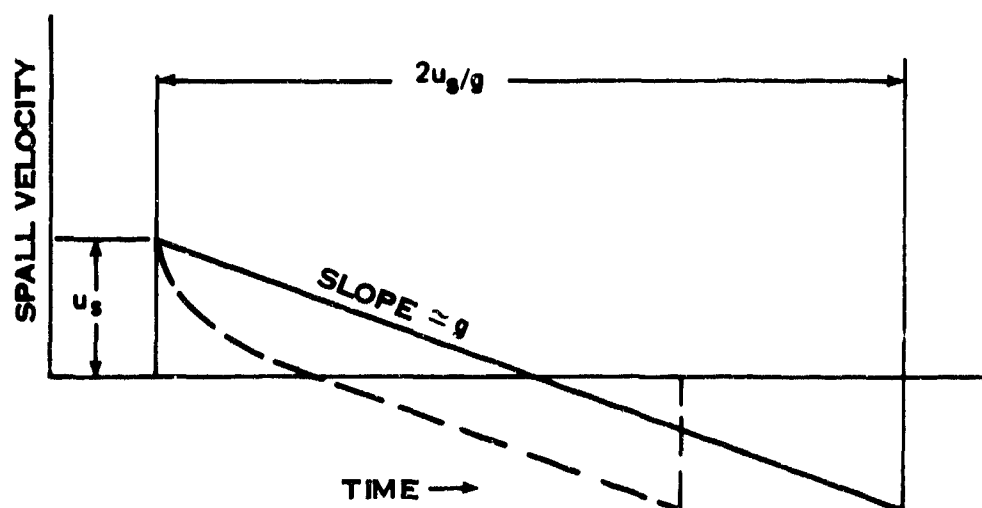
Figure 17. Velocity-time behavior for a cavitated interface with surface spallation.

Both the acoustic interface and the spalled interface produce the same initial value of surface velocity, namely u_s, as indicated in figures 16 and 17, and described in equation (90). For this reason, the spalled interface assumption will yield the same peak value for the P_1 wave as that obtained by the acoustic approximation, in agreement with the data produced and discussed by Pittman.

The P_2 air blast pulse discussed by Pittman--that is, the pressure wave diffracted into the air due to surface motion in the neighborhood of surface-zero-- will have inordinately larger magnitude for the long-duration N-wave surface motion typified by figure 17 when compared with the P_2 wave produced by the very short duration--relatively impulsive--motion typified by figure 16.

B. Highlights of Towne and Arons' Analysis

Figure 18 shows the geometry of the air blast problem. A charge of weight W is burst at a depth d below the water surface. We are interested in describing the pressure-time curve for the air blast at the point (x,z). Because of assumed symmetry about the vertical passing through the charge, the coordinate x is the horizontal radius from surface-zero, while the coordinate-z is the altitude above the (undisturbed) water surface.

Figure 19 shows Towne and Arons' pressure versus time curve in air at the water surface for a charge which is burst at the dimensionless depth η of 0.5; and for angles of α (see figure 18) of 15° and 60°. The dimensionless depth η is measured in wavelengths of the assumed exponential underwater shockwave; in other words

$$\eta = d/c_w \tau \qquad (119)$$

where d is the depth of burst; c_w is the speed of sound in water; and τ is the time constant of the pressure wave in the water, assumed to be of the form

$$p = p_o \exp[-(t - r/c_w)/\tau] \qquad . \qquad (120)$$
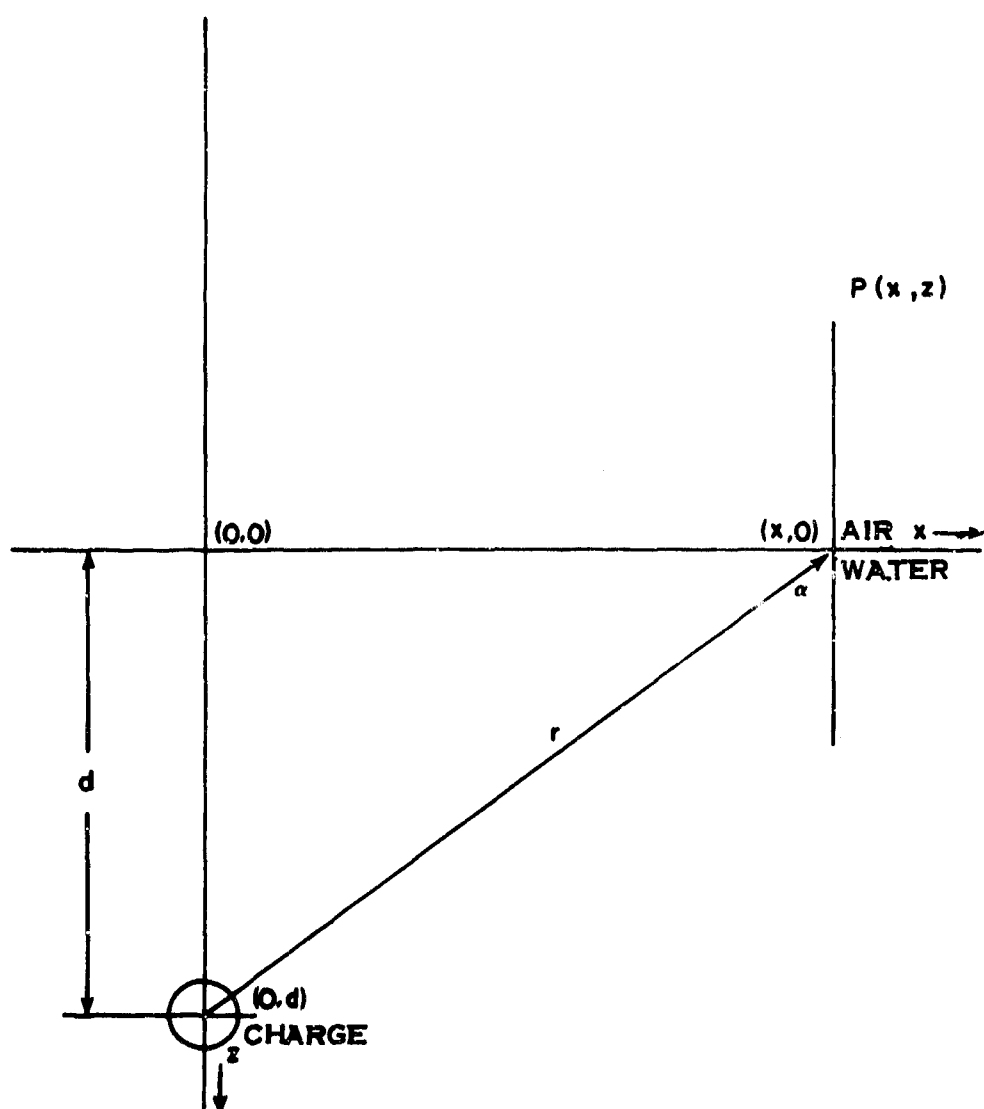
Figure 18. Geometry for the air blast analysis.
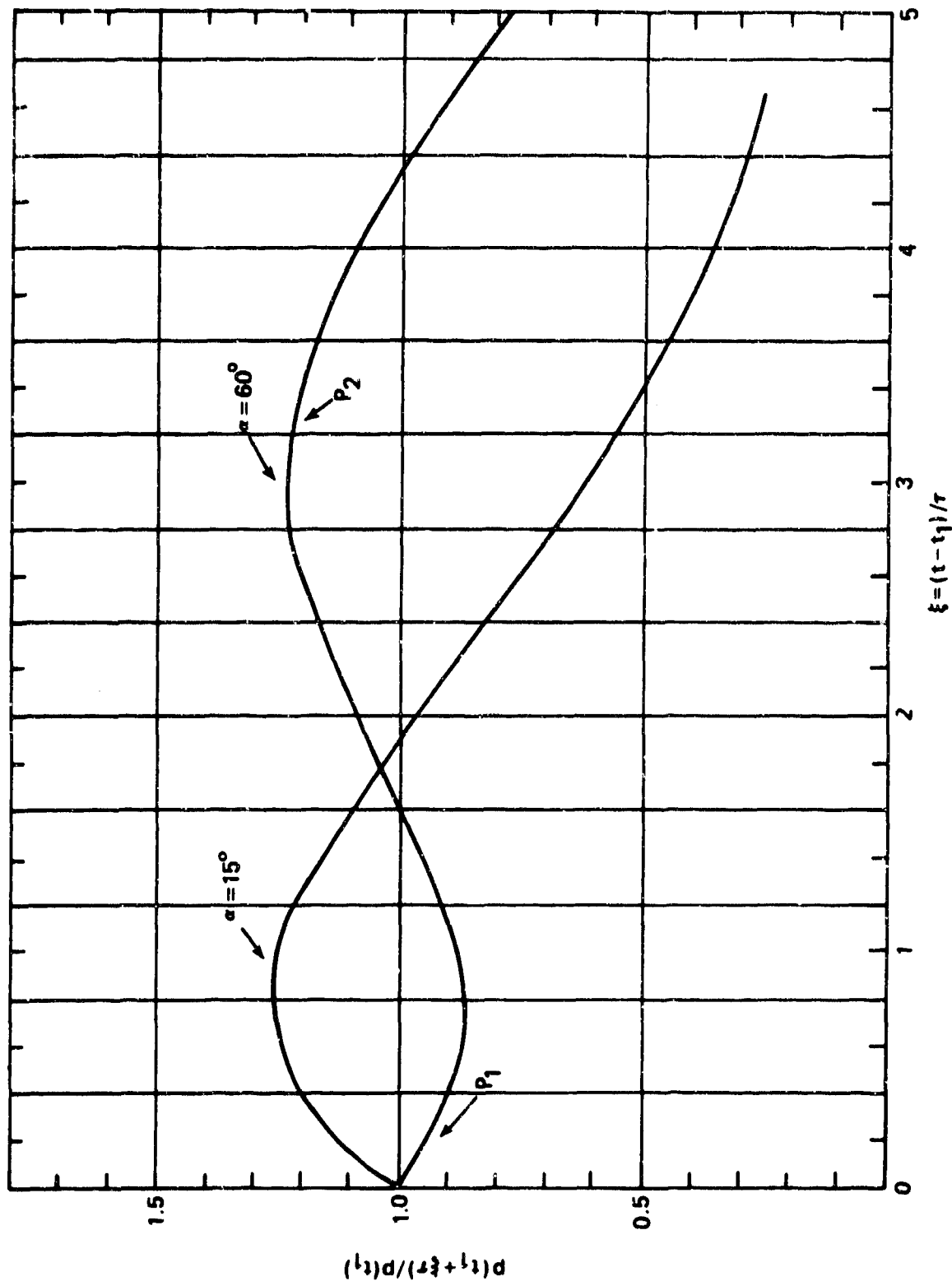
Figure 19. Pressure versus time curves--derived by Towne and Arons, assuming an acoustic interface behavior --at an altitude of zero, dimensionless burst depth $\eta = 0.5$, and various values of α. The first arrival occurs at the time t_1; the pressure at this front is $p(t_1)$. For larger distances from surface-zero ($\alpha = 60^0$), a second wave--the P_2 wave--begins to be discernible as distinct from the first arrival wave, the P_1 wave. Nearer surface-zero ($\alpha = 15^0$), the P_1 wave and the P_2 wave tend to coalesce.

73

Both pressure-time curves in figure 19 are normalized relative to the first arrival pressure front $p(t_1)$, which arrives at time t_1.

Figure 20 shows Towne and Arons' pressure versus time curves in the air at the surface for $\alpha = 60^{\circ}$, and for various values of burst depth η.

From figure 20 we see that as the burst depth η becomes sufficiently deep, the incident shockwave in the water spproaches that of a plane wave as it nears the surface, and therefore the pressure-time curve in the air approaches $e^{-(t-t_1)/\tau}$, i.e., approaches the wave shape of the pressure disturbance in the water. For small values of dimensionless burst depth η we discern that the over-all pressure wave in the air takes on the aspect of two pulses, which can be identified with the P_1 and P_2 pulse described by Pittman. In figure 20 we see the P_1 wave is essentially the first arrival wave, while the P_2 wave arrives somewhat later. In figure 19, for the curve corresponding to $\alpha = 15^{\circ}$ (i.e., a location on the surface rather near surface-zero), we see that the P_1 wave and the P_2 wave tend to coalesce*.

As we retreat further from surface-zero--that is, as $\alpha \rightarrow 90^{\circ}$ --we find from Towne and Arons[13] that:

    (1)   The secondary pulse P_2 takes on the behavior of an isolated arrival occurring at a time equal to x/c_a, where c_a is the speed of sound in air.

---

*Indeed, for a position this close to surface-zero, we can imagine the pressure wave is sufficiently strong so that the rather smooth pressure-versus-time curve might appear more shocked up.

[13]ibid, p. 24

$\xi = (t-t_1)/\tau$
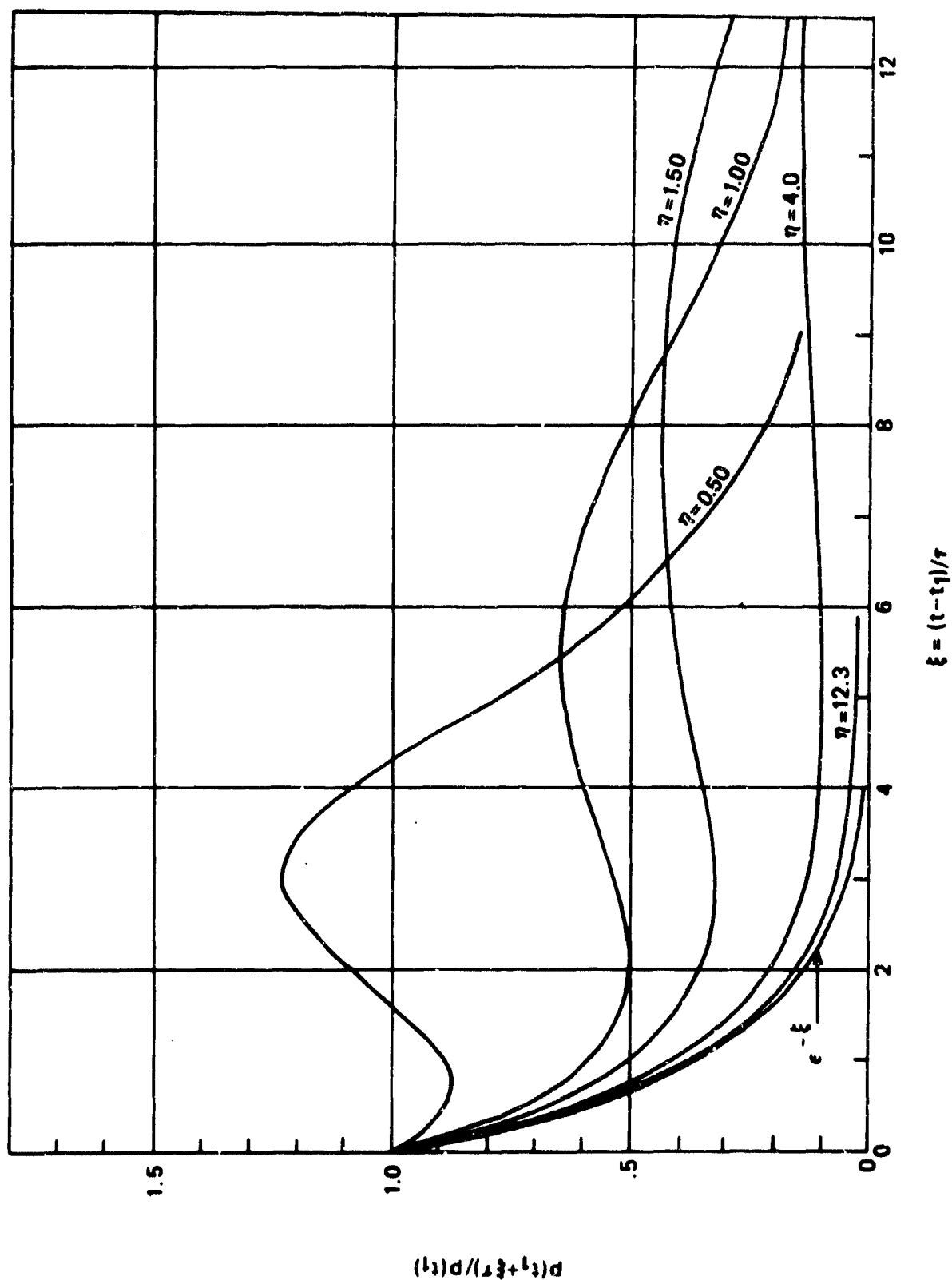
Figure 20. Pressure versus time curves--computed by Towne and Arons, who assumed an acoustic interface behavior--at an altitude of zero, for $\alpha = 60^\circ$, and various values of dimensionless burst depth η. All pressure time curves are normalized relative to the first arrival pressure front $p(t_1)$ which arrives at time t_1. For sufficiently deep burst depths, the incident wave approaches the exponential character of the incident underwater shockwave.

(2) The secondary pulse P_2 becomes predominantly important in comparison with the initial arrival pulse P_1. The initial arrival pulse becomes negligible because the underwater shockwave is incident on the surface at a grazing angle, and the transmission coefficient is small.

(3) The secondary pulse P_2 appears to correspond to waves which propagate as inhomogeneous plane waves through the water, enter the air in the neighborhood of surface-zero, and then propagate through the air as ordinary plane waves.

C. Arrival Time of SZ Diffracted Pulse

In figure 11 of Section V, we have already plotted, as a function of dimensionless horizontal distance X: (1) T_1, which is the dimensionless time of arrival of the main shock front, and therefore is the time at which the spall begins its upward motion; and (2) T_c, which is the dimensionless time of cavitation closure, that is, the time at which the spall completes its trajectory. These are replotted in figure 21; and in addition, we plot T_2, which is the dimensionless time of arrival of the air blast wave diffracted from the neighborhood of surface-zero. To compute T_2, we note that, after the underwater shockwave arrives at surface-zero, the diffracted air blast pulse arrives at a horizontal radius x at a time the order of x/c_a, where c_a is the speed of sound in the air. In other words, the SZ-diffracted pulse arrives at a time t_2 given by

$$t_2 = t_o + x/c_a \qquad , \qquad (121)$$

where t_o is the time (in the acoustic approximation) at which the main shockwave arrives at surface-zero, as described by equation (89) in Section V. Following the format of that section, we define the dimensionless time T_2 as

Figure 21. Dimensionless time of arrival T_1 of main shockwave, dimensional time of closure T_c of cavitation, and dimensionless time of arrival T_2 of surface-zero diffracted air wave--as a function of dimensionless distance X from surface-zero. Time of closure is plotted for two charge weights--10 pounds and 10 kilotons --each burst at the cube-root-scaled depth λ_d of 0.5.
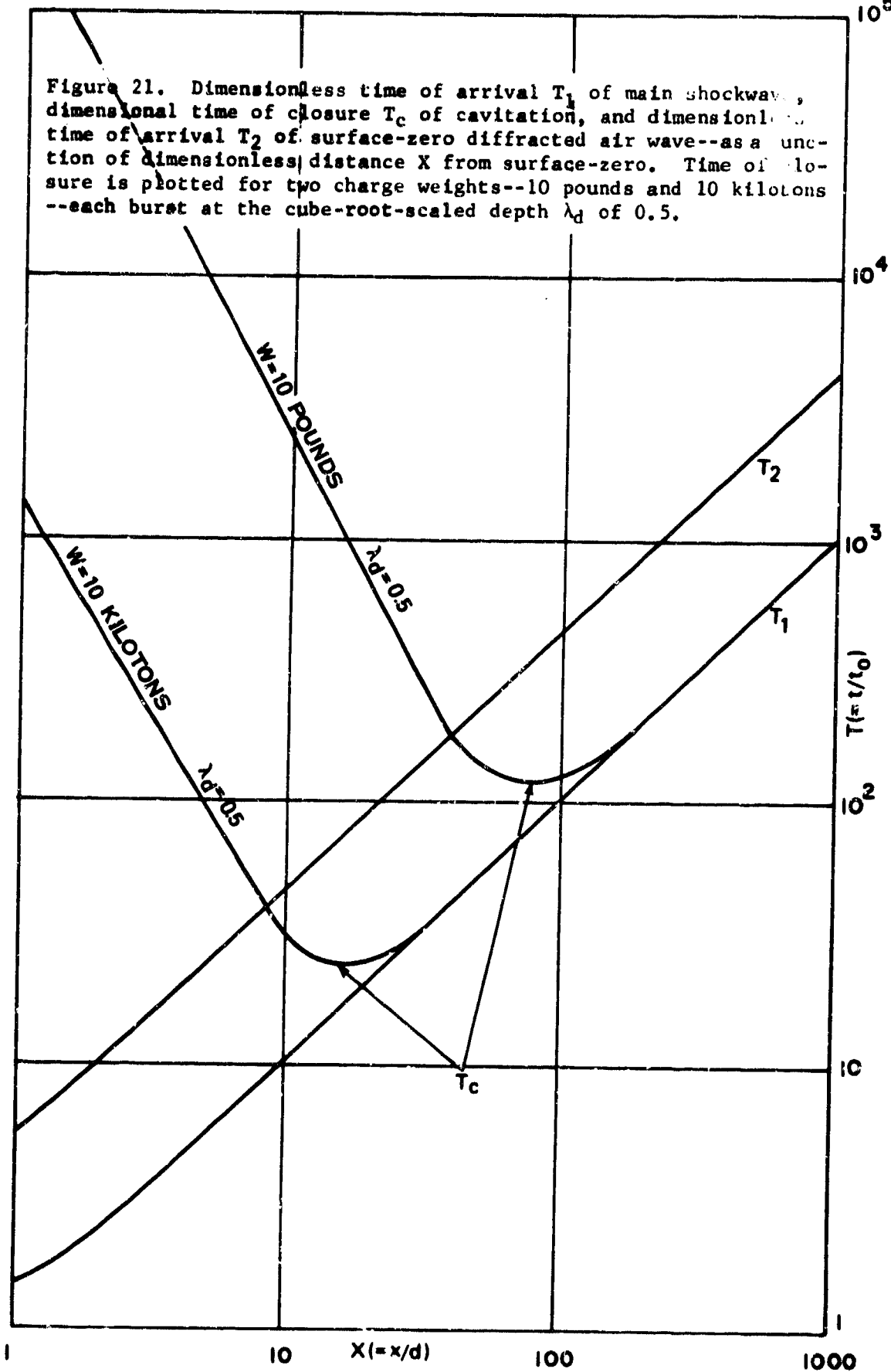
$$T_2 \equiv t_2/t_o \tag{122}$$

so that equation (121) can be written as

$$T_2 = 1 + (c_w/c_a) X \tag{123}$$

where c_w/c_a is the ratio of sound speed in water to that in air and X is the dimensionless horizontal distance defined in equation (75). T_2 is plotted as a function of X in figure 21 for a sound speed ratio of 4.5.

D. Air Blast Pulse Arrival Times

In order to get a general picture of air blast pulse relationships, we have in this section limited ourselves to the acoustic approximation in water and in air; and have assumed that the spalled water surface is acted upon only by gravity. If we restrict our discussion now to locations in the air at or just above the water surface, we can, with the information developed, see the difference in behavior for small charges when compared with large charges.

The first arrival pressure pulse--the P_1 pulse--commences at a time T_1, as indicated in figure 21. For small values of X, dX/dT_1 (which is equal to the mach number in water) is supersonic, i.e., this derivative is greater than unity in the dimensionless plot of figure 21. The derivative asymptotically approaches unity for large values of X.

An upper bound for the conclusion of the P_1 pulse (near the water surface) is the time at which the spall closes. That is to say, the P_1 pulse is over at a time not greater than T_c. More complete diffraction analysis is required in order to sharpen this estimate of the P_1 pulse duration. But it appears that the estimate is adequate provided

$$\frac{dT_c}{dX} \leq 1 \quad . \tag{124}$$

The inequality (124) provides that the locus of the spall closure point is not moving subsonically relative to the speed of sound in water. For example, in figure 21 for the 10 pound T_c curve, our estimate that the P_1 pulse is completed at a time T_c is probably good for values of X greater than about 55. For values less than 55, the locus of spall closure is traveling subsonically, and a more thorough diffraction analysis is required in order to find when the P_1 pulse effectively is concluded.

For the 10 kiloton charge shown in figure 21, our identification of T_c as the termination of the P_1 pulse is probably good for values of X greater than about 12. For values of X considerably less tl.n 12, T_c is an upper bound for the conclusion of the P_1 pulse, but an increasingly poor estimate as X gets considerably smaller than 12. Similar conjectures hold for the 10 pound T_c curve for values of X less than 55.

In figure 21, the T_2 curve indicates the time of arrival of the P_2 pulse, i.e., the air blast pulse which is diffracted from the neighborhood of surface-zero. If our air blast gage is located near the surface at the dimensionless distance 15 ($\approx$X) from surface-zero, we see that, for the large 10 kiloton charge, the P_2 pulse arrives after T_c, i.e., after the completion of the P_1 pulse. On the other hand, for the 10 pound charge at the same scaled burst depth of 0.5, we see that the P_2 pulse arrives while the P_1 pulse is still extant.

E. Comparison With Experiment

Figure 22 is identical with figure 94 of Pittman's report, and shows the Umbrella air blast pressure histories for gage locations near the surface. All of these records indicate that the P_1 pulse is over with long before arrival of the P_2 pulse. Furthermore, the shape of the P_1 pressure wave at the 2070 foot station has the same N-wave shape as the spalled surface motion; this suggests
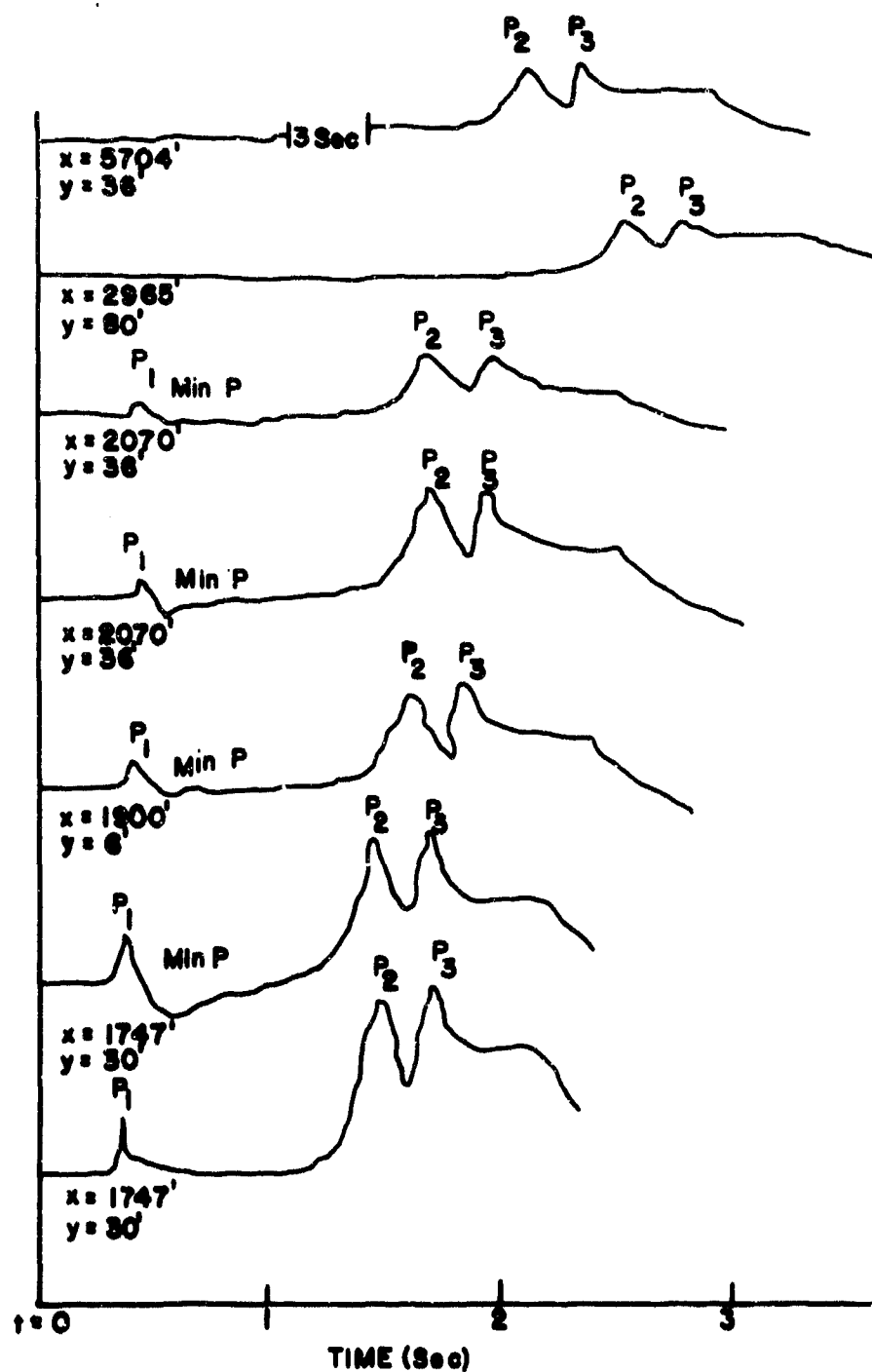
Figure 22.   Umbrella air blast pressure histories as reported by Pittman.

that the P_1 wave is quite coherent with the surface motion. The interpretation is that at this station the air blast wave can be explained in terms of a plane wave traveling vertically from the surface, and therefore suggests that the 2070 foot station is quite near the place of first spall closure, i.e., quite near the place where $dT_c/dX = 0$. At this 2070 foot station the P_2 pulse arrives at about 1.8 seconds, which is about the transit time through the air of a pressure pulse whose origin is at surface-zero. The P_1 pulse is essentially over with by about 0.6 or 0.7 seconds.

The P_3 pulse in figure 22 indicates that the water column or bubble blow-out took effect (in producing the P_3 pulse) about 0.3 seconds after the underwater shock front arrival at surface-zero, i.e., about 0.3 seconds after the origin of the P_2 pulse.

Figure 23 is identical with figure 53 in Pittman's report. Here we can see the effect of charge weight ranging from 8.6 pounds up to 8 kilotons. According to the analysis in this section, we see that for the small charges the P_2 wave arrives much before the conclusion of the P_1 wave, i.e., much before the spall has closed. For the large charges, the P_2 wave arrives after the spall has closed, i.e., after the P_1 wave has subsided. Again, this is particularly evident on the very large nuclear charge.

82
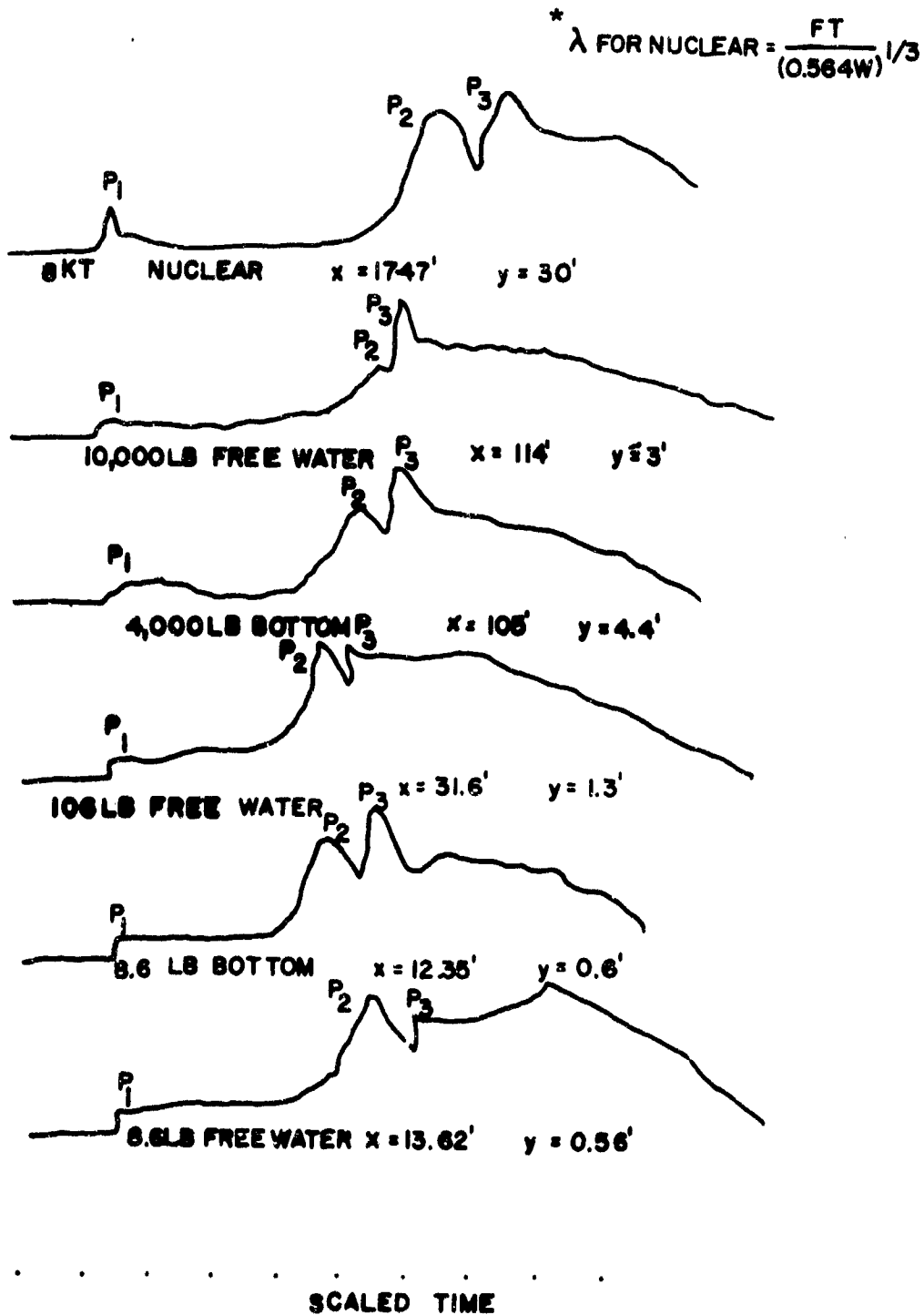
Figure 23.   Pittman's comparison of air blast pressure histories from under-water nuclear and HBX-1 burst; λ_d = sin 9.726*; $\lambda_x \approx 6.6$; λ_y = 0.12 to 0.27.

Appendix A

SPALL DYNAMICS,
HIGH PRESSURE LIMIT ANALYSIS

```
            PROGRAM EP1062
      C
      C
      C     SPALL DYNAMICS, HIGH PRESSURE LIMIT ANALYSIS,
      C     INCIDENT PRESSURE WAVE HAS SHOCK RISE WITH EXPONENTIAL TAIL-OFF,
      C     WAVELENGTH IS LENGTH FOR PRESSURE TO FALL TO 1/E,
      C     IN TABLES,
      C               TIME IS NORMALIZED TO CLOSURE TIME
      C               SPALL THICKNESS IS NORMALIZED TO CLOSURE DEPTH
      C               SURFACE POSITION IS NORMALIZED TO MAXIMUM
      C                   SURFACE EXCURSION
      C               SURFACE VELOCITY IS NORMALIZED TO VERTICAL COMPONENT
      C                   OF INCIDENT PEAK PARTICLE VELOCITY
      C               SURFACE ACCELERATION IS IN UNITS OF GRAVITY ACCELERATION
      C               LOWER CAVITY BOUNDARY IS NORMALIZED TO CLOSURE DEPTH
      C
      C
      C     FOR SHOCKWAVE INCIDENT AT ANGLE A, USE TABLES REPLACING
      C           (1) WAVELENGTH BY SHOCK WAVELENGTH TIMES SECANT(A)
      C           (2) PRESSURE BY SHOCK PEAK PRESSURE TIMES COSINE(A)
      C
      1     READ (60,100) WMAX,WMIN,R,R1,R2
            R = EXPF(LOGF(10,)/R)
            I = 1
            W = WMIN
      2     PW = 64,4*W/(14,7*144,)
            D = SQRTF(1,/PW)
      3     V = EXPF(2,*D)
            F0 = V-(1,+2,*D)-2,/PW
            F1 = 2,*(V-D)
            D1 = D -F0/F1
            DD = ABSF(D1-D)
            D = D1
            IF (DD*10,**6-D) 4,4,3
      4     DZS = D
            D = (SQRTF(1,+8,*PW)-1,)/(4,*PW)
      5     V = EXPF(2,*D)
            F0 = 1,-(PW+1,/(2,*D))*(V-1,-2,*D)
            F1 = -2,*(PW+1,/(2,*D))*(V-1,)+(1,/(2,*D*D))*(V-1,-2,*D)
            D1 = D -F0/F1
            DD = ABSF(D1-D)
            D = D1
            IF (DD*10,**6-D) 6,6,5
      6     DJS = D
            V = EXPF(-2,*D)
            TZSMAX = 1,-(1,+2,*D)*V
            ZSMAX =-2,*(V-PW*TZSMAX/2,)*TZSMAX
            D = DZS
            V = EXPF(2,*D)
            F0= 4,*(1,+PW*D) -(1,/(2,*D*D))*(V-1,-2,*D)
            IF (F0) 7,8,8
      7     V = EXPF(2,*D)
            F0 = 4,*(1,+PW*D) -(1,/(2,*D*D))*(V-1,-2,*D)
            F1 = 4,*PW -(1,/(D*D))*(V-1,) +(1,/(D**3))*(V-1,-2,*D)
            D1 = D -F0/F1
            DD = ABSF(D1-D)
            D = D1
            IF (DD*10,**6-D) 9,9,7
```

```
 8    DGS = D
      L = 2
      GO TO 22
 9    DGS = D
      L = 1
22    DZSW = DZS*W
      TDZS = 1. -(1.+2.*DZS)*EXPF(-2.*DZS)
      TDZSP = 2.*W*TDZS/73.5
      DZ1 = DUS/R1
      DZ2 = (DZS -DUS)/R2
      ZSMAXP = 576. * W * ZSMAX/1470.
      WRITE (61,106)
      WRITE (61,101) I
      I = I+1
      WRITE (61,102)
      WRITE (61,103) W,ZSMAXP,DZSW,TDZSP
      WRITE (61,104)
      Z = 0.
10    V = EXPF(-2.*Z)
      ZN = Z/DZS
      T = 1.-(1.+2.*Z)*V
      TN = T/TDZS
      US =-2.*(V-(PW+1./(2.*Z))*T)
      ZS =-2.*(V-PW*T/2.)*T
      ZSN = ZS/ZSMAX
      IF (Z) 11,11,12
11    GS = 1000000.
      ZBN= 1000000.
      GO TO 13
12    GS = 1.+(1.-T/(8.*
     1                     Z*Z*V))/(PW*Z)
      ZBN = 1. - LOGF(TN)/ (2. * DZS)
13    WRITE (61,105)TN,ZN,ZSN,US,GS, ZBN
      IF (Z-DUS+ DZ1/2.) 14,15,15
14    Z = Z + DZ1
      GO TO 10
15    GO TO (16,19,21) L
16    IF (Z+DZ2-DGS) 19,18,17
17    L = 3
      ZM = Z
      Z = DGS
      GO TO 10
18    L = 2
19    Z = Z+DZ2
      IF (Z - DZS - DZ2/2.)  10,20,20
20    W = R*W
      IF (W-WMAX) 2,2,50
21    L = 2
      Z = ZM
      GO TO 19
100 FORMAT (2F7.2,3F3.0)
101 FORMAT (36X,5HPAGE .I3//)
102 FORMAT (33X,14HSPALL DYNAMICS/26X,28HHIGH PRESSURE LIMIT ANALYSIS)
103 FORMAT (///22X,13HWAVELENGTH = ,F10.5,5H FEET/ 7X,
   1 28HMAXIMUM SURFACE EXCURSION = ,F10.5,
   2 30H FEET PER THOUSAND PSI SQUARED/19X,16HCLOSURE DEPTH = ,F10.5,
```

```
      3 5H FEET/20X,15HCLOSURE TIME = ,F10.5,
      4 25H SECONDS PER THOUSAND PSI//)
  104 FORMAT (7X,4HTIME,6X,5HSPALL,4X,7HSURFACE,4X,7HSURFACE,5X,
      5 7HSURFACE, 8X,5HLOWER/15X,9HTHICKNESS,2X,8HPOSITION,3X,
      6 8HVELOCITY,2X,
      X                 12HACCELERATION,4X,6HCAVITY/48X,9H(IN GEES),
      7 5X,8HBOUNDARY/)
  105 FORMAT (6X,F6,3,4X,F6,3,5X,F6,3,5X,F6,3,5X,F8,2,5X,F7,2)
  106 FORMAT (1H1)
   50 END
```

SPALL DYNAMICS
HIGH PRESSURE LIMIT ANALYSIS

```
              WAVELENGTH =      0.01000 FEET
MAXIMUM SURFACE EXCURSION =     -0.00080 FEET PER THOUSAND PSI SQUARED
            CLOSURE DEPTH =      0.04396 FEET
             CLOSURE TIME =      0.00027 SECONDS PER THOUSAND PSI
```

TIME	SPALL THICKNESS	SURFACE POSITION	SURFACE VELOCITY	SURFACE ACCELERATION (IN GEES)	LOWER CAVITY BOUNDARY
0.000	0.000	0.000	-2.000	********	*******
0.002	0.007	0.017	-1.818	77947.45	1.71
0.007	0.014	0.063	-1.648	38687.02	1.56
0.015	0.021	0.128	-1.490	25594.03	1.47
0.027	0.029	0.204	-1.343	19042.71	1.41
0.040	0.036	0.288	-1.206	15107.91	1.37
0.056	0.043	0.374	-1.078	12481.25	1.33
0.073	0.050	0.459	-0.959	10601.97	1.30
0.091	0.057	0.541	-0.848	9189.70	1.27
0.111	0.064	0.617	-0.745	8088.47	1.25
0.131	0.071	0.688	-0.649	7205.41	1.23
0.153	0.079	0.751	-0.560	6480.45	1.22
0.173	0.086	0.807	-0.478	5874.12	1.20
0.197	0.093	0.856	-0.401	5353.98	1.18
0.220	0.100	0.897	-0.330	4915.39	1.17
0.243	0.107	0.930	-0.264	4528.97	1.16
0.265	0.114	0.957	-0.203	4188.03	1.15
0.290	0.121	0.976	-0.146	3887.01	1.14
0.313	0.129	0.990	-0.093	3616.78	1.13
0.335	0.136	0.998	-0.045	3373.17	1.12
0.359	0.143	1.000	0.000	3152.10	1.12
0.485	0.186	0.932	0.204	2150.22	1.08
0.595	0.229	0.785	0.326	1469.45	1.06
0.690	0.271	0.621	0.394	944.53	1.04
0.764	0.314	0.472	0.426	496.76	1.03
0.822	0.357	0.348	0.437	61.01	1.02
0.832	0.366	0.327	0.437	-0.00	1.02
0.867	0.400	0.251	0.434	-333.53	1.02
0.902	0.443	0.179	0.422	-771.79	1.01
0.925	0.486	0.126	0.406	-1257.37	1.01
0.947	0.529	0.088	0.388	-1815.46	1.01
0.962	0.571	0.061	0.370	-2475.20	1.00
0.973	0.614	0.042	0.351	-3272.16	1.00
0.980	0.657	0.028	0.333	-4251.07	1.00
0.985	0.700	0.019	0.316	-5469.26	1.00
0.991	0.743	0.013	0.301	-7001.05	1.00
0.994	0.786	0.008	0.286	-8943.61	1.00
0.995	0.829	0.005	0.272	********	1.00
0.997	0.871	0.003	0.260	********	1.00
0.999	0.914	0.002	0.248	********	1.00
0.999	0.957	0.001	0.237	********	1.00
1.000	1.000	0.000	0.227	********	1.00

SPALL DYNAMICS
HIGH PRESSURE LIMIT ANALYSIS

WAVELENGTH =	0.01334	FEET
MAXIMUM SURFACE EXCURSION =	-0.00106	FEET PER THOUSAND PSI SQUARED
CLOSURE DEPTH =	0.05671	FEET
CLOSURE TIME =	0.00036	SECONDS PER THOUSAND PSI

TIME	SPALL THICKNESS	SURFACE POSITION	SURFACE VELOCITY	SURFACE ACCELERATION (IN GEES)	LOWER CAVITY BOUNDARY
0.000	0.000	0.000	-2.000	********	*******
0.002	0.007	0.017	-1.818	58457.55	1.74
0.007	0.015	0.063	-1.648	29013.90	1.58
0.015	0.022	0.127	-1.490	19194.72	1.49
0.027	0.030	0.204	-1.343	14281.51	1.43
0.040	0.037	0.288	-1.206	11330.58	1.38
0.056	0.044	0.374	-1.078	9360.70	1.34
0.073	0.052	0.459	-0.959	7951.32	1.31
0.091	0.059	0.541	-0.848	6892.17	1.28
0.111	0.066	0.617	-0.745	6066.45	1.26
0.131	0.074	0.688	-0.649	5404.05	1.24
0.153	0.081	0.751	-0.560	4860.36	1.22
0.175	0.089	0.807	-0.478	4405.64	1.20
0.197	0.096	0.856	-0.401	4019.31	1.19
0.220	0.103	0.897	-0.330	3686.64	1.18
0.243	0.111	0.930	-0.264	3396.84	1.17
0.267	0.118	0.957	-0.203	3141.83	1.16
0.290	0.126	0.976	-0.146	2915.40	1.15
0.313	0.133	0.990	-0.093	2712.74	1.14
0.336	0.140	0.998	-0.045	2530.05	1.13
0.359	0.148	1.000	-0.000	2364.26	1.12
0.482	0.190	0.936	0.198	1635.94	1.09
0.590	0.233	0.797	0.319	1136.10	1.06
0.680	0.276	0.640	0.388	749.93	1.05
0.754	0.318	0.493	0.423	421.83	1.03
0.812	0.361	0.369	0.436	119.41	1.02
0.832	0.378	0.326	0.437	0.00	1.02
0.855	0.403	0.271	0.435	-177.74	1.02
0.894	0.446	0.196	0.426	-487.98	1.01
0.921	0.489	0.140	0.412	-826.65	1.01
0.942	0.531	0.099	0.395	-1210.05	1.01
0.957	0.574	0.069	0.377	-1656.59	1.01
0.969	0.616	0.048	0.359	-2188.26	1.00
0.979	0.659	0.033	0.342	-2832.18	1.00
0.984	0.702	0.023	0.325	-3622.59	1.00
0.989	0.744	0.015	0.309	-4603.21	1.00
0.992	0.787	0.010	0.294	-5830.48	1.00
0.995	0.830	0.006	0.281	-7377.54	1.00
0.997	0.872	0.004	0.268	-9339.73	1.00
0.998	0.915	0.002	0.256	********	1.00
0.999	0.957	0.001	0.245	********	1.00
1.000	1.000	0.000	0.235	********	1.00

SPALL DYNAMICS
HIGH PRESSURE LIMIT ANALYSIS

```
              WAVELENGTH  =    0.01778 FEET
MAXIMUM SURFACE EXCURSION =   -0.00142 FEET PER THOUSAND PSI SQUARED
           CLOSURE DEPTH  =    0.07307 FEET
           CLOSURE TIME   =    0.00048 SECONDS PER THOUSAND PSI
```

TIME	SPALL THICKNESS	SURFACE POSITION	SURFACE VELOCITY	SURFACE ACCELERATION (IN GEES)	LOWER CAVITY BOUNDARY
0.000	0.000	0.000	-2.000	********	*******
0.002	0.008	0.017	-1.818	43842.18	1.76
0.007	0.015	0.063	-1.648	21760.09	1.60
0.015	0.023	0.127	-1.490	14395.91	1.51
0.027	0.031	0.204	-1.343	10711.11	1.44
0.040	0.038	0.288	-1.206	8497.98	1.39
0.055	0.046	0.374	-1.078	7020.41	1.35
0.073	0.053	0.459	-0.959	5963.61	1.32
0.091	0.061	0.540	-0.848	5169.28	1.29
0.111	0.069	0.617	-0.745	4550.00	1.27
0.132	0.076	0.688	-0.649	4053.22	1.25
0.153	0.084	0.751	-0.560	3645.46	1.23
0.175	0.092	0.807	-0.478	3304.44	1.21
0.198	0.099	0.856	-0.401	3014.70	1.20
0.220	0.107	0.897	-0.330	2765.20	1.18
0.243	0.115	0.930	-0.264	2547.87	1.17
0.267	0.122	0.957	-0.203	2356.61	1.16
0.290	0.130	0.976	-0.146	2186.80	1.15
0.313	0.138	0.990	-0.093	2034.81	1.14
0.335	0.145	0.998	-0.045	1897.80	1.13
0.359	0.153	1.000	0.000	1773.46	1.12
0.479	0.195	0.941	0.192	1244.75	1.09
0.582	0.238	0.809	0.312	878.18	1.07
0.671	0.280	0.658	0.382	594.26	1.05
0.744	0.322	0.514	0.419	353.85	1.04
0.802	0.365	0.391	0.435	134.33	1.03
0.833	0.391	0.326	0.437	0.00	1.02
0.849	0.407	0.292	0.437	-79.51	1.02
0.885	0.449	0.214	0.429	-299.46	1.01
0.914	0.492	0.155	0.417	-536.05	1.01
0.935	0.534	0.112	0.401	-799.88	1.01
0.952	0.576	0.079	0.384	-1102.61	1.01
0.963	0.619	0.056	0.367	-1457.80	1.00
0.974	0.661	0.039	0.350	-1881.91	1.00
0.982	0.703	0.027	0.334	-2395.33	1.00
0.987	0.746	0.018	0.318	-3023.73	1.00
0.991	0.788	0.012	0.303	-3799.78	1.00
0.994	0.831	0.008	0.289	-4765.27	1.00
0.996	0.873	0.005	0.277	-5973.96	1.00
0.998	0.915	0.003	0.265	-7495.27	1.00
0.999	0.958	0.001	0.254	-9419.09	1.00
1.000	1.000	0.000	0.243	********	1.00

SPALL DYNAMICS
HIGH PRESSURE LIMIT ANALYSIS

                    WAVELENGTH =   0.02371 FEET
MAXIMUM SURFACE EXCURSION =   -0.00189 FEET PER THOUSAND PSI SQUARED
            CLOSURE DEPTH =   0.09403 FEET
            CLOSURE TIME =   0.00064 SECONDS PER THOUSAND PSI

TIME	SPALL THICKNESS	SURFACE POSITION	SURFACE VELOCITY	SURFACE ACCELERATION (IN GFES)	LOWER CAVITY BOUNDARY
0.000	0.000	0.000	-2.000	********	*******
0.002	0.008	0.017	-1.818	32882.20	1.79
0.007	0.016	0.063	-1.648	16320.49	1.62
0.015	0.024	0.127	-1.490	10797.31	1.52
0.027	0.032	0.204	-1.343	8033.69	1.46
0.040	0.040	0.288	-1.206	6373.83	1.41
0.056	0.047	0.374	-1.078	5265.80	1.36
0.073	0.055	0.459	-0.959	4473.04	1.33
0.091	0.063	0.540	-0.848	3877.29	1.30
0.111	0.071	0.617	-0.745	3412.83	1.28
0.132	0.079	0.688	-0.650	3040.24	1.26
0.153	0.087	0.751	-0.561	2734.42	1.24
0.175	0.095	0.807	-0.478	2478.65	1.22
0.198	0.103	0.856	-0.401	2261.34	1.20
0.221	0.111	0.897	-0.330	2074.22	1.19
0.244	0.119	0.930	-0.264	1911.22	1.18
0.267	0.127	0.957	-0.203	1767.78	1.17
0.290	0.135	0.976	-0.146	1640.42	1.16
0.313	0.142	0.990	-0.093	1526.44	1.15
0.336	0.150	0.998	-0.045	1423.67	1.14
0.359	0.158	1.000	0.000	1330.43	1.13
0.473	0.200	0.945	0.186	947.21	1.09
0.575	0.242	0.821	0.304	678.70	1.07
0.661	0.285	0.676	0.376	470.11	1.05
0.733	0.327	0.536	0.415	293.98	1.04
0.792	0.369	0.414	0.434	134.32	1.03
0.834	0.405	0.325	0.438	-0.00	1.02
0.839	0.411	0.314	0.438	-19.53	1.02
0.875	0.453	0.234	0.433	-175.70	1.02
0.905	0.495	0.172	0.422	-341.28	1.01
0.929	0.537	0.125	0.408	-523.17	1.01
0.946	0.579	0.091	0.392	-728.77	1.01
0.960	0.621	0.065	0.375	-966.45	1.01
0.971	0.663	0.046	0.359	-1246.19	1.00
0.979	0.705	0.032	0.343	-1580.13	1.00
0.985	0.747	0.022	0.327	-1983.39	1.00
0.989	0.790	0.015	0.313	-2474.53	1.00
0.993	0.832	0.010	0.299	-3077.65	1.00
0.995	0.874	0.006	0.286	-3822.87	1.00
0.997	0.916	0.003	0.274	-4748.70	1.00
0.999	0.958	0.001	0.263	-5904.39	1.00
1.000	1.000	-0.000	0.252	-7353.12	1.00

SPALL DYNAMICS
HIGH PRESSURE LIMIT ANALYSIS

	WAVELENGTH =	0.03162 FEET			
MAXIMUM SURFACE EXCURSION =		-0.00252 FEET PER THOUSAND PSI SQUARED			
CLOSURE DEPTH =		0.12086 FEET			
CLOSURE TIME =		0.00086 SECONDS PER THOUSAND PSI			

TIME	SPALL THICKNESS	SURFACE POSITION	SURFACE VELOCITY	SURFACE ACCELERATION (IN GEES)	LOWER CAVITY BOUNDARY
0.000	0.000	0.000	-2.000	*******	*******
0.002	0.008	0.017	-1.818	24663.38	1.82
0.007	0.016	0.063	-1.649	12241.37	1.64
0.015	0.025	0.127	-1.490	8098.75	1.54
0.027	0.033	0.204	-1.343	6025.91	1.47
0.040	0.041	0.288	-1.206	4780.94	1.42
0.056	0.049	0.374	-1.078	3949.87	1.38
0.073	0.057	0.459	-0.959	3355.27	1.34
0.091	0.066	0.540	-0.848	2908.43	1.31
0.111	0.074	0.617	-0.745	2560.07	1.29
0.132	0.082	0.688	-0.650	2280.61	1.27
0.153	0.090	0.751	-0.561	2051.23	1.25
0.175	0.099	0.807	-0.478	1859.40	1.23
0.198	0.107	0.856	-0.401	1696.41	1.21
0.221	0.115	0.897	-0.330	1556.06	1.20
0.244	0.123	0.930	-0.264	1433.81	1.18
0.267	0.131	0.957	-0.203	1326.22	1.17
0.290	0.140	0.976	-0.146	1230.70	1.16
0.313	0.148	0.990	-0.093	1145.21	1.15
0.336	0.156	0.998	-0.045	1068.13	1.14
0.359	0.164	1.000	-0.000	998.19	1.13
0.469	0.206	0.949	0.180	720.89	1.10
0.567	0.248	0.833	0.296	524.47	1.07
0.651	0.290	0.695	0.369	371.35	1.06
0.722	0.331	0.559	0.411	242.34	1.04
0.781	0.373	0.438	0.431	126.17	1.03
0.829	0.415	0.337	0.438	15.36	1.02
0.834	0.421	0.324	0.438	-0.00	1.02
0.867	0.457	0.255	0.435	-95.71	1.02
0.897	0.499	0.	0.426	-211.81	1.01
0.921	0.540	0.	0.414	-337.46	1.01
0.940	0.582	0.103	0.399	-477.37	1.01
0.953	0.624	0.075	0.384	-636.72	1.01
0.966	0.666	0.054	0.368	-821.55	1.00
0.975	0.707	0.038	0.352	-1039.07	1.00
0.982	0.749	0.027	0.337	-1298.08	1.00
0.987	0.791	0.018	0.322	-1609.42	1.00
0.991	0.833	0.012	0.309	-1986.61	1.00
0.995	0.875	0.008	0.296	-2446.56	1.00
0.997	0.916	0.004	0.284	-3010.56	1.00
0.999	0.958	0.002	0.272	-3705.91	1.00
1.000	1.000	-0.000	0.262	-4565.45	1.00

SPALL DYNAMICS
HIGH PRESSURE LIMIT ANALYSIS

WAVELENGTH = 0.04217 FEET
MAXIMUM SURFACE EXCURSION = -0.00336 FEET PER THOUSAND PSI SQUARED
CLOSURE DEPTH = 0.15512 FEET
CLOSURE TIME = 0.00114 SECONDS PER THOUSAND PSI

TIME	SPALL THICKNESS	SURFACE POSITION	SURFACE VELOCITY	SURFACE ACCELERATION (IN GFES)	LOWER CAVITY BOUNDARY
0.000	0.000	0.000	-2.000	*******	*******
0.002	0.009	0.017	-1.818	18500.12	1.85
0.007	0.017	0.063	-1.649	9182.46	1.67
0.015	0.026	0.127	-1.491	6075.10	1.56
0.027	0.034	0.204	-1.343	4520.29	1.49
0.040	0.043	0.288	-1.206	3586.44	1.44
0.056	0.051	0.373	-1.078	2963.06	1.39
0.073	0.060	0.459	-0.959	2517.06	1.36
0.091	0.068	0.540	-0.849	2181.89	1.33
0.111	0.077	0.617	-0.746	1920.59	1.30
0.132	0.085	0.688	-0.650	1710.97	1.28
0.153	0.094	0.751	-0.561	1538.92	1.25
0.175	0.102	0.807	-0.478	1395.02	1.24
0.198	0.111	0.856	-0.401	1272.77	1.22
0.221	0.119	0.897	-0.330	1167.50	1.21
0.244	0.128	0.930	-0.264	1075.90	1.19
0.267	0.136	0.957	-0.203	995.10	1.18
0.290	0.145	0.976	-0.146	923.45	1.17
0.313	0.154	0.990	-0.093	859.32	1.16
0.336	0.162	0.998	-0.045	801.51	1.15
0.359	0.171	1.000	-0.000	749.06	1.14
0.465	0.212	0.953	0.173	548.75	1.10
0.559	0.254	0.845	0.288	405.28	1.08
0.642	0.295	0.713	0.361	292.99	1.06
0.711	0.336	0.582	0.405	198.51	1.05
0.770	0.378	0.463	0.429	113.95	1.04
0.819	0.419	0.361	0.438	34.05	1.03
0.836	0.437	0.323	0.439	-0.00	1.02
0.957	0.461	0.278	0.437	-45.06	1.02
0.889	0.502	0.211	0.431	-126.63	1.02
0.913	0.544	0.158	0.420	-213.62	1.01
0.933	0.585	0.118	0.407	-309.04	1.01
0.949	0.627	0.087	0.392	-416.10	1.01
0.962	0.668	0.063	0.377	-538.46	1.01
0.972	0.710	0.045	0.362	-680.42	1.00
0.979	0.751	0.032	0.347	-847.08	1.00
0.985	0.793	0.022	0.333	-1044.69	1.00
0.990	0.834	0.015	0.319	-1280.89	1.00
0.993	0.876	0.009	0.306	-1565.12	1.00
0.996	0.917	0.005	0.294	-1909.12	1.00
0.999	0.959	0.002	0.282	-2327.48	1.00
1.000	1.000	-0.000	0.272	-2838.50	1.00

SPALL DYNAMICS
HIGH PRESSURE LIMIT ANALYSIS

```
            WAVELENGTH =     0.05623 FEET
MAXIMUM SURFACE EXCURSION =  -0.00448 FEET PER THOUSAND PSI SQUARED
            CLOSURE DEPTH =  0.19881 FEET
            CLOSURE TIME =   0.00152 SECONDS PER THOUSAND PSI
```

TIME	SPALL THICKNESS	SURFACE POSITION	SURFACE VELOCITY	SURFACE ACCELERATION (IN GEES)	LOWER CAVITY BOUNDARY
0.000	0.000	0.000	-2.000	********	*******
0.002	0.009	0.017	-1.818	13878.73	1.89
0.007	0.018	0.063	-1.649	6888.40	1.70
0.015	0.027	0.127	-1.491	4557.59	1.59
0.027	0.035	0.204	-1.343	3391.22	1.51
0.040	0.044	0.288	-1.206	2690.70	1.45
0.056	0.053	0.373	-1.078	2223.16	1.41
0.073	0.062	0.458	-0.959	1888.49	1.37
0.091	0.071	0.540	-0.849	1637.06	1.34
0.111	0.080	0.617	-0.746	1441.04	1.31
0.132	0.089	0.688	-0.650	1283.80	1.29
0.153	0.098	0.751	-0.561	1154.73	1.27
0.176	0.106	0.807	-0.478	1046.79	1.25
0.199	0.115	0.856	-0.402	955.08	1.23
0.221	0.124	0.897	-0.330	876.11	1.21
0.244	0.133	0.930	-0.264	807.32	1.20
0.267	0.142	0.957	-0.203	746.79	1.19
0.291	0.151	0.976	-0.146	693.05	1.17
0.314	0.160	0.990	-0.094	644.94	1.16
0.337	0.169	0.998	-0.045	601.58	1.15
0.359	0.177	1.000	0.000	562.23	1.14
0.460	0.219	0.957	0.167	417.82	1.11
0.552	0.260	0.856	0.280	313.19	1.08
0.632	0.301	0.732	0.354	230.93	1.06
0.700	0.342	0.602	0.399	161.78	1.05
0.755	0.383	0.488	0.425	100.21	1.04
0.806	0.424	0.387	0.437	42.54	1.03
0.837	0.455	0.321	0.439	-0.00	1.03
0.846	0.465	0.302	0.439	-13.91	1.02
0.879	0.506	0.232	0.435	-71.34	1.02
0.905	0.548	0.177	0.426	-131.71	1.01
0.925	0.589	0.134	0.414	-196.94	1.01
0.943	0.630	0.100	0.401	-269.04	1.01
0.957	0.671	0.074	0.386	-350.24	1.01
0.967	0.712	0.054	0.372	-443.07	1.00
0.976	0.753	0.038	0.358	-550.52	1.00
0.983	0.794	0.027	0.344	-676.16	1.00
0.989	0.835	0.018	0.330	-824.31	1.00
0.992	0.877	0.012	0.317	-1000.22	1.00
0.995	0.918	0.007	0.305	-1210.31	1.00
0.998	0.959	0.003	0.293	-1462.51	1.00
1.000	1.000	0.000	0.283	-1766.58	1.00

SPALL DYNAMICS
HIGH PRESSURE LIMIT ANALYSIS

WAVELENGTH =	0.07499 FEET		
MAXIMUM SURFACE EXCURSION =	=0.00597 FEET PER THOUSAND PSI SQUARED		
CLOSURE DEPTH =	0.25440 FEET		
CLOSURE TIME =	0.00202 SECONDS PER THOUSAND PSI		

TIME	SPALL THICKNESS	SURFACE POSITION	SURFACE VELOCITY	SURFACE ACCELERATION (IN GEES)	LOWER CAVITY BOUNDARY
0.000	0.000	0.000	=2.000	*******	*******
0.002	0.009	0.017	=1.818	10412.48	1.92
0.007	0.018	0.063	=1.649	5168.44	1.73
0.016	0.028	0.127	=1.491	3419.41	1.61
0.027	0.037	0.204	=1.344	2544.55	1.53
0.040	0.046	0.287	=1.206	2018.08	1.47
0.056	0.055	0.373	=1.079	1668.14	1.43
0.073	0.065	0.458	=0.960	1417.13	1.39
0.092	0.074	0.540	=0.849	1228.49	1.35
0.111	0.083	0.617	=0.746	1081.43	1.32
0.132	0.092	0.687	=0.650	963.46	1.30
0.154	0.102	0.751	=0.561	866.63	1.28
0.176	0.111	0.807	=0.479	785.45	1.26
0.198	0.120	0.856	=0.402	716.85	1.24
0.221	0.129	0.897	=0.330	657.41	1.22
0.249	0.139	0.930	=0.264	606.00	1.21
0.269	0.148	0.957	=0.203	560.59	1.19
0.291	0.157	0.976	=0.146	520.27	1.18
0.314	0.166	0.990	=0.094	484.18	1.17
0.337	0.176	0.998	=0.045	451.65	1.16
0.360	0.185	1.000	=0.000	422.13	1.15
0.456	0.226	0.961	0.160	318.22	1.12
0.544	0.266	0.867	0.271	242.06	1.09
0.622	0.307	0.750	0.345	181.87	1.07
0.689	0.348	0.629	0.393	131.29	1.05
0.746	0.389	0.515	0.421	86.45	1.04
0.795	0.429	0.414	0.436	44.79	1.03
0.835	0.470	0.327	0.440	4.45	1.03
0.839	0.475	0.319	0.440	0.00	1.03
0.869	0.511	0.256	0.438	=36.08	1.02
0.896	0.552	0.198	0.431	=78.08	1.02
0.918	0.592	0.151	0.421	=122.79	1.01
0.935	0.633	0.115	0.409	=171.49	1.01
0.951	0.674	0.086	0.396	=225.50	1.01
0.963	0.715	0.063	0.382	=286.36	1.01
0.972	0.755	0.046	0.369	=355.90	1.00
0.980	0.796	0.032	0.355	=435.85	1.00
0.986	0.837	0.022	0.342	=528.95	1.00
0.991	0.878	0.014	0.329	=638.01	1.00
0.995	0.918	0.008	0.317	-766.53	1.00
0.998	0.959	0.004	0.305	=918.80	1.00
1.000	1.000	=0.000	0.294	-1100.01	1.00

SPALL DYNAMICS
HIGH PRESSURE LIMIT ANALYSIS

WAVELENGTH = 0.10000 FEET
MAXIMUM SURFACE EXCURSION = -0.00796 FEET PER THOUSAND PSI SQUARED
CLOSURE DEPTH = 0.32498 FEET
CLOSURE TIME = 0.00269 SECONDS PER THOUSAND PSI

TIME	SPALL THICKNESS	SURFACE POSITION	SURFACE VELOCITY	SURFACE ACCELERATION (IN GEES)	LOWER CAVITY BOUNDARY
0.000	0.000	0.000	-2.000	*******	*******
0.002	0.010	0.017	-1.818	7813.44	1.96
0.007	0.019	0.043	-1.649	3878.50	1.76
0.015	0.029	0.127	-1.491	2566.24	1.64
0.027	0.039	0.204	-1.344	1909.63	1.56
0.040	0.048	0.287	-1.207	1515.26	1.49
0.056	0.058	0.373	-1.079	1252.00	1.44
0.073	0.067	0.458	-0.960	1063.66	1.40
0.092	0.077	0.540	-0.849	922.11	1.37
0.111	0.087	0.617	-0.746	811.77	1.34
0.132	0.096	0.687	-0.651	723.25	1.31
0.154	0.106	0.751	-0.562	650.59	1.29
0.175	0.116	0.807	-0.479	589.83	1.27
0.199	0.125	0.856	-0.402	538.20	1.25
0.222	0.135	0.896	-0.331	493.75	1.23
0.243	0.145	0.930	-0.265	455.03	1.22
0.269	0.154	0.956	-0.203	420.95	1.20
0.292	0.164	0.976	-0.146	390.70	1.19
0.315	0.174	0.990	-0.094	363.62	1.18
0.338	0.183	0.998	-0.045	339.21	1.17
0.361	0.193	1.000	-0.000	317.07	1.16
0.452	0.233	0.964	0.154	242.47	1.12
0.537	0.274	0.878	0.262	187.13	1.10
0.612	0.314	0.768	0.337	143.16	1.08
0.677	0.354	0.652	0.386	106.18	1.06
0.734	0.395	0.542	0.416	73.53	1.05
0.782	0.435	0.441	0.434	43.41	1.04
0.823	0.475	0.355	0.441	14.53	1.03
0.841	0.496	0.316	0.442	-0.00	1.03
0.857	0.516	0.281	0.441	-14.13	1.02
0.885	0.556	0.221	0.436	-43.43	1.02
0.909	0.596	0.171	0.428	-74.18	1.01
0.929	0.637	0.131	0.417	-107.16	1.01
0.944	0.677	0.100	0.405	-143.20	1.01
0.957	0.717	0.074	0.393	-183.21	1.01
0.968	0.758	0.055	0.380	-228.20	1.01
0.975	0.798	0.039	0.367	-279.34	1.00
0.983	0.839	0.027	0.354	-337.98	1.00
0.989	0.879	0.017	0.342	-405.74	1.00
0.993	0.919	0.010	0.330	-484.53	1.00
0.997	0.960	0.004	0.318	-576.44	1.00
1.000	1.000	-0.000	0.307	-684.82	1.00

SPALL DYNAMICS
HIGH PRESSURE LIMIT ANALYSIS

                    WAVELENGTH =   0.13335 FEET
MAXIMUM SURFACE EXCURSION =   -0.01061 FEET PER THOUSAND PSI SQUARED
         CLOSURE DEPTH =   0.41439 FEET
         CLOSURE TIME =   0.00358 SECONDS PER THOUSAND PSI

TIME	SPALL THICKNESS	SURFACE POSITION	SURFACE VELOCITY	SURFACE ACCELERATION (IN GEES)	LOWER CAVITY BOUNDARY
0.000	0.000	0.000	-2.000	*******	******
0.002	0.017	0.017	-1.819	5864.43	2.01
0.007	0.020	0.063	-1.649	2911.98	1.79
0.015	0.030	0.127	-1.491	1926.30	1.67
0.027	0.040	0.204	-1.344	1433.50	1.58
0.040	0.050	0.287	-1.207	1137.52	1.52
0.056	0.060	0.373	-1.080	939.95	1.46
0.073	0.071	0.458	-0.961	798.59	1.42
0.092	0.081	0.540	-0.850	692.36	1.38
0.112	0.091	0.616	-0.747	609.54	1.35
0.132	0.101	0.687	-0.651	543.11	1.33
0.154	0.111	0.751	-0.562	488.58	1.30
0.176	0.121	0.807	-0.479	442.98	1.28
0.199	0.131	0.855	-0.402	404.23	1.26
0.222	0.141	0.896	-0.331	370.87	1.24
0.245	0.151	0.930	-0.265	341.81	1.23
0.269	0.161	0.956	-0.203	316.24	1.21
0.292	0.171	0.976	-0.147	293.54	1.20
0.315	0.181	0.990	-0.094	273.22	1.19
0.339	0.191	0.998	-0.045	254.90	1.17
0.361	0.201	1.000	0.000	238.28	1.16
0.449	0.241	0.967	0.147	184.85	1.13
0.529	0.281	0.889	0.253	144.73	1.10
0.602	0.321	0.786	0.327	112.65	1.08
0.666	0.361	0.676	0.378	85.45	1.07
0.722	0.401	0.569	0.411	61.87	1.05
0.770	0.441	0.470	0.431	40.07	1.04
0.811	0.481	0.383	0.441	19.37	1.03
0.844	0.519	0.312	0.443	-0.00	1.03
0.845	0.521	0.306	0.443	-0.94	1.03
0.875	0.561	0.245	0.441	-21.44	1.02
0.900	0.601	0.193	0.434	-42.55	1.02
0.920	0.641	0.150	0.426	-65.07	1.01
0.937	0.681	0.115	0.415	-89.20	1.01
0.952	0.721	0.087	0.404	-115.60	1.01
0.963	0.760	0.065	0.392	-144.44	1.01
0.973	0.800	0.047	0.379	-177.40	1.00
0.981	0.840	0.033	0.367	-214.65	1.00
0.987	0.880	0.021	0.355	-256.96	1.00
0.992	0.920	0.013	0.343	-305.27	1.00
0.997	0.960	0.006	0.332	-361.12	1.00
1.000	1.000	-0.000	0.321	-425.95	1.00

SPALL DYNAMICS
HIGH PRESSURE LIMIT ANALYSIS

```
                    WAVELENGTH =      0.17783 FEET
    MAXIMUM SURFACE EXCURSION =     =0.01414 FEET PER THOUSAND PSI SQUARED
              CLOSURE DEPTH =        0.52737 FEET
              CLOSURE TIME =         0.00475 SECONDS PER THOUSAND PSI
```

TIME	SPALL THICKNESS	SURFACE POSITION	SURFACE VELOCITY	SURFACE ACCELERATION (IN GEES)	LOWER CAVITY BOUNDARY
0.000	0.000	0.000	=2.000	*******	******
0.002	0.011	0.017	=1.819	4402.88	2.06
0.007	0.021	0.063	=1.650	2185.79	1.83
0.015	0.032	0.127	=1.492	1446.42	1.70
0.027	0.042	0.204	=1.345	1076.46	1.61
0.041	0.053	0.287	=1.208	854.26	1.54
0.056	0.063	0.373	=1.080	705.93	1.49
0.073	0.074	0.458	=0.961	599.81	1.44
0.092	0.084	0.539	=0.851	520.07	1.40
0.112	0.095	0.616	=0.748	457.90	1.37
0.133	0.105	0.687	=0.652	408.02	1.34
0.154	0.116	0.750	=0.563	367.09	1.31
0.177	0.127	0.807	=0.480	332.86	1.29
0.200	0.137	0.855	=0.403	303.77	1.27
0.223	0.148	0.896	=0.332	278.73	1.25
0.246	0.158	0.930	=0.265	256.91	1.24
0.269	0.169	0.956	=0.204	237.72	1.22
0.293	0.179	0.976	=0.147	220.68	1.21
0.315	0.190	0.990	=0.094	205.42	1.19
0.339	0.200	0.998	=0.045	191.67	1.18
0.362	0.211	1.000	0.000	179.20	1.17
0.443	0.250	0.971	0.140	141.03	1.14
0.522	0.290	0.899	0.243	112.60	1.11
0.592	0.329	0.803	0.318	88.64	1.09
0.654	0.369	0.700	0.370	68.94	1.07
0.709	0.408	0.597	0.405	51.65	1.06
0.757	0.448	0.500	0.427	35.85	1.05
0.799	0.487	0.413	0.440	20.98	1.04
0.834	0.527	0.337	0.445	6.95	1.03
0.849	0.545	0.306	0.445	=0.00	1.03
0.864	0.566	0.272	0.445	=7.83	1.02
0.890	0.605	0.217	0.441	=22.51	1.02
0.912	0.645	0.171	0.434	=37.80	1.02
0.930	0.684	0.135	0.425	=54.03	1.01
0.945	0.724	0.102	0.415	=71.51	1.01
0.959	0.763	0.077	0.404	=90.59	1.01
0.969	0.803	0.056	0.393	=111.66	1.01
0.977	0.842	0.039	0.381	=135.14	1.00
0.985	0.882	0.026	0.369	=161.52	1.00
0.991	0.921	0.015	0.358	=191.36	1.00
0.995	0.961	0.007	0.347	=225.92	1.00
1.000	1.000	=0.000	0.336	=264.15	1.00

SPALL DYNAMICS
HIGH PRESSURE LIMIT ANALYSIS

WAVELENGTH = 0.23714 FEET
MAXIMUM SURFACE EXCURSION = -0.01884 FEET PER THOUSAND PSI SQUARED
CLOSURE DEPTH = 0.66974 FEET
CLOSURE TIME = 0.00630 SECONDS PER THOUSAND PSI

TIME	SPALL THICKNESS	SURFACE POSITION	SURFACE VELOCITY	SURFACE ACCELERATION (IN GEES)	LOWER CAVITY BOUNDARY
0.000	0.000	0.000	-2.000	*******	******
0.002	0.011	0.017	-1.819	3306.85	2.11
0.007	0.022	0.063	-1.650	1641.92	1.87
0.016	0.033	0.127	-1.493	1086.55	1.73
0.027	0.044	0.203	-1.346	808.71	1.64
0.041	0.055	0.287	-1.209	641.94	1.57
0.055	0.066	0.372	-1.081	530.45	1.51
0.074	0.077	0.457	-0.962	450.75	1.46
0.092	0.088	0.539	-0.852	390.96	1.42
0.112	0.100	0.616	-0.749	344.17	1.39
0.133	0.111	0.686	-0.653	306.72	1.36
0.155	0.122	0.750	-0.564	275.98	1.33
0.177	0.133	0.806	-0.481	250.27	1.31
0.200	0.144	0.855	-0.404	228.43	1.28
0.223	0.155	0.896	-0.332	209.63	1.27
0.247	0.166	0.930	-0.266	193.25	1.25
0.270	0.177	0.956	-0.204	178.83	1.23
0.294	0.188	0.976	-0.147	166.04	1.22
0.317	0.199	0.990	-0.094	154.58	1.20
0.340	0.210	0.998	-0.045	144.26	1.19
0.364	0.221	1.000	-0.000	134.89	1.18
0.442	0.260	0.974	0.134	107.69	1.14
0.515	0.299	0.908	0.234	86.74	1.12
0.582	0.338	0.820	0.308	69.77	1.10
0.643	0.377	0.723	0.361	55.41	1.08
0.697	0.416	0.624	0.398	42.82	1.06
0.744	0.455	0.530	0.423	31.38	1.05
0.785	0.494	0.444	0.438	20.70	1.04
0.821	0.533	0.368	0.446	10.42	1.03
0.852	0.572	0.301	0.448	0.30	1.03
0.853	0.573	0.299	0.448	-0.00	1.03
0.879	0.611	0.243	0.447	-9.90	1.02
0.902	0.650	0.194	0.442	-20.37	1.02
0.922	0.688	0.153	0.435	-31.33	1.01
0.939	0.727	0.119	0.426	-42.96	1.01
0.952	0.766	0.090	0.417	-55.46	1.01
0.964	0.805	0.067	0.406	-69.07	1.01
0.974	0.844	0.047	0.396	-84.01	1.00
0.982	0.883	0.032	0.385	-100.57	1.00
0.989	0.922	0.019	0.374	-119.03	1.00
0.995	0.961	0.008	0.363	-139.75	1.00
1.000	1.000	0.000	0.353	-163.14	1.00

SPALL DYNAMICS
HIGH PRESSURE LIMIT ANALYSIS

WAVELENGTH = 0.31623 FEET
MAXIMUM SURFACE EXCURSION = -0.02508 FEET PER THOUSAND PSI SQUARED
CLOSURE DEPTH = 0.84852 FEET
CLOSURE TIME = 0.00635 SECONDS PER THOUSAND PSI

TIME	SPALL THICKNESS	SURFACE POSITION	SURFACE VELOCITY	SURFACE ACCELERATION (IN GEES)	LOWER CAVITY BOUNDARY
0.000	0.000	0.000	-2.000	********	******
0.002	0.012	0.017	-1.819	2484.92	2.17
0.007	0.023	0.062	-1.651	1233.98	1.91
0.015	0.035	0.127	-1.495	816.48	1.77
0.027	0.046	0.203	-1.347	607.92	1.67
0.041	0.058	0.286	-1.210	462.54	1.60
0.056	0.070	0.372	-1.082	398.65	1.54
0.074	0.081	0.457	-0.964	338.97	1.49
0.093	0.093	0.539	-0.853	293.97	1.44
0.113	0.105	0.615	-0.750	258.99	1.41
0.134	0.116	0.686	-0.654	230.75	1.38
0.155	0.128	0.750	-0.565	207.86	1.35
0.178	0.139	0.806	-0.482	188.35	1.32
0.201	0.151	0.855	-0.405	171.94	1.30
0.224	0.163	0.896	-0.333	157.81	1.28
0.248	0.174	0.930	-0.267	145.50	1.26
0.271	0.186	0.956	-0.205	134.69	1.24
0.295	0.197	0.976	-0.148	125.06	1.23
0.318	0.209	0.990	-0.095	116.46	1.21
0.342	0.221	0.998	-0.045	108.70	1.20
0.365	0.232	1.000	-0.000	101.67	1.19
0.439	0.271	0.977	0.127	82.34	1.15
0.509	0.309	0.917	0.224	67.26	1.13
0.573	0.347	0.837	0.297	54.95	1.10
0.632	0.386	0.746	0.351	44.50	1.09
0.684	0.424	0.652	0.391	35.34	1.07
0.731	0.463	0.561	0.418	27.66	1.06
0.772	0.501	0.476	0.436	19.36	1.05
0.809	0.539	0.400	0.447	12.03	1.04
0.840	0.578	0.331	0.452	4.89	1.03
0.860	0.604	0.289	0.452	-0.00	1.03
0.868	0.616	0.271	0.452	-2.22	1.03
0.892	0.655	0.219	0.450	-9.43	1.02
0.913	0.693	0.175	0.445	-16.86	1.02
0.930	0.731	0.137	0.438	-24.64	1.01
0.946	0.770	0.106	0.430	-32.88	1.01
0.959	0.808	0.079	0.421	-41.71	1.01
0.970	0.846	0.057	0.411	-51.27	1.01
0.979	0.885	0.038	0.401	-61.71	1.00
0.987	0.923	0.023	0.391	-73.19	1.00
0.994	0.962	0.010	0.381	-85.89	1.00
1.000	1.000	0.000	0.371	-100.03	1.00

SPALL DYNAMICS
HIGH PRESSURE LIMIT ANALYSIS

```
              WAVELENGTH =      0.42170 FEET
MAXIMUM SURFACE EXCURSION =     -0.03338 FEET PER THOUSAND PSI SQUARED
            CLOSURE DEPTH =      1.07268 FEET
             CLOSURE TIME =      0.01104 SECONDS PER THOUSAND PSI
```

TIME	SPALL THICKNESS	SURFACE POSITION	SURFACE VELOCITY	SURFACE ACCELERATION (IN GEES)	LOWER CAVITY BOUNDARY
0.000	0.000	0.000	-2.000	*******	*******
0.002	0.012	0.017	-1.820	1868.55	2.23
0.007	0.024	0.042	-1.651	927.07	1.96
0.015	0.037	0.126	-1.494	614.29	1.81
0.027	0.049	0.203	-1.348	457.34	1.71
0.041	0.061	0.286	-1.211	363.18	1.63
0.057	0.073	0.371	-1.084	300.16	1.56
0.074	0.086	0.456	-0.965	255.14	1.51
0.093	0.098	0.538	-0.855	221.31	1.47
0.113	0.110	0.615	-0.751	194.94	1.43
0.134	0.122	0.685	-0.655	173.78	1.39
0.156	0.134	0.749	-0.566	156.42	1.37
0.179	0.147	0.805	-0.483	141.90	1.34
0.202	0.159	0.854	-0.406	129.57	1.31
0.225	0.171	0.895	-0.334	118.95	1.29
0.249	0.183	0.929	-0.267	109.70	1.27
0.273	0.196	0.956	-0.206	101.56	1.26
0.295	0.208	0.976	-0.148	94.33	1.24
0.320	0.220	0.990	-0.095	87.87	1.22
0.343	0.232	0.997	-0.046	82.04	1.21
0.367	0.244	1.000	0.000	76.75	1.20
0.437	0.282	0.979	0.120	63.05	1.16
0.503	0.320	0.926	0.214	52.23	1.14
0.564	0.358	0.852	0.287	43.32	1.11
0.621	0.396	0.768	0.342	35.73	1.09
0.672	0.433	0.680	0.383	29.08	1.08
0.715	0.471	0.592	0.412	23.07	1.07
0.759	0.509	0.509	0.433	17.53	1.05
0.796	0.547	0.433	0.446	12.28	1.04
0.829	0.584	0.363	0.454	7.22	1.04
0.855	0.622	0.301	0.458	2.25	1.03
0.868	0.639	0.276	0.458	0.00	1.03
0.881	0.660	0.247	0.457	-2.74	1.02
0.903	0.698	0.199	0.455	-7.81	1.02
0.922	0.736	0.158	0.450	-13.04	1.02
0.939	0.773	0.123	0.443	-18.50	1.01
0.953	0.811	0.093	0.436	-24.27	1.01
0.965	0.849	0.068	0.428	-30.42	1.01
0.976	0.887	0.046	0.419	-37.04	1.00
0.985	0.924	0.028	0.409	-44.21	1.00
0.993	0.962	0.013	0.400	-52.15	1.00
1.000	1.000	-0.000	0.391	-60.44	1.00

SPALL DYNAMICS
HIGH PRESSURE LIMIT ANALYSIS

```
             WAVELENGTH =    0.56234 FEET
MAXIMUM SURFACE EXCURSION =   -0.04440 FEET PER THOUSAND PSI SQUARED
           CLOSURE DEPTH =    1.35239 FEET
            CLOSURE TIME =    0.01458 SECONDS PER THOUSAND PSI
```

TIME	SPALL THICKNESS	SURFACE POSITION	SURFACE VELOCITY	SURFACE ACCELERATION (IN GEES)	LOWER CAVITY BOUNDARY
0.000	0.000	0.000	-2.000	*******	*******
0.002	0.013	0.017	-1.820	1406.30	2.30
0.007	0.026	0.062	-1.653	698.54	2.02
0.016	0.039	0.126	-1.496	462.52	1.86
0.027	0.052	0.202	-1.350	344.42	1.75
0.041	0.064	0.285	-1.213	273.49	1.66
0.057	0.077	0.370	-1.086	226.15	1.60
0.074	0.090	0.455	-0.967	192.27	1.54
0.093	0.103	0.537	-0.857	166.82	1.49
0.114	0.116	0.614	-0.754	146.98	1.45
0.135	0.129	0.684	-0.658	131.06	1.42
0.157	0.142	0.748	-0.568	118.00	1.39
0.180	0.155	0.805	-0.485	107.07	1.36
0.203	0.167	0.854	-0.408	97.79	1.33
0.226	0.180	0.895	-0.336	89.80	1.31
0.250	0.193	0.929	-0.269	82.85	1.29
0.274	0.206	0.956	-0.207	76.72	1.27
0.298	0.219	0.976	-0.149	71.29	1.25
0.322	0.232	0.990	-0.095	66.42	1.24
0.345	0.245	0.997	-0.046	62.04	1.22
0.369	0.258	1.000	0.000	58.07	1.21
0.433	0.295	0.982	0.114	48.39	1.17
0.497	0.332	0.934	0.205	40.64	1.15
0.555	0.369	0.867	0.276	34.21	1.12
0.610	0.406	0.789	0.331	28.70	1.10
0.660	0.443	0.707	0.374	23.87	1.09
0.705	0.480	0.623	0.406	19.52	1.07
0.745	0.517	0.542	0.429	15.52	1.06
0.782	0.555	0.467	0.446	11.76	1.05
0.815	0.592	0.397	0.456	8.17	1.04
0.844	0.629	0.333	0.462	4.47	1.04
0.870	0.666	0.276	0.465	1.20	1.03
0.879	0.679	0.258	0.465	-0.00	1.03
0.893	0.703	0.226	0.464	-2.27	1.02
0.914	0.740	0.181	0.462	-5.51	1.02
0.931	0.777	0.143	0.457	-9.45	1.01
0.947	0.814	0.109	0.452	-13.25	1.01
0.961	0.852	0.080	0.445	-17.24	1.01
0.973	0.889	0.055	0.437	-21.47	1.01
0.983	0.926	0.034	0.429	-25.98	1.00
0.992	0.963	0.016	0.421	-30.84	1.00
1.000	1.000	-0.000	0.412	-36.10	1.00

SPALL DYNAMICS
HIGH PRESSURE LIMIT ANALYSIS

WAVELENGTH =	0.74989 FEET
MAXIMUM SURFACE EXCURSION =	-0.05908 FEET PER THOUSAND PSI SQUARED
CLOSURE DEPTH =	1.70029 FEET
CLOSURE TIME =	0.01919 SECONDS PER THOUSAND PSI

TIME	SPALL THICKNESS	SURFACE POSITION	SURFACE VELOCITY	SURFACE ACCELERATION (IN GEES)	LOWER CAVITY BOUNDARY
0.000	0.000	0.000	-2.000	*******	******
0.002	0.014	0.017	-1.821	1059.42	2.38
0.007	0.027	0.062	-1.654	526.48	2.08
0.016	0.041	0.125	-1.498	348.49	1.91
0.027	0.054	0.201	-1.352	259.73	1.79
0.041	0.068	0.284	-1.216	206.30	1.70
0.057	0.082	0.369	-1.089	170.64	1.63
0.075	0.095	0.454	-0.970	145.12	1.57
0.094	0.109	0.536	-0.860	125.95	1.52
0.114	0.122	0.612	-0.756	111.01	1.48
0.135	0.136	0.683	-0.660	99.02	1.44
0.159	0.150	0.747	-0.571	89.18	1.41
0.181	0.163	0.804	-0.487	80.95	1.38
0.204	0.177	0.853	-0.410	73.96	1.35
0.228	0.190	0.894	-0.338	67.95	1.33
0.252	0.204	0.929	-0.270	62.71	1.30
0.275	0.218	0.956	-0.208	58.10	1.28
0.300	0.231	0.976	-0.150	54.00	1.27
0.324	0.245	0.990	-0.096	50.34	1.25
0.348	0.258	0.997	-0.046	47.04	1.23
0.372	0.272	1.000	-0.000	44.05	1.22
0.433	0.308	0.984	0.108	37.23	1.18
0.492	0.345	0.942	0.195	31.70	1.16
0.548	0.381	0.882	0.265	27.07	1.13
0.600	0.418	0.810	0.321	23.09	1.11
0.648	0.454	0.733	0.365	19.58	1.10
0.692	0.490	0.654	0.399	16.43	1.08
0.733	0.527	0.576	0.425	13.54	1.07
0.769	0.563	0.501	0.444	10.84	1.06
0.802	0.600	0.431	0.458	8.28	1.05
0.832	0.636	0.366	0.467	5.81	1.04
0.859	0.672	0.307	0.472	3.39	1.03
0.883	0.709	0.254	0.474	0.99	1.03
0.892	0.724	0.234	0.475	0.00	1.03
0.905	0.745	0.206	0.474	-1.42	1.02
0.924	0.782	0.164	0.472	-3.87	1.02
0.941	0.818	0.127	0.468	-6.39	1.01
0.955	0.854	0.094	0.463	-8.99	1.01
0.969	0.891	0.065	0.458	-11.72	1.01
0.981	0.927	0.040	0.451	-14.59	1.00
0.991	0.964	0.019	0.444	-17.63	1.00
1.000	1.000	0.000	0.436	-20.87	1.00

SPALL DYNAMICS
HIGH PRESSURE LIMIT ANALYSIS

```
                  WAVELENGTH =    1.00000 FEET
MAXIMUM SURFACE EXCURSION =   -0.07831 FEET PER THOUSAND PSI SQUARED
           CLOSURE DEPTH =     2.13135 FEET
           CLOSURE TIME =      0.02519 SECONDS PER THOUSAND PSI
```

TIME	SPALL THICKNESS	SURFACE POSITION	SURFACE VELOCITY	SURFACE ACCELERATION (IN GEES)	LOWER CAVITY BOUNDARY
0.000	0.000	0.000	-2.000	*******	*******
0.002	0.014	0.017	-1.822	799.40	2.46
0.007	0.029	0.051	-1.656	397.43	2.15
0.015	0.043	0.125	-1.500	263.31	1.97
0.029	0.058	0.200	-1.355	196.21	1.84
0.041	0.072	0.283	-1.219	155.91	1.75
0.057	0.086	0.368	-1.092	129.01	1.67
0.075	0.101	0.452	-0.974	109.76	1.61
0.094	0.115	0.534	-0.863	95.30	1.55
0.115	0.129	0.611	-0.760	84.03	1.51
0.136	0.144	0.682	-0.664	74.96	1.47
0.159	0.158	0.746	-0.574	67.56	1.43
0.182	0.173	0.803	-0.491	61.36	1.40
0.205	0.187	0.852	-0.413	56.09	1.37
0.229	0.201	0.894	-0.340	51.55	1.35
0.254	0.216	0.928	-0.273	47.60	1.32
0.279	0.230	0.955	-0.210	44.12	1.30
0.302	0.245	0.975	-0.151	41.04	1.28
0.326	0.259	0.989	-0.097	38.28	1.26
0.351	0.273	0.997	-0.047	35.79	1.25
0.375	0.288	1.000	0.000	33.54	1.23
0.433	0.323	0.986	0.102	28.74	1.20
0.489	0.359	0.949	0.185	24.91	1.17
0.541	0.395	0.895	0.254	21.48	1.14
0.591	0.430	0.830	0.310	18.60	1.12
0.637	0.466	0.758	0.356	16.07	1.11
0.680	0.501	0.683	0.392	13.78	1.09
0.720	0.537	0.609	0.420	11.70	1.08
0.755	0.573	0.536	0.442	9.76	1.07
0.790	0.608	0.466	0.459	7.92	1.06
0.820	0.644	0.401	0.471	6.17	1.05
0.849	0.679	0.340	0.479	4.47	1.04
0.873	0.715	0.284	0.484	2.80	1.03
0.895	0.751	0.234	0.487	1.15	1.03
0.909	0.775	0.201	0.487	-0.00	1.02
0.915	0.786	0.188	0.487	-0.51	1.02
0.934	0.822	0.147	0.486	-2.20	1.02
0.950	0.858	0.110	0.483	-3.92	1.01
0.965	0.893	0.077	0.479	-5.69	1.01
0.979	0.929	0.048	0.474	-7.53	1.01
0.990	0.964	0.023	0.469	-9.45	1.00
1.000	1.000	0.000	0.463	-11.48	1.00

SPALL DYNAMICS
HIGH PRESSURE LIMIT ANALYSIS

WAVELENGTH = 1.33352 FEET
MAXIMUM SURFACE EXCURSION = -0.10380 FEET PER THOUSAND PSI SQUARED
CLOSURE DEPTH = 2.66329 FEET
CLOSURE TIME = 0.03295 SECONDS PER THOUSAND PSI

TIME	SPALL THICKNESS	SURFACE POSITION	SURFACE VELOCITY	SURFACE ACCELERATION (IN GEES)	LOWER CAVITY BOUNDARY
0.000	0.000	0.000	-2.000	*******	*******
0.002	0.015	0.017	-1.823	604.54	2.56
0.009	0.030	0.061	-1.658	300.42	2.22
0.015	0.046	0.124	-1.503	199.27	2.03
0.025	0.061	0.199	-1.359	148.56	1.90
0.042	0.076	0.281	-1.223	118.10	1.80
0.055	0.091	0.366	-1.097	97.77	1.71
0.075	0.107	0.450	-0.979	83.23	1.65
0.095	0.122	0.532	-0.868	72.30	1.59
0.116	0.137	0.609	-0.765	63.79	1.54
0.137	0.152	0.680	-0.668	56.95	1.50
0.160	0.168	0.744	-0.579	51.35	1.46
0.183	0.183	0.801	-0.495	46.66	1.42
0.207	0.198	0.851	-0.416	42.68	1.39
0.231	0.213	0.893	-0.343	39.25	1.37
0.256	0.228	0.927	-0.275	36.27	1.34
0.280	0.244	0.955	-0.212	33.64	1.32
0.305	0.259	0.975	-0.153	31.31	1.30
0.329	0.274	0.989	-0.098	29.23	1.28
0.354	0.289	0.997	-0.047	27.35	1.26
0.379	0.305	1.000	0.000	25.65	1.24
0.433	0.339	0.988	0.096	22.29	1.21
0.485	0.374	0.955	0.176	19.49	1.18
0.535	0.409	0.907	0.244	17.11	1.16
0.582	0.444	0.848	0.300	15.04	1.14
0.627	0.478	0.782	0.346	13.20	1.12
0.669	0.513	0.712	0.384	11.55	1.10
0.709	0.548	0.641	0.415	10.04	1.09
0.744	0.583	0.570	0.440	8.64	1.07
0.777	0.618	0.501	0.460	7.33	1.06
0.809	0.652	0.436	0.475	6.08	1.05
0.836	0.687	0.374	0.486	4.88	1.04
0.862	0.722	0.316	0.495	3.71	1.04
0.886	0.757	0.262	0.500	2.57	1.03
0.907	0.791	0.213	0.503	1.43	1.02
0.927	0.826	0.168	0.504	0.29	1.02
0.931	0.835	0.157	0.504	0.00	1.02
0.944	0.861	0.127	0.504	-0.86	1.01
0.960	0.896	0.090	0.502	-2.02	1.01
0.975	0.930	0.057	0.500	-3.22	1.01
0.989	0.965	0.027	0.496	-4.45	1.00
1.000	1.000	0.000	0.491	-5.72	1.00

SPALL DYNAMICS
HIGH PRESSURE LIMIT ANALYSIS

WAVELENGTH =	1.77828	FEET	
MAXIMUM SURFACE EXCURSION =	-0.13732	FEET PER THOUSAND PSI SQUARED	
CLOSURE DEPTH =	3.31690	FEET	
CLOSURE TIME =	0.04290	SECONDS PER THOUSAND PSI	

TIME	SPALL THICKNESS	SURFACE POSITION	SURFACE VELOCITY	SURFACE ACCELERATION (IN GEES)	LOWER CAVITY BOUNDARY
0.000	0.000	0.000	-2.000	*******	******
0.002	0.016	0.017	-1.825	458.19	2.67
0.005	0.032	0.060	-1.661	227.98	2.31
0.015	0.048	0.123	-1.507	151.21	2.10
0.029	0.065	0.197	-1.364	112.80	1.96
0.042	0.081	0.279	-1.229	89.74	1.85
0.059	0.097	0.363	-1.103	74.34	1.76
0.075	0.113	0.448	-0.985	63.32	1.69
0.095	0.129	0.529	-0.874	55.05	1.63
0.115	0.145	0.606	-0.771	48.60	1.58
0.138	0.161	0.677	-0.674	43.42	1.53
0.161	0.178	0.742	-0.584	39.18	1.49
0.185	0.194	0.799	-0.500	35.43	1.45
0.209	0.210	0.849	-0.421	32.42	1.42
0.233	0.226	0.891	-0.348	30.02	1.39
0.259	0.242	0.926	-0.279	27.76	1.36
0.283	0.258	0.954	-0.215	25.78	1.34
0.308	0.274	0.975	-0.155	24.01	1.32
0.333	0.291	0.989	-0.100	22.44	1.29
0.358	0.307	0.997	-0.048	21.02	1.28
0.382	0.323	1.000	-0.000	19.73	1.26
0.433	0.357	0.989	0.090	17.38	1.22
0.482	0.391	0.961	0.168	15.40	1.20
0.530	0.424	0.918	0.234	13.69	1.17
0.573	0.458	0.865	0.290	12.20	1.15
0.618	0.492	0.804	0.337	10.87	1.13
0.658	0.526	0.739	0.377	9.68	1.11
0.695	0.560	0.671	0.410	8.59	1.10
0.732	0.594	0.603	0.438	7.58	1.08
0.765	0.628	0.536	0.461	6.63	1.07
0.795	0.661	0.471	0.479	5.74	1.06
0.823	0.695	0.408	0.494	4.89	1.05
0.852	0.729	0.348	0.505	4.06	1.04
0.876	0.763	0.292	0.514	3.26	1.04
0.899	0.797	0.239	0.520	2.48	1.03
0.919	0.831	0.191	0.524	1.70	1.02
0.939	0.865	0.146	0.527	0.93	1.02
0.956	0.898	0.104	0.527	0.15	1.01
0.959	0.905	0.097	0.527	0.00	1.01
0.972	0.932	0.066	0.527	-0.64	1.01
0.987	0.966	0.031	0.526	-1.43	1.00
1.000	1.000	0.000	0.523	-2.25	1.00

SPALL DYNAMICS
HIGH PRESSURE LIMIT ANALYSIS

WAVELENGTH = 2.37137 FEET
MAXIMUM SURFACE EXCURSION = -0.18122 FEET PER THOUSAND PSI SQUARED
CLOSURE DEPTH = 4.11643 FEET
CLOSURE TIME = 0.05556 SECONDS PER THOUSAND PSI

TIME	SPALL THICKNESS	SURFACE POSITION	SURFACE VELOCITY	SURFACE ACCELERATION (IN GEES)	LOWER CAVITY BOUNDARY
0.000	0.000	0.000	-2.000	*******	*******
0.002	0.017	0.016	-1.827	348.33	2.79
0.008	0.034	0.059	-1.665	173.46	2.41
0.015	0.051	0.121	-1.513	115.14	2.18
0.028	0.069	0.195	-1.370	85.96	2.03
0.042	0.086	0.276	-1.236	68.44	1.91
0.058	0.103	0.360	-1.110	56.75	1.82
0.077	0.120	0.444	-0.993	48.38	1.74
0.096	0.137	0.526	-0.882	42.10	1.67
0.117	0.154	0.603	-0.779	37.20	1.62
0.140	0.171	0.674	-0.682	33.27	1.57
0.163	0.188	0.739	-0.592	30.05	1.52
0.185	0.206	0.797	-0.507	27.35	1.48
0.211	0.223	0.847	-0.427	25.06	1.45
0.235	0.240	0.890	-0.353	23.09	1.42
0.261	0.257	0.925	-0.284	21.38	1.39
0.285	0.274	0.953	-0.219	19.87	1.36
0.311	0.291	0.974	-0.158	18.53	1.34
0.337	0.308	0.989	-0.102	17.34	1.31
0.362	0.325	0.997	-0.049	16.26	1.29
0.387	0.343	1.000	-0.000	15.28	1.27
0.433	0.375	0.991	0.085	13.64	1.24
0.481	0.408	0.966	0.159	12.24	1.21
0.525	0.441	0.928	0.224	11.02	1.19
0.569	0.474	0.880	0.280	9.95	1.16
0.610	0.507	0.825	0.328	8.99	1.14
0.649	0.540	0.764	0.370	8.13	1.12
0.686	0.573	0.701	0.406	7.34	1.11
0.721	0.606	0.635	0.436	6.60	1.09
0.754	0.638	0.570	0.462	5.92	1.08
0.785	0.671	0.505	0.483	5.28	1.07
0.814	0.704	0.442	0.501	4.47	1.06
0.841	0.737	0.381	0.516	4.09	1.05
0.867	0.770	0.322	0.528	3.53	1.04
0.890	0.803	0.267	0.538	2.98	1.03
0.912	0.836	0.214	0.545	2.44	1.03
0.933	0.869	0.165	0.551	1.91	1.02
0.952	0.901	0.119	0.554	1.39	1.01
0.969	0.934	0.076	0.557	0.86	1.01
0.985	0.967	0.037	0.558	0.33	1.00
0.993	0.988	0.013	0.558	0.00	1.00
1.000	1.000	0.000	0.558	-0.20	1.00

SPALL DYNAMICS
HIGH PRESSURE LIMIT ANALYSIS

WAVELENGTH = 3.16228 FEET
MAXIMUM SURFACE EXCURSION = -0.23842 FEET PER THOUSAND PSI SQUARED
CLOSURE DEPTH = 5.08998 FEET
CLOSURE TIME = 0.07153 SECONDS PER THOUSAND PSI

TIME	SPALL THICKNESS	SURFACE POSITION	SURFACE VELOCITY	SURFACE ACCELERATION (IN GEES)	LOWER CAVITY BOUNDARY
0.000	0.000	0.000	-2.000	*******	******
0.002	0.018	0.016	-1.830	265.82	2.93
0.009	0.036	0.059	-1.670	132.51	2.52
0.015	0.055	0.119	-1.519	88.05	2.28
0.029	0.073	0.193	-1.378	65.81	2.11
0.042	0.091	0.273	-1.245	52.45	1.98
0.059	0.109	0.357	-1.120	43.53	1.88
0.077	0.127	0.440	-1.003	37.16	1.80
0.097	0.145	0.522	-0.892	32.37	1.72
0.119	0.164	0.599	-0.789	28.63	1.66
0.141	0.182	0.670	-0.692	25.64	1.61
0.164	0.200	0.736	-0.601	23.18	1.56
0.189	0.218	0.794	-0.515	21.13	1.52
0.213	0.236	0.845	-0.435	19.39	1.48
0.239	0.254	0.888	-0.360	17.89	1.45
0.264	0.273	0.924	-0.290	16.58	1.41
0.289	0.291	0.952	-0.224	15.43	1.39
0.315	0.309	0.974	-0.162	14.42	1.36
0.341	0.327	0.989	-0.105	13.51	1.33
0.367	0.345	0.997	-0.050	12.69	1.31
0.393	0.363	1.000	0.000	11.94	1.29
0.437	0.395	0.992	0.081	10.80	1.26
0.480	0.427	0.970	0.152	9.80	1.23
0.523	0.459	0.937	0.215	8.94	1.20
0.564	0.491	0.894	0.271	8.16	1.18
0.603	0.523	0.843	0.320	7.47	1.16
0.641	0.554	0.787	0.364	6.85	1.14
0.677	0.586	0.728	0.401	6.27	1.12
0.711	0.618	0.666	0.434	5.74	1.11
0.744	0.650	0.602	0.463	5.25	1.09
0.775	0.682	0.538	0.488	4.79	1.08
0.804	0.714	0.475	0.510	4.35	1.07
0.832	0.745	0.413	0.528	3.93	1.06
0.859	0.777	0.353	0.543	3.53	1.05
0.882	0.809	0.295	0.556	3.15	1.04
0.905	0.841	0.239	0.567	2.77	1.03
0.927	0.873	0.186	0.576	2.40	1.02
0.947	0.905	0.135	0.583	2.04	1.02
0.965	0.936	0.087	0.589	1.69	1.01
0.984	0.968	0.042	0.593	1.33	1.01
1.000	1.000	-0.000	0.596	0.98	1.00

SPALL DYNAMICS
HIGH PRESSURE LIMIT ANALYSIS

WAVELENGTH = 4.21697 FEET
MAXIMUM SURFACE EXCURSION = -0.31244 FEET PER THOUSAND PSI SQUARED
CLOSURE DEPTH = 6.26985 FEET
CLOSURE TIME = 0.03144 SECONDS PER THOUSAND PSI

TIME	SPALL THICKNESS	SURFACE POSITION	SURFACE VELOCITY	SURFACE ACCELERATION (IN GEES)	LOWER CAVITY BOUNDARY
0.000	0.000	0.000	-2.000	*******	******
0.002	0.019	0.016	-1.833	203.79	3.09
0.008	0.039	0.057	-1.676	101.72	2.64
0.017	0.058	0.117	-1.527	67.48	2.38
0.025	0.077	0.189	-1.388	50.65	2.20
0.043	0.096	0.269	-1.256	40.42	2.06
0.059	0.116	0.352	-1.132	33.40	1.95
0.079	0.135	0.435	-1.015	28.72	1.86
0.099	0.154	0.516	-0.905	25.05	1.78
0.119	0.173	0.594	-0.802	22.19	1.72
0.142	0.193	0.666	-0.704	19.90	1.66
0.166	0.212	0.731	-0.613	18.02	1.60
0.190	0.231	0.790	-0.526	16.45	1.56
0.215	0.250	0.841	-0.445	15.12	1.52
0.241	0.270	0.885	-0.369	13.97	1.48
0.267	0.289	0.922	-0.297	12.97	1.44
0.293	0.308	0.951	-0.230	12.10	1.41
0.320	0.327	0.973	-0.167	11.32	1.38
0.346	0.347	0.988	-0.108	10.62	1.36
0.372	0.366	0.997	-0.052	10.00	1.33
0.399	0.385	1.000	-0.000	9.43	1.31
0.440	0.416	0.993	0.077	8.63	1.28
0.481	0.447	0.974	0.146	7.92	1.25
0.521	0.477	0.944	0.208	7.30	1.22
0.560	0.508	0.906	0.263	6.75	1.20
0.597	0.539	0.860	0.313	6.25	1.17
0.634	0.570	0.808	0.358	5.80	1.15
0.669	0.600	0.753	0.398	5.38	1.14
0.702	0.631	0.694	0.434	5.00	1.12
0.735	0.662	0.632	0.466	4.64	1.10
0.765	0.693	0.570	0.494	4.30	1.09
0.795	0.723	0.507	0.519	3.98	1.08
0.823	0.754	0.445	0.541	3.68	1.07
0.849	0.785	0.383	0.560	3.40	1.05
0.875	0.816	0.323	0.577	3.12	1.05
0.899	0.846	0.264	0.591	2.86	1.04
0.921	0.877	0.206	0.604	2.60	1.03
0.943	0.908	0.151	0.615	2.35	1.02
0.963	0.939	0.099	0.624	2.10	1.01
0.982	0.969	0.048	0.632	1.86	1.01
1.000	1.000	-0.000	0.638	1.62	1.00

SPALL DYNAMICS
HIGH PRESSURE LIMIT ANALYSIS

WAVELENGTH = 5.62341 FEET
MAXIMUM SURFACE EXCURSION = -0.40746 FEET PER THOUSAND PSI SQUARED
CLOSURE DEPTH = 7.69304 FEET
CLOSURE TIME = 0.11596 SECONDS PER THOUSAND PSI

TIME	SPALL THICKNESS	SURFACE POSITION	SURFACE VELOCITY	SURFACE ACCELERATION (IN GEES)	LOWER CAVITY BOUNDARY
0.000	0.000	0.000	-2.000	********	*******
0.002	0.020	0.015	-1.837	157.09	3.27
0.009	0.041	0.056	-1.683	78.54	2.78
0.017	0.061	0.115	-1.537	52.34	2.50
0.028	0.082	0.186	-1.400	39.24	2.30
0.043	0.102	0.264	-1.270	31.37	2.15
0.059	0.122	0.346	-1.147	26.12	2.03
0.079	0.143	0.429	-1.031	22.36	1.93
0.099	0.163	0.510	-0.921	19.54	1.85
0.120	0.184	0.587	-0.817	17.34	1.78
0.143	0.204	0.660	-0.719	15.58	1.71
0.167	0.224	0.726	-0.627	14.14	1.65
0.192	0.245	0.785	-0.540	12.93	1.60
0.217	0.265	0.837	-0.458	11.90	1.56
0.244	0.286	0.882	-0.380	11.02	1.52
0.270	0.306	0.919	-0.307	10.25	1.48
0.297	0.326	0.949	-0.238	9.58	1.44
0.324	0.347	0.972	-0.173	8.98	1.41
0.351	0.367	0.988	-0.112	8.45	1.38
0.379	0.388	0.997	-0.054	7.97	1.36
0.405	0.408	1.000	-0.000	7.53	1.33
0.444	0.438	0.994	0.073	6.97	1.30
0.482	0.467	0.977	0.140	6.47	1.27
0.520	0.497	0.951	0.201	6.03	1.24
0.557	0.526	0.916	0.257	5.63	1.21
0.593	0.556	0.875	0.308	5.27	1.19
0.629	0.586	0.827	0.354	4.94	1.17
0.662	0.615	0.775	0.396	4.64	1.15
0.695	0.645	0.719	0.434	4.36	1.13
0.725	0.674	0.660	0.469	4.09	1.12
0.757	0.704	0.600	0.501	3.85	1.10
0.785	0.734	0.537	0.529	3.62	1.09
0.813	0.763	0.475	0.555	3.40	1.07
0.842	0.793	0.412	0.578	3.19	1.06
0.869	0.822	0.349	0.599	2.99	1.05
0.892	0.852	0.288	0.617	2.80	1.04
0.915	0.882	0.227	0.634	2.62	1.03
0.938	0.911	0.168	0.649	2.44	1.02
0.960	0.941	0.110	0.662	2.27	1.01
0.981	0.970	0.054	0.673	2.10	1.01
1.000	1.000	0.000	0.684	1.94	1.00

SPALL DYNAMICS
HIGH PRESSURE LIMIT ANALYSIS

WAVELENGTH = 7.49894 FEET
MAXIMUM SURFACE EXCURSION = -0.52822 FEET PER THOUSAND PSI SQUARED
CLOSURE DEPTH = 9.40171 FEET
CLOSURE TIME = 0.14574 SECONDS PER THOUSAND PSI

TIME	SPALL THICKNESS	SURFACE POSITION	SURFACE VELOCITY	SURFACE ACCELERATION (IN GEES)	LOWER CAVITY BOUNDARY
0.000	0.000	0.000	-2.000	********	*******
0.002	0.022	0.015	-1.842	121.86	3.48
0.008	0.043	0.054	-1.692	62.05	2.94
0.017	0.065	0.112	-1.549	40.77	2.64
0.029	0.086	0.181	-1.414	30.63	2.42
0.043	0.108	0.258	-1.285	24.54	2.26
0.060	0.129	0.340	-1.164	20.47	2.13
0.078	0.151	0.422	-1.049	17.57	2.02
0.099	0.173	0.503	-0.940	15.38	1.92
0.121	0.194	0.580	-0.836	13.68	1.84
0.144	0.216	0.653	-0.738	12.32	1.77
0.168	0.237	0.719	-0.644	11.20	1.71
0.194	0.259	0.780	-0.556	10.27	1.65
0.220	0.280	0.833	-0.473	9.47	1.60
0.246	0.302	0.878	-0.393	8.79	1.56
0.273	0.323	0.917	-0.318	8.20	1.52
0.301	0.345	0.947	-0.247	7.68	1.48
0.328	0.367	0.971	-0.180	7.22	1.44
0.356	0.388	0.987	-0.117	6.81	1.41
0.384	0.410	0.997	-0.057	6.44	1.38
0.412	0.431	1.000	-0.000	6.10	1.35
0.448	0.460	0.995	0.070	5.70	1.32
0.484	0.488	0.980	0.135	5.35	1.29
0.520	0.517	0.957	0.196	5.03	1.26
0.555	0.545	0.925	0.251	4.74	1.23
0.590	0.573	0.887	0.303	4.48	1.2.
0.623	0.602	0.844	0.351	4.24	1.19
0.655	0.630	0.795	0.395	4.02	1.17
0.688	0.659	0.742	0.436	3.81	1.15
0.720	0.687	0.685	0.474	3.62	1.13
0.750	0.716	0.626	0.509	3.44	1.11
0.779	0.744	0.565	0.541	3.27	1.10
0.807	0.773	0.503	0.570	3.11	1.09
0.835	0.801	0.439	0.597	2.96	1.07
0.861	0.829	0.375	0.622	2.82	1.06
0.887	0.858	0.311	0.645	2.68	1.05
0.911	0.886	0.247	0.666	2.55	1.04
0.935	0.915	0.184	0.685	2.42	1.03
0.957	0.943	0.121	0.702	2.29	1.02
0.979	0.972	0.060	0.718	2.18	1.01
1.000	1.000	-0.000	0.733	2.06	1.00

SPALL DYNAMICS
HIGH PRESSURE LIMIT ANALYSIS

WAVELENGTH = 10.00000 FEET
MAXIMUM SURFACE EXCURSION = -0.67992 FEET PER THOUSAND PSI SQUARED
CLOSURE DEPTH = 11.44378 FEET
CLOSURE TIME = 0.18137 SECONDS PER THOUSAND PSI

TIME	SPALL THICKNESS	SURFACE POSITION	SURFACE VELOCITY	SURFACE ACCELERATION (IN GEES)	LOWER CAVITY BOUNDARY
0.000	0.000	0.000	-2.000	*******	*******
0.002	0.023	0.014	-1.848	95.20	3.72
0.009	0.045	0.052	-1.702	47.82	3.13
0.016	0.068	0.108	-1.564	32.02	2.79
0.029	0.091	0.176	-1.431	24.11	2.56
0.043	0.114	0.252	-1.305	19.37	2.38
0.060	0.136	0.332	-1.185	16.20	2.23
0.079	0.159	0.413	-1.071	13.94	2.11
0.099	0.182	0.494	-0.962	12.23	2.01
0.121	0.205	0.571	-0.858	10.91	1.92
0.145	0.227	0.644	-0.759	9.85	1.84
0.169	0.250	0.712	-0.665	8.98	1.78
0.195	0.273	0.773	-0.576	8.25	1.71
0.222	0.296	0.827	-0.490	7.63	1.66
0.249	0.318	0.874	-0.402	7.10	1.61
0.275	0.341	0.913	-0.332	6.64	1.56
0.304	0.364	0.945	-0.259	6.24	1.52
0.333	0.383	0.970	-0.189	5.88	1.48
0.361	0.409	0.987	-0.123	5.56	1.44
0.390	0.432	0.997	-0.060	5.27	1.41
0.419	0.455	1.000	-0.000	5.01	1.38
0.453	0.482	0.995	0.068	4.73	1.35
0.487	0.509	0.982	0.132	4.48	1.31
0.521	0.536	0.961	0.191	4.25	1.28
0.555	0.564	0.933	0.248	4.04	1.26
0.588	0.591	0.898	0.300	3.85	1.23
0.620	0.618	0.858	0.350	3.67	1.21
0.652	0.646	0.812	0.396	3.51	1.19
0.683	0.673	0.762	0.440	3.36	1.17
0.714	0.700	0.708	0.481	3.22	1.15
0.744	0.727	0.650	0.519	3.08	1.13
0.773	0.755	0.590	0.554	2.96	1.11
0.801	0.782	0.528	0.588	2.84	1.10
0.829	0.809	0.464	0.619	2.73	1.08
0.855	0.836	0.399	0.648	2.62	1.07
0.882	0.864	0.333	0.675	2.52	1.06
0.907	0.891	0.266	0.700	2.42	1.04
0.931	0.918	0.199	0.724	2.33	1.03
0.953	0.945	0.132	0.746	2.24	1.02
0.979	0.973	0.066	0.766	2.15	1.01
1.000	1.000	0.000	0.785	2.07	1.00

SPALL DYNAMICS
HIGH PRESSURE LIMIT ANALYSIS

WAVELENGTH = 13.33521 FEET
MAXIMUM SURFACE EXCURSION = -0.86790 FEET PER THOUSAND PSI SQUARED
CLOSURE DEPTH = 13.87364 FEET
CLOSURE TIME = 0.22331 SECONDS PER THOUSAND PSI

TIME	SPALL THICKNESS	SURFACE POSITION	SURFACE VELOCITY	SURFACE ACCELERATION (IN GEES)	LOWER CAVITY BOUNDARY
0.000	0.000	0.000	-2.000	********	*******
0.002	0.024	0.014	-1.854	74.96	4.00
0.009	0.048	0.050	-1.714	37.76	3.35
0.015	0.072	0.104	-1.580	25.36	2.98
0.029	0.096	0.170	-1.451	19.16	2.72
0.043	0.119	0.245	-1.328	15.44	2.52
0.059	0.143	0.323	-1.209	12.95	2.36
0.079	0.167	0.404	-1.096	11.18	2.22
0.099	0.191	0.484	-0.988	9.84	2.11
0.121	0.215	0.561	-0.884	8.90	2.01
0.145	0.239	0.635	-0.785	7.97	1.93
0.170	0.263	0.703	-0.690	7.29	1.85
0.195	0.287	0.765	-0.599	6.72	1.78
0.223	0.311	0.821	-0.511	6.23	1.72
0.251	0.334	0.849	-0.428	5.82	1.66
0.279	0.358	0.909	-0.348	5.46	1.61
0.305	0.382	0.943	-0.272	5.14	1.57
0.337	0.406	0.968	-0.200	4.86	1.52
0.367	0.430	0.986	-0.130	4.61	1.48
0.395	0.454	0.997	-0.063	4.38	1.44
0.425	0.478	1.000	-0.000	4.18	1.41
0.459	0.504	0.996	0.066	3.98	1.37
0.491	0.530	0.984	0.129	3.80	1.34
0.523	0.556	0.965	0.189	3.63	1.31
0.555	0.582	0.940	0.245	3.48	1.28
0.587	0.608	0.908	0.299	3.34	1.26
0.619	0.634	0.870	0.351	3.21	1.23
0.649	0.661	0.827	0.399	3.09	1.21
0.679	0.687	0.779	0.445	2.98	1.19
0.709	0.713	0.727	0.489	2.87	1.17
0.739	0.739	0.672	0.530	2.77	1.15
0.769	0.765	0.613	0.570	2.68	1.13
0.796	0.791	0.551	0.607	2.59	1.11
0.824	0.817	0.487	0.642	2.51	1.09
0.851	0.843	0.421	0.676	2.43	1.08
0.877	0.869	0.353	0.707	2.35	1.06
0.903	0.896	0.284	0.737	2.28	1.05
0.929	0.922	0.214	0.765	2.21	1.04
0.953	0.948	0.143	0.792	2.15	1.02
0.977	0.974	0.071	0.817	2.08	1.01
1.000	1.000	0.000	0.841	2.02	1.00

SPALL DYNAMICS
HIGH PRESSURE LIMIT ANALYSIS

WAVELENGTH =	17.78279 FEET
MAXIMUM SURFACE EXCURSION =	-1.09729 FEET PER THOUSAND PSI SQUARED
CLOSURE DEPTH =	16.75300 FEET
CLOSURE TIME =	0.27182 SECONDS PER THOUSAND PSI

TIME	SPALL THICKNESS	SURFACE POSITION	SURFACE VELOCITY	SURFACE ACCELERATION (IN GEES)	LOWER CAVITY BOUNDARY
0.000	0.000	0.000	-2.000	*******	*******
0.002	0.025	0.013	-1.861	59.51	4.32
0.007	0.050	0.048	-1.727	30.09	3.60
0.015	0.075	0.100	-1.598	20.29	3.19
0.028	0.100	0.164	-1.473	15.38	2.90
0.042	0.125	0.237	-1.353	12.44	2.68
0.059	0.150	0.314	-1.237	10.47	2.50
0.078	0.175	0.394	-1.125	9.07	2.35
0.099	0.200	0.473	-1.017	8.01	2.23
0.121	0.225	0.550	-0.913	7.19	2.12
0.145	0.250	0.624	-0.813	6.53	2.02
0.171	0.275	0.693	-0.717	5.99	1.94
0.197	0.300	0.757	-0.625	5.54	1.86
0.225	0.325	0.813	-0.535	5.16	1.79
0.253	0.350	0.863	-0.450	4.83	1.73
0.282	0.375	0.905	-0.367	4.55	1.67
0.311	0.400	0.940	-0.288	4.30	1.62
0.341	0.425	0.966	-0.212	4.08	1.57
0.372	0.450	0.985	-0.138	3.88	1.53
0.402	0.475	0.996	-0.068	3.70	1.48
0.433	0.500	1.000	0.000	3.54	1.44
0.464	0.525	0.996	0.065	3.40	1.41
0.495	0.550	0.986	0.127	3.27	1.37
0.525	0.575	0.969	0.187	3.14	1.34
0.555	0.600	0.945	0.245	3.03	1.31
0.585	0.625	0.915	0.300	2.93	1.28
0.617	0.650	0.880	0.353	2.83	1.26
0.647	0.675	0.839	0.404	2.74	1.23
0.676	0.700	0.794	0.453	2.66	1.21
0.705	0.725	0.744	0.499	2.58	1.18
0.735	0.750	0.690	0.544	2.50	1.16
0.763	0.775	0.632	0.587	2.43	1.14
0.792	0.800	0.571	0.628	2.37	1.12
0.819	0.825	0.507	0.668	2.31	1.11
0.847	0.850	0.440	0.705	2.25	1.09
0.874	0.875	0.371	0.742	2.19	1.07
0.900	0.900	0.300	0.776	2.14	1.06
0.925	0.925	0.227	0.809	2.08	1.04
0.951	0.950	0.152	0.841	2.03	1.03
0.975	0.975	0.077	0.871	1.99	1.01
1.000	1.000	-0.000	0.900	1.94	1.00

SPALL DYNAMICS
HIGH PRESSURE LIMIT ANALYSIS

WAVELENGTH = 23.71374 FEET
MAXIMUM SURFACE EXCURSION = -1.37248 FEET PER THOUSAND PSI SQUARED
CLOSURE DEPTH = 20.15203 FEET
CLOSURE TIME = 0.32692 SECONDS PER THOUSAND PSI

TIME	SPALL THICKNESS	SURFACE POSITION	SURFACE VELOCITY	SURFACE ACCELERATION (IN GEES)	LOWER CAVITY BOUNDARY
0.000	0.000	0.000	-2.000	*******	******
0.002	0.026	0.012	-1.869	47.64	4.69
0.007	0.052	0.046	-1.741	24.20	3.89
0.015	0.078	0.096	-1.617	16.39	3.43
0.029	0.104	0.158	-1.497	12.48	3.11
0.042	0.130	0.228	-1.380	10.13	2.87
0.059	0.157	0.304	-1.267	8.57	2.67
0.078	0.183	0.382	-1.156	7.45	2.50
0.099	0.209	0.461	-1.050	6.61	2.36
0.121	0.235	0.539	-0.946	5.95	2.24
0.143	0.261	0.613	-0.846	5.43	2.14
0.171	0.287	0.683	-0.748	5.00	2.04
0.199	0.313	0.747	-0.654	4.64	1.95
0.225	0.339	0.805	-0.562	4.34	1.88
0.254	0.365	0.857	-0.474	4.08	1.81
0.284	0.391	0.900	-0.388	3.85	1.74
0.314	0.418	0.936	-0.305	3.65	1.68
0.345	0.444	0.964	-0.225	3.48	1.63
0.375	0.470	0.984	-0.148	3.32	1.58
0.409	0.496	0.996	-0.073	3.18	1.53
0.440	0.522	1.000	0.000	3.05	1.48
0.469	0.546	0.997	0.064	2.94	1.45
0.499	0.570	0.987	0.127	2.85	1.41
0.529	0.594	0.971	0.187	2.76	1.38
0.558	0.618	0.949	0.246	2.67	1.34
0.587	0.641	0.922	0.302	2.60	1.31
0.615	0.665	0.888	0.357	2.52	1.28
0.645	0.689	0.850	0.410	2.46	1.26
0.675	0.713	0.807	0.462	2.39	1.23
0.703	0.737	0.758	0.512	2.33	1.21
0.732	0.761	0.706	0.560	2.28	1.18
0.760	0.785	0.649	0.606	2.22	1.16
0.789	0.809	0.589	0.651	2.17	1.14
0.815	0.833	0.525	0.695	2.13	1.12
0.843	0.857	0.457	0.737	2.08	1.10
0.870	0.880	0.387	0.778	2.04	1.08
0.897	0.904	0.314	0.817	2.00	1.06
0.923	0.928	0.239	0.855	1.96	1.05
0.949	0.952	0.161	0.892	1.92	1.03
0.975	0.976	0.081	0.927	1.88	1.01
1.000	1.000	-0.000	0.962	1.85	1.00

SPALL DYNAMICS
HIGH PRESSURE LIMIT ANALYSIS

WAVELENGTH = 31.62278 FEET
MAXIMUM SURFACE EXCURSION = -1.69661 FEET PER THOUSAND PSI SQUARED
CLOSURE DEPTH = 24.15062 FEET
CLOSURE TIME = 0.38834 SECONDS PER THOUSAND PSI

TIME	SPALL THICKNESS	SURFACE POSITION	SURFACE VELOCITY	SURFACE ACCELERATION (IN GEES)	LOWER CAVITY BOUNDARY
0.000	0.000	0.000	-2.000	*******	*******
0.002	0.027	0.012	-1.877	38.48	5.12
0.007	0.054	0.044	-1.756	19.65	4.23
0.016	0.081	0.091	-1.638	13.37	3.72
0.027	0.108	0.151	-1.523	10.23	3.36
0.041	0.136	0.220	-1.409	8.35	3.08
0.059	0.163	0.294	-1.299	7.09	2.86
0.077	0.190	0.371	-1.190	6.19	2.68
0.099	0.217	0.449	-1.085	5.52	2.52
0.120	0.244	0.526	-0.981	4.99	2.39
0.143	0.271	0.601	-0.880	4.57	2.27
0.171	0.298	0.672	-0.782	4.23	2.16
0.195	0.325	0.737	-0.686	3.94	2.06
0.225	0.352	0.797	-0.592	3.70	1.97
0.255	0.380	0.850	-0.501	3.49	1.89
0.285	0.407	0.895	-0.412	3.31	1.82
0.317	0.434	0.933	-0.325	3.15	1.75
0.349	0.461	0.962	-0.240	3.01	1.69
0.380	0.488	0.983	-0.158	2.88	1.63
0.413	0.515	0.996	-0.078	2.77	1.58
0.445	0.542	1.000	-0.000	2.67	1.53
0.474	0.565	0.997	0.064	2.59	1.49
0.503	0.588	0.988	0.127	2.52	1.45
0.531	0.611	0.973	0.188	2.45	1.41
0.559	0.634	0.953	0.248	2.39	1.38
0.588	0.657	0.927	0.306	2.33	1.35
0.615	0.680	0.895	0.363	2.27	1.32
0.645	0.702	0.859	0.418	2.22	1.29
0.673	0.725	0.817	0.473	2.17	1.26
0.702	0.748	0.771	0.525	2.13	1.23
0.730	0.771	0.719	0.577	2.08	1.21
0.758	0.794	0.664	0.627	2.04	1.18
0.786	0.817	0.604	0.676	2.01	1.16
0.813	0.840	0.540	0.724	1.97	1.14
0.841	0.863	0.472	0.770	1.93	1.11
0.869	0.886	0.401	0.816	1.90	1.09
0.895	0.908	0.327	0.860	1.87	1.07
0.922	0.931	0.249	0.903	1.84	1.05
0.948	0.954	0.169	0.945	1.81	1.03
0.974	0.977	0.086	0.985	1.73	1.02
1.000	1.000	-0.000	1.025	1.75	1.00

SPALL DYNAMICS
HIGH PRESSURE LIMIT ANALYSIS

WAVELENGTH = 42,16965 FEET
MAXIMUM SURFACE EXCURSION = -2,07102 FEET PER THOUSAND PSI SQUARED
CLOSURE DEPTH = 38,83996 FEET
CLOSURE TIME = 0,45555 SECONDS PER THOUSAND PSI

TIME	SPALL THICKNESS	SURFACE POSITION	SURFACE VELOCITY	SURFACE ACCELERATION (IN GEES)	LOWER CAVITY BOUNDARY
0,000	0,000	0,000	-2,000	*******	*******
0,002	0,028	0,011	-1,885	31,34	5,62
0,007	0,056	0,041	-1,772	16,10	4,62
0,015	0,084	0,087	-1,660	11,02	4,05
0,027	0,112	0,144	-1,550	8,48	3,65
0,041	0,140	0,211	-1,440	6,96	3,34
0,057	0,168	0,285	-1,333	5,94	3,09
0,075	0,196	0,359	-1,226	5,21	2,86
0,097	0,224	0,437	-1,122	4,47	2,71
0,120	0,252	0,514	-1,019	4,24	2,55
0,144	0,280	0,589	-0,918	3,90	2,42
0,170	0,309	0,660	-0,818	3,63	2,29
0,198	0,337	0,727	-0,720	3,39	2,19
0,225	0,365	0,788	-0,624	3,20	2,09
0,255	0,393	0,842	-0,529	3,03	2,00
0,287	0,421	0,889	-0,437	2,98	1,91
0,319	0,449	0,929	-0,346	2,75	1,84
0,351	0,477	0,960	-0,257	2,64	1,77
0,384	0,505	0,982	-0,169	2,54	1,70
0,418	0,533	0,995	-0,084	2,45	1,64
0,452	0,561	1,000	0,000	2,36	1,58
0,479	0,583	0,997	0,064	2,31	1,54
0,505	0,605	0,989	0,128	2,25	1,50
0,534	0,627	0,975	0,190	2,20	1,46
0,562	0,649	0,956	0,251	2,15	1,42
0,589	0,671	0,931	0,311	2,11	1,39
0,617	0,693	0,901	0,370	2,07	1,35
0,645	0,715	0,866	0,428	2,03	1,32
0,673	0,737	0,826	0,485	1,99	1,29
0,700	0,759	0,781	0,541	1,95	1,26
0,728	0,780	0,731	0,596	1,92	1,23
0,755	0,802	0,676	0,649	1,89	1,20
0,784	0,824	0,617	0,702	1,86	1,18
0,811	0,846	0,553	0,754	1,83	1,15
0,839	0,868	0,485	0,805	1,80	1,13
0,865	0,890	0,414	0,855	1,78	1,11
0,893	0,912	0,338	0,904	1,75	1,08
0,920	0,934	0,259	0,952	1,73	1,06
0,947	0,956	0,176	0,999	1,71	1,04
0,974	0,978	0,089	1,045	1,69	1,02
1,000	1,000	-0,000	1,090	1,66	1,00

SPALL DYNAMICS
HIGH PRESSURE LIMIT ANALYSIS

```
            WAVELENGTH =    56.23413 FEET
MAXIMUM SURFACE EXCURSION =   -2.49488 FEET PER THOUSAND PSI SQUARED
           CLOSURE DEPTH =    34.32446 FEET
            CLOSURE TIME =     0.52771 SECONDS PER THOUSAND PSI
```

TIME	SPALL THICKNESS	SURFACE POSITION	SURFACE VELOCITY	SURFACE ACCELERATION (IN GEES)	LOWER CAVITY BOUNDARY
0.000	0.000	0.000	-2.000	*******	*******
0.002	0.029	0.010	-1.894	25.74	6.19
0.007	0.058	0.039	-1.788	13.32	5.08
0.015	0.087	0.083	-1.682	9.18	4.40
0.025	0.116	0.138	-1.577	7.11	3.98
0.040	0.145	0.202	-1.472	5.87	3.63
0.057	0.173	0.273	-1.367	5.04	3.35
0.073	0.202	0.348	-1.264	4.45	3.12
0.096	0.231	0.424	-1.160	4.00	2.92
0.119	0.260	0.501	-1.058	3.45	2.75
0.143	0.289	0.576	-0.956	3.38	2.59
0.169	0.318	0.648	-0.856	3.15	2.45
0.197	0.347	0.716	-0.756	2.96	2.33
0.225	0.376	0.779	-0.657	2.80	2.22
0.255	0.405	0.835	-0.560	2.66	2.11
0.288	0.434	0.884	-0.463	2.54	2.02
0.320	0.463	0.925	-0.368	2.44	1.93
0.353	0.491	0.957	-0.274	2.35	1.85
0.388	0.520	0.981	-0.181	2.27	1.78
0.422	0.549	0.995	-0.090	2.19	1.71
0.458	0.578	1.000	0.000	2.12	1.64
0.484	0.599	0.997	0.065	2.08	1.59
0.510	0.620	0.990	0.129	2.04	1.55
0.537	0.641	0.977	0.192	2.00	1.51
0.564	0.663	0.958	0.255	1.96	1.47
0.591	0.684	0.935	0.317	1.93	1.43
0.618	0.705	0.906	0.378	1.90	1.39
0.645	0.726	0.872	0.439	1.87	1.36
0.672	0.747	0.833	0.498	1.84	1.33
0.700	0.768	0.789	0.557	1.81	1.29
0.727	0.789	0.740	0.615	1.78	1.26
0.755	0.810	0.686	0.673	1.76	1.23
0.782	0.831	0.628	0.729	1.74	1.20
0.809	0.852	0.564	0.785	1.71	1.17
0.837	0.873	0.497	0.840	1.69	1.15
0.864	0.895	0.424	0.895	1.67	1.12
0.892	0.916	0.347	0.948	1.65	1.09
0.919	0.937	0.267	1.001	1.63	1.07
0.945	0.958	0.182	1.053	1.62	1.05
0.973	0.979	0.093	1.104	1.60	1.02
1.000	1.000	-0.000	1.155	1.58	1.00

SPALL DYNAMICS
HIGH PRESSURE LIMIT ANALYSIS

WAVELENGTH =	74.98942 FEET		
MAXIMUM SURFACE EXCURSION =	-2.96504 FEET PER THOUSAND PSI SQUARED		
CLOSURE DEPTH =	40.72393 FEET		
CLOSURE TIME =	0.60377 SECONDS PER THOUSAND PSI		

TIME	SPALL THICKNESS	SURFACE POSITION	SURFACE VELOCITY	SURFACE ACCELERATION (IN GEES)	LOWER CAVITY BOUNDARY
0.000	0.000	0.000	-2.000	********	*******
0.002	0.030	0.010	-1.903	21.31	6.86
0.007	0.059	0.037	-1.804	11.12	5.60
0.013	0.089	0.079	-1.705	7.72	4.88
0.025	0.119	0.132	-1.605	6.02	4.37
0.039	0.148	0.194	-1.504	5.00	3.98
0.056	0.178	0.263	-1.403	4.32	3.66
0.074	0.208	0.336	-1.301	3.84	3.39
0.095	0.238	0.412	-1.199	3.47	3.17
0.113	0.267	0.489	-1.098	3.19	2.97
0.142	0.297	0.564	-0.996	2.96	2.80
0.169	0.327	0.637	-0.894	2.77	2.64
0.196	0.356	0.706	-0.793	2.62	2.50
0.225	0.386	0.770	-0.692	2.49	2.37
0.256	0.416	0.827	-0.591	2.37	2.25
0.289	0.445	0.878	-0.491	2.28	2.15
0.321	0.475	0.921	-0.391	2.19	2.05
0.355	0.505	0.955	-0.292	2.12	1.95
0.390	0.534	0.980	-0.194	2.05	1.87
0.425	0.564	0.995	-0.097	1.99	1.79
0.463	0.594	1.000	0.000	1.93	1.71
0.488	0.614	0.998	0.066	1.90	1.66
0.514	0.634	0.990	0.131	1.87	1.61
0.540	0.655	0.978	0.196	1.84	1.57
0.566	0.675	0.960	0.260	1.81	1.52
0.592	0.695	0.938	0.324	1.78	1.48
0.619	0.716	0.910	0.387	1.76	1.44
0.645	0.736	0.877	0.450	1.73	1.40
0.672	0.756	0.839	0.512	1.71	1.37
0.699	0.777	0.796	0.574	1.69	1.33
0.725	0.797	0.748	0.636	1.47	1.29
0.754	0.817	0.695	0.697	1.65	1.26
0.781	0.838	0.637	0.757	1.63	1.23
0.808	0.858	0.574	0.817	1.61	1.20
0.835	0.878	0.506	0.876	1.59	1.17
0.863	0.898	0.433	0.935	1.58	1.14
0.890	0.919	0.356	0.993	1.56	1.11
0.918	0.939	0.274	1.050	1.55	1.08
0.945	0.959	0.187	1.108	1.53	1.05
0.973	0.980	0.096	1.164	1.52	1.03
1.000	1.000	-0.000	1.220	1.51	1.00

SPALL DYNAMICS
HIGH PRESSURE LIMIT ANALYSIS

WAVELENGTH = 100.00008 FEET
MAXIMUM SURFACE EXCURSION = -3.47604 FEET PER THOUSAND PSI SQUARED
CLOSURE DEPTH = 48.17618 FEET
CLOSURE TIME = 0.68252 SECONDS PER THOUSAND PSI

TIME	SPALL THICKNESS	SURFACE POSITION	SURFACE VELOCITY	SURFACE ACCELERATION (IN GEES)	LOWER CAVITY BOUNDARY
0.000	0.000	0.000	-2.000	*******	*******
0.002	0.030	0.009	-1.911	17.78	7.63
0.007	0.061	0.035	-1.820	9.36	6.21
0.015	0.091	0.075	-1.727	6.56	5.39
0.023	0.122	0.126	-1.632	5.15	4.82
0.039	0.152	0.186	-1.536	4.31	4.37
0.055	0.182	0.255	-1.438	3.75	4.01
0.073	0.213	0.325	-1.339	3.35	3.71
0.094	0.243	0.400	-1.239	3.05	3.46
0.115	0.274	0.476	-1.137	2.81	3.23
0.141	0.304	0.552	-1.036	2.62	3.03
0.167	0.334	0.625	-0.933	2.47	2.86
0.193	0.365	0.695	-0.830	2.34	2.69
0.223	0.395	0.760	-0.727	2.23	2.55
0.255	0.426	0.820	-0.623	2.14	2.41
0.289	0.456	0.872	-0.519	2.06	2.29
0.322	0.486	0.916	-0.415	1.99	2.18
0.357	0.517	0.952	-0.311	1.93	2.07
0.393	0.547	0.978	-0.207	1.87	1.97
0.430	0.577	0.995	-0.103	1.82	1.88
0.467	0.608	1.000	-0.000	1.78	1.79
0.492	0.627	0.998	0.067	1.75	1.74
0.517	0.647	0.991	0.133	1.73	1.68
0.542	0.667	0.979	0.199	1.70	1.63
0.568	0.686	0.962	0.265	1.68	1.59
0.594	0.706	0.940	0.331	1.66	1.54
0.620	0.726	0.913	0.397	1.64	1.50
0.645	0.745	0.881	0.462	1.62	1.45
0.673	0.765	0.844	0.527	1.60	1.41
0.699	0.784	0.802	0.592	1.59	1.37
0.725	0.804	0.755	0.657	1.57	1.33
0.753	0.824	0.702	0.721	1.55	1.29
0.780	0.843	0.645	0.785	1.54	1.26
0.807	0.863	0.582	0.848	1.52	1.22
0.835	0.882	0.514	0.912	1.51	1.19
0.862	0.902	0.441	0.975	1.50	1.15
0.890	0.922	0.363	1.037	1.49	1.12
0.917	0.941	0.279	1.099	1.47	1.09
0.945	0.961	0.191	1.161	1.46	1.06
0.972	0.980	0.098	1.223	1.45	1.03
1.000	1.000	-0.000	1.284	1.44	1.00

SPALL DYNAMICS
HIGH PRESSURE LIMIT ANALYSIS

	WAVELENGTH =	133.35214 FEET
MAXIMUM SURFACE EXCURSION =		-4.02048 FEET PER THOUSAND PSI SQUARED
CLOSURE DEPTH =		56.83991 FEET
CLOSURE TIME =		0.76268 SECONDS PER THOUSAND PSI

TIME	SPALL THICKNESS	SURFACE POSITION	SURFACE VELOCITY	SURFACE ACCELERATION (IN GEES)	LOWER CAVITY BOUNDARY
0.000	0.000	0.000	-2.000	*******	******
0.002	0.031	0.009	-1.919	14.94	8.53
0.005	0.062	0.033	-1.835	7.95	6.92
0.014	0.093	0.071	-1.748	5.62	5.99
0.025	0.124	0.120	-1.658	4.45	5.34
0.039	0.155	0.179	-1.566	3.75	4.83
0.054	0.186	0.245	-1.472	3.29	4.43
0.072	0.217	0.315	-1.375	2.95	4.08
0.093	0.248	0.389	-1.277	2.70	3.79
0.115	0.279	0.465	-1.177	2.51	3.54
0.140	0.310	0.541	-1.075	2.35	3.31
0.166	0.341	0.614	-0.972	2.23	3.11
0.194	0.372	0.685	-0.867	2.12	2.92
0.224	0.403	0.752	-0.761	2.03	2.75
0.255	0.434	0.812	-0.655	1.95	2.60
0.289	0.465	0.866	-0.547	1.89	2.46
0.323	0.496	0.912	-0.439	1.83	2.33
0.358	0.527	0.950	-0.330	1.78	2.20
0.395	0.558	0.977	-0.220	1.73	2.09
0.433	0.589	0.994	-0.110	1.69	1.98
0.471	0.620	1.000	0.000	1.65	1.88
0.495	0.639	0.998	0.068	1.63	1.82
0.520	0.658	0.991	0.135	1.61	1.77
0.545	0.677	0.979	0.203	1.59	1.71
0.570	0.696	0.963	0.271	1.57	1.66
0.595	0.715	0.942	0.339	1.56	1.61
0.621	0.734	0.916	0.406	1.54	1.56
0.647	0.753	0.885	0.474	1.53	1.51
0.673	0.772	0.849	0.542	1.51	1.46
0.699	0.791	0.807	0.610	1.50	1.42
0.725	0.810	0.760	0.677	1.49	1.38
0.753	0.829	0.709	0.745	1.47	1.33
0.780	0.848	0.651	0.812	1.46	1.29
0.807	0.867	0.589	0.879	1.45	1.25
0.834	0.886	0.521	0.947	1.44	1.21
0.861	0.905	0.447	1.014	1.43	1.18
0.889	0.924	0.369	1.080	1.42	1.14
0.915	0.943	0.285	1.147	1.41	1.10
0.944	0.962	0.195	1.213	1.40	1.07
0.972	0.981	0.100	1.280	1.39	1.03
1.000	1.000	-0.000	1.346	1.38	1.00

SPALL DYNAMICS
HIGH PRESSURE LIMIT ANALYSIS

```
                WAVELENGTH =    177.82794 FEET
MAXIMUM SURFACE EXCURSION =     -4.58946 FEET PER THOUSAND PSI SQUARED
            CLOSURE DEPTH =     66.89820 FEET
            CLOSURE TIME =       0.84296 SECONDS PER THOUSAND PSI
```

TIME	SPALL THICKNESS	SURFACE POSITION	SURFACE VELOCITY	SURFACE ACCELERATION (IN GEES)	LOWER CAVITY BOUNDARY
0.000	0.000	0.000	-2.000	*******	*******
0.003	0.032	0.008	-1.927	12.44	9.56
0.005	0.063	0.032	-1.849	6.90	7.74
0.014	0.095	0.068	-1.768	4.96	6.68
0.024	0.126	0.116	-1.684	3.99	5.94
0.037	0.158	0.172	-1.596	3.30	5.37
0.053	0.189	0.236	-1.505	2.91	4.90
0.071	0.221	0.306	-1.411	2.64	4.51
0.091	0.253	0.379	-1.314	2.43	4.18
0.114	0.284	0.454	-1.215	2.26	3.89
0.139	0.316	0.530	-1.113	2.13	3.63
0.165	0.347	0.604	-1.009	2.03	3.40
0.193	0.379	0.676	-0.903	1.94	3.18
0.223	0.410	0.743	-0.796	1.86	2.99
0.253	0.442	0.805	-0.686	1.80	2.82
0.285	0.474	0.861	-0.575	1.74	2.65
0.323	0.505	0.909	-0.462	1.70	2.50
0.359	0.537	0.947	-0.348	1.65	2.36
0.397	0.568	0.976	-0.233	1.61	2.23
0.435	0.600	0.994	-0.117	1.58	2.11
0.473	0.631	1.000	-0.000	1.55	1.99
0.493	0.650	0.998	0.069	1.53	1.92
0.523	0.668	0.991	0.138	1.52	1.86
0.547	0.687	0.980	0.207	1.50	1.80
0.572	0.705	0.964	0.277	1.49	1.74
0.597	0.724	0.944	0.346	1.47	1.69
0.622	0.742	0.918	0.416	1.46	1.63
0.648	0.760	0.888	0.486	1.45	1.58
0.673	0.779	0.852	0.557	1.44	1.53
0.700	0.797	0.811	0.627	1.43	1.47
0.726	0.816	0.765	0.698	1.42	1.43
0.752	0.834	0.714	0.768	1.41	1.38
0.779	0.853	0.657	0.839	1.40	1.33
0.805	0.871	0.594	0.910	1.39	1.29
0.833	0.889	0.526	0.980	1.38	1.24
0.861	0.908	0.453	1.051	1.37	1.20
0.889	0.926	0.374	1.122	1.36	1.16
0.915	0.945	0.289	1.193	1.35	1.12
0.944	0.963	0.198	1.264	1.35	1.08
0.972	0.982	0.102	1.335	1.34	1.04
1.000	1.000	-0.000	1.406	1.33	1.00

SPALL DYNAMICS
HIGH PRESSURE LIMIT ANALYSIS

WAVELENGTH = 237.13737 FEET
MAXIMUM SURFACE EXCURSION = -5.17329 FEET PER THOUSAND PSI SQUARED
CLOSURE DEPTH = 78.56243 FEET
CLOSURE TIME = 0.92216 SECONDS PER THOUSAND PSI

TIME	SPALL THICKNESS	SURFACE POSITION	SURFACE VELOCITY	SURFACE ACCELERATION (IN GEES)	LOWER CAVITY BOUNDARY
0.000	0.000	0.000	-2.000	********	*******
0.002	0.032	0.008	-1.934	10.76	10.76
0.005	0.064	0.030	-1.863	5.87	8.69
0.014	0.096	0.065	-1.787	4.24	7.48
0.024	0.128	0.111	-1.708	3.42	6.64
0.037	0.160	0.166	-1.624	2.93	5.98
0.052	0.192	0.229	-1.536	2.61	5.46
0.070	0.224	0.297	-1.444	2.37	5.01
0.090	0.256	0.370	-1.349	2.20	4.63
0.113	0.289	0.444	-1.251	2.06	4.29
0.137	0.321	0.520	-1.150	1.95	4.00
0.164	0.353	0.594	-1.045	1.87	3.73
0.192	0.385	0.667	-0.938	1.79	3.49
0.222	0.417	0.735	-0.829	1.73	3.27
0.254	0.449	0.799	-0.716	1.67	3.07
0.288	0.481	0.856	-0.602	1.63	2.88
0.323	0.513	0.905	-0.485	1.59	2.70
0.360	0.545	0.945	-0.367	1.55	2.54
0.398	0.577	0.975	-0.246	1.52	2.39
0.437	0.609	0.994	-0.124	1.49	2.25
0.478	0.641	1.000	-0.000	1.46	2.11
0.501	0.659	0.998	0.070	1.45	2.04
0.525	0.677	0.992	0.140	1.44	1.97
0.549	0.695	0.981	0.211	1.43	1.90
0.573	0.713	0.965	0.282	1.41	1.84
0.599	0.731	0.945	0.354	1.40	1.78
0.623	0.749	0.920	0.426	1.39	1.71
0.649	0.767	0.890	0.498	1.38	1.65
0.674	0.785	0.855	0.571	1.37	1.60
0.700	0.803	0.815	0.644	1.36	1.54
0.725	0.821	0.769	0.717	1.36	1.48
0.752	0.839	0.718	0.791	1.35	1.43
0.779	0.856	0.661	0.865	1.34	1.38
0.805	0.874	0.599	0.939	1.33	1.33
0.833	0.892	0.531	1.013	1.32	1.28
0.860	0.910	0.458	1.087	1.32	1.23
0.888	0.928	0.378	1.162	1.31	1.18
0.915	0.946	0.293	1.237	1.30	1.13
0.944	0.964	0.201	1.312	1.30	1.09
0.972	0.982	0.104	1.387	1.29	1.04
1.000	1.000	-0.000	1.462	1.29	1.00

SPALL DYNAMICS
HIGH PRESSURE LIMIT ANALYSIS

```
                 WAVELENGTH =    316.22777 FEET
MAXIMUM SURFACE EXCURSION =     -5.76209 FEET PER THOUSAND PSI SQUARED
            CLOSURE DEPTH =     92.07664 FEET
            CLOSURE TIME =       0.99921 SECONDS PER THOUSAND PSI
```

TIME	SPALL THICKNESS	SURFACE POSITION	SURFACE VELOCITY	SURFACE ACCELERATION (IN GEES)	LOWER CAVITY BOUNDARY
0.000	0.000	0.000	-2.000	********	*******
0.002	0.032	0.007	-1.940	9.22	12.14
0.005	0.065	0.029	-1.875	5.10	9.78
0.013	0.097	0.063	-1.805	3.73	8.41
0.023	0.130	0.107	-1.730	3.04	7.44
0.035	0.162	0.161	-1.650	2.63	6.70
0.051	0.195	0.222	-1.565	2.36	6.09
0.069	0.227	0.289	-1.476	2.16	5.59
0.089	0.260	0.361	-1.383	2.01	5.15
0.112	0.292	0.435	-1.286	1.90	4.77
0.136	0.325	0.511	-1.184	1.81	4.43
0.163	0.357	0.586	-1.080	1.73	4.12
0.191	0.390	0.659	-0.971	1.67	3.84
0.221	0.422	0.728	-0.860	1.62	3.59
0.254	0.455	0.793	-0.745	1.57	3.36
0.288	0.487	0.851	-0.628	1.53	3.14
0.323	0.520	0.901	-0.507	1.50	2.94
0.361	0.552	0.943	-0.384	1.47	2.75
0.399	0.585	0.974	-0.258	1.44	2.58
0.439	0.617	0.995	-0.130	1.41	2.41
0.461	0.650	1.000	0.000	1.39	2.26
0.504	0.667	0.998	0.071	1.38	2.18
0.527	0.685	0.992	0.143	1.37	2.10
0.551	0.702	0.981	0.215	1.36	2.02
0.575	0.720	0.966	0.288	1.35	1.95
0.599	0.737	0.946	0.362	1.34	1.88
0.624	0.755	0.922	0.435	1.34	1.81
0.649	0.772	0.892	0.510	1.33	1.74
0.674	0.790	0.857	0.585	1.32	1.68
0.700	0.807	0.818	0.660	1.31	1.61
0.725	0.825	0.772	0.736	1.30	1.55
0.752	0.842	0.722	0.812	1.30	1.49
0.779	0.860	0.665	0.889	1.29	1.43
0.805	0.877	0.603	0.966	1.29	1.37
0.833	0.895	0.535	1.044	1.28	1.31
0.860	0.912	0.462	1.122	1.27	1.26
0.887	0.930	0.382	1.200	1.27	1.20
0.915	0.947	0.296	1.278	1.26	1.15
0.943	0.965	0.203	1.357	1.26	1.10
0.972	0.982	0.105	1.437	1.25	1.05
1.000	1.000	-0.000	1.516	1.25	1.00

SPALL DYNAMICS
HIGH PRESSURE LIMIT ANALYSIS

WAVELENGTH = 421.69650 FEET
MAXIMUM SURFACE EXCURSION = -6.34640 FEET PER THOUSAND PSI SQUARED
CLOSURE DEPTH = 107.72292 FEET
CLOSURE TIME = 1.07321 SECONDS PER THOUSAND PSI

TIME	SPALL THICKNESS	SURFACE POSITION	SURFACE VELOCITY	SURFACE ACCELERATION (IN GEES)	LOWER CAVITY BOUNDARY
0.000	0.000	0.000	-2.000	*******	*******
0.001	0.033	0.007	-1.947	7.95	13.74
0.005	0.066	0.028	-1.887	4.47	11.05
0.013	0.099	0.060	-1.822	3.31	9.48
0.023	0.131	0.103	-1.751	2.73	8.38
0.036	0.164	0.156	-1.674	2.38	7.53
0.051	0.197	0.216	-1.592	2.15	6.83
0.069	0.230	0.282	-1.506	1.98	6.25
0.089	0.263	0.353	-1.414	1.86	5.75
0.110	0.296	0.427	-1.318	1.76	5.31
0.133	0.329	0.502	-1.217	1.68	4.92
0.161	0.362	0.577	-1.112	1.62	4.57
0.190	0.394	0.651	-1.003	1.57	4.25
0.221	0.427	0.721	-0.890	1.52	3.96
0.253	0.460	0.787	-0.773	1.48	3.69
0.287	0.493	0.846	-0.652	1.45	3.44
0.323	0.526	0.898	-0.528	1.42	3.21
0.361	0.559	0.941	-0.401	1.40	2.99
0.400	0.592	0.973	-0.270	1.37	2.79
0.441	0.624	0.993	-0.137	1.35	2.60
0.483	0.657	1.000	0.000	1.33	2.42
0.505	0.674	0.998	0.072	1.33	2.33
0.529	0.692	0.992	0.145	1.32	2.25
0.553	0.709	0.982	0.219	1.31	2.16
0.575	0.726	0.967	0.294	1.30	2.08
0.600	0.743	0.947	0.369	1.29	2.00
0.625	0.760	0.923	0.444	1.29	1.92
0.650	0.777	0.894	0.521	1.28	1.84
0.675	0.794	0.860	0.598	1.27	1.77
0.700	0.812	0.820	0.676	1.27	1.70
0.725	0.829	0.775	0.754	1.26	1.63
0.752	0.846	0.725	0.833	1.26	1.56
0.779	0.863	0.669	0.912	1.25	1.49
0.805	0.880	0.607	0.992	1.25	1.42
0.832	0.897	0.539	1.073	1.24	1.36
0.860	0.914	0.465	1.154	1.24	1.30
0.887	0.931	0.385	1.235	1.23	1.23
0.915	0.949	0.298	1.317	1.23	1.17
0.943	0.966	0.205	1.400	1.22	1.11
0.971	0.983	0.106	1.483	1.22	1.06
1.000	1.000	-0.000	1.566	1.21	1.00

SPALL DYNAMICS
HIGH PRESSURE LIMIT ANALYSIS

```
              WAVELENGTH =  562.34133 FEET
MAXIMUM SURFACE EXCURSION =   -6.91771 FEET PER THOUSAND PSI SQUARED
           CLOSURE DEPTH =  125.82708 FEET
            CLOSURE TIME =    1.14345 SECONDS PER THOUSAND PSI
```

TIME	SPALL THICKNESS	SURFACE POSITION	SURFACE VELOCITY	SURFACE ACCELERATION (IN GEES)	LOWER CAVITY BOUNDARY
0.000	0.000	0.000	-2.000	*******	*******
0.001	0.033	0.007	-1.952	6.99	15.59
0.005	0.066	0.027	-1.898	3.94	12.51
0.013	0.100	0.058	-1.837	2.96	10.72
0.023	0.133	0.100	-1.769	2.47	9.46
0.035	0.166	0.152	-1.696	2.17	8.48
0.050	0.199	0.210	-1.617	1.97	7.69
0.068	0.232	0.276	-1.533	1.83	7.02
0.087	0.266	0.346	-1.443	1.73	6.45
0.109	0.299	0.419	-1.348	1.65	5.94
0.134	0.332	0.495	-1.247	1.58	5.49
0.160	0.365	0.570	-1.142	1.53	5.09
0.189	0.398	0.644	-1.032	1.48	4.72
0.220	0.431	0.715	-0.917	1.44	4.39
0.252	0.465	0.782	-0.798	1.41	4.08
0.287	0.498	0.842	-0.675	1.38	3.79
0.323	0.531	0.895	-0.548	1.36	3.52
0.361	0.564	0.939	-0.416	1.34	3.28
0.401	0.597	0.972	-0.281	1.32	3.04
0.443	0.631	0.993	-0.142	1.30	2.82
0.485	0.664	1.000	0.000	1.28	2.61
0.509	0.681	0.998	0.073	1.28	2.51
0.531	0.697	0.992	0.148	1.27	2.42
0.554	0.714	0.982	0.223	1.26	2.32
0.579	0.731	0.967	0.299	1.26	2.23
0.602	0.748	0.948	0.375	1.25	2.14
0.625	0.765	0.924	0.453	1.25	2.05
0.650	0.781	0.895	0.531	1.24	1.96
0.675	0.798	0.861	0.610	1.23	1.88
0.701	0.815	0.822	0.690	1.23	1.79
0.728	0.832	0.777	0.771	1.22	1.71
0.752	0.849	0.727	0.852	1.22	1.64
0.779	0.866	0.671	0.934	1.22	1.56
0.805	0.882	0.610	1.016	1.21	1.48
0.832	0.899	0.542	1.100	1.21	1.41
0.859	0.916	0.468	1.184	1.20	1.34
0.887	0.933	0.387	1.268	1.20	1.27
0.915	0.950	0.301	1.353	1.20	1.20
0.943	0.966	0.207	1.439	1.19	1.13
0.971	0.983	0.107	1.525	1.19	1.06
1.000	1.000	-0.000	1.612	1.18	1.00

SPALL DYNAMICS
HIGH PRESSURE LIMIT ANALYSIS

```
              WAVELENGTH =   749.89421 FEET
MAXIMUM SURFACE EXCURSION =    -7.46873 FEET PER THOUSAND PSI SQUARED
            CLOSURE DEPTH =   146.76588 FEET
             CLOSURE TIME =     1.20940 SECONDS PER THOUSAND PSI
```

TIME	SPALL THICKNESS	SURFACE POSITION	SURFACE VELOCITY	SURFACE ACCELERATION (IN GEES)	LOWER CAVITY BOUNDARY
0.000	0.000	0.000	-2.000	*******	*******
0.001	0.033	0.007	-1.957	6.01	17.72
0.005	0.067	0.026	-1.907	3.50	14.20
0.013	0.100	0.056	-1.850	2.47	12.15
0.022	0.134	0.097	-1.787	2.25	10.71
0.035	0.167	0.148	-1.717	2.00	9.59
0.049	0.201	0.206	-1.640	1.83	8.68
0.067	0.234	0.270	-1.558	1.71	7.91
0.085	0.268	0.340	-1.469	1.42	7.25
0.109	0.301	0.413	-1.375	1.55	6.67
0.133	0.335	0.488	-1.275	1.49	6.16
0.159	0.368	0.563	-1.170	1.45	5.69
0.189	0.402	0.638	-1.059	1.41	5.27
0.219	0.435	0.709	-0.943	1.38	4.88
0.251	0.469	0.777	-0.822	1.35	4.53
0.286	0.502	0.838	-0.696	1.33	4.20
0.323	0.536	0.892	-0.566	1.31	3.89
0.361	0.569	0.937	-0.431	1.29	3.60
0.402	0.603	0.971	-0.292	1.27	3.33
0.444	0.636	0.992	-0.148	1.26	3.08
0.489	0.670	1.000	-0.000	1.24	2.84
0.510	0.686	0.998	0.074	1.24	2.72
0.532	0.703	0.992	0.150	1.23	2.61
0.555	0.719	0.982	0.226	1.23	2.50
0.579	0.736	0.968	0.304	1.22	2.40
0.602	0.752	0.949	0.382	1.22	2.29
0.627	0.769	0.925	0.461	1.21	2.19
0.651	0.785	0.896	0.541	1.21	2.10
0.675	0.802	0.863	0.622	1.20	2.00
0.701	0.818	0.824	0.703	1.20	1.91
0.727	0.835	0.779	0.786	1.19	1.82
0.752	0.851	0.729	0.869	1.19	1.73
0.779	0.868	0.674	0.954	1.19	1.64
0.805	0.884	0.612	1.039	1.18	1.55
0.832	0.901	0.544	1.124	1.18	1.47
0.859	0.917	0.470	1.211	1.18	1.39
0.887	0.934	0.390	1.298	1.17	1.31
0.915	0.950	0.303	1.386	1.17	1.23
0.943	0.967	0.209	1.475	1.17	1.15
0.971	0.983	0.108	1.565	1.16	1.07
1.000	1.000	-0.000	1.655	1.16	1.00

SPALL DYNAMICS
HIGH PRESSURE LIMIT ANALYSIS

WAVELENGTH = 1000.00008 FEET
MAXIMUM SURFACE EXCURSION = -7.99364 FEET PER THOUSAND PSI SQUARED
CLOSURE DEPTH = 170.97435 FEET
CLOSURE TIME = 1.27079 SECONDS PER THOUSAND PSI

TIME	SPALL THICKNESS	SURFACE POSITION	SURFACE VELOCITY	SURFACE ACCELERATION (IN GEES)	LOWER CAVITY BOUNDARY
0.000	0.000	0.000	-2.000	********	*******
0.001	0.034	0.006	-1.962	5.27	20.19
0.005	0.067	0.025	-1.916	3.13	16.16
0.013	0.101	0.055	-1.863	2.42	13.81
0.022	0.135	0.095	-1.802	2.06	12.15
0.034	0.169	0.144	-1.735	1.85	10.87
0.049	0.202	0.201	-1.661	1.71	9.82
0.065	0.236	0.265	-1.580	1.61	8.94
0.085	0.270	0.334	-1.493	1.53	8.18
0.108	0.304	0.407	-1.400	1.47	7.52
0.132	0.337	0.482	-1.300	1.42	6.92
0.159	0.371	0.557	-1.195	1.38	6.39
0.187	0.405	0.632	-1.084	1.35	5.90
0.219	0.438	0.704	-0.967	1.32	5.46
0.251	0.472	0.772	-0.844	1.30	5.04
0.286	0.506	0.835	-0.716	1.28	4.66
0.323	0.540	0.890	-0.583	1.26	4.31
0.362	0.573	0.935	-0.444	1.25	3.98
0.402	0.607	0.970	-0.301	1.23	3.66
0.445	0.641	0.992	-0.153	1.22	3.37
0.489	0.675	1.000	0.000	1.21	3.09
0.511	0.691	0.998	0.075	1.20	2.96
0.534	0.707	0.992	0.152	1.20	2.84
0.555	0.723	0.982	0.229	1.19	2.71
0.580	0.740	0.968	0.308	1.19	2.59
0.603	0.756	0.949	0.388	1.18	2.48
0.627	0.772	0.926	0.468	1.18	2.36
0.652	0.788	0.897	0.550	1.18	2.25
0.676	0.805	0.864	0.632	1.17	2.14
0.701	0.821	0.825	0.716	1.17	2.04
0.727	0.837	0.781	0.800	1.17	1.93
0.753	0.854	0.731	0.886	1.16	1.83
0.779	0.870	0.676	0.972	1.16	1.73
0.805	0.886	0.614	1.059	1.16	1.63
0.832	0.902	0.546	1.147	1.15	1.54
0.859	0.919	0.472	1.236	1.15	1.44
0.887	0.935	0.392	1.326	1.15	1.35
0.915	0.951	0.304	1.417	1.15	1.26
0.943	0.967	0.210	1.508	1.14	1.17
0.971	0.984	0.109	1.601	1.14	1.09
1.000	1.000	-0.000	1.694	1.14	1.00

SPALL DYNAMICS
HIGH PRESSURE LIMIT ANALYSIS

WAVELENGTH = 1333.52143 FEET
MAXIMUM SURFACE EXCURSION = -8.48813 FEET PER THOUSAND PSI SQUARED
CLOSURE DEPTH = 198.95529 FEET
CLOSURE TIME = 1.32733 SECONDS PER THOUSAND PSI

TIME	SPALL THICKNESS	SURFACE POSITION	SURFACE VELOCITY	SURFACE ACCELERATION (IN GEES)	LOWER CAVITY BOUNDARY
0.000	0.000	0.000	-2.000	*******	*******
0.001	0.034	0.006	-1.966	4.45	23.04
0.005	0.068	0.024	-1.923	2.92	18.42
0.012	0.102	0.054	-1.874	2.21	15.72
0.022	0.136	0.093	-1.816	1.91	13.82
0.034	0.170	0.141	-1.752	1.73	12.34
0.048	0.204	0.198	-1.680	1.60	11.14
0.065	0.238	0.261	-1.601	1.52	10.13
0.085	0.272	0.329	-1.515	1.45	9.26
0.107	0.305	0.401	-1.423	1.40	8.49
0.131	0.339	0.476	-1.324	1.36	7.81
0.159	0.373	0.552	-1.218	1.33	7.19
0.186	0.407	0.627	-1.106	1.30	6.63
0.217	0.441	0.700	-0.988	1.28	6.12
0.250	0.475	0.769	-0.864	1.26	5.64
0.285	0.509	0.832	-0.734	1.24	5.20
0.322	0.543	0.887	-0.598	1.22	4.79
0.362	0.577	0.934	-0.457	1.21	4.41
0.403	0.611	0.969	-0.310	1.20	4.05
0.446	0.645	0.992	-0.158	1.19	3.71
0.491	0.679	1.000	-0.000	1.18	3.39
0.512	0.695	0.998	0.076	1.17	3.24
0.535	0.711	0.992	0.154	1.17	3.10
0.557	0.727	0.982	0.232	1.17	2.96
0.580	0.743	0.968	0.312	1.16	2.82
0.604	0.759	0.950	0.393	1.16	2.69
0.629	0.775	0.926	0.475	1.16	2.56
0.652	0.791	0.898	0.558	1.15	2.43
0.677	0.807	0.865	0.642	1.15	2.31
0.702	0.823	0.826	0.727	1.15	2.19
0.727	0.839	0.782	0.813	1.14	2.07
0.753	0.855	0.733	0.900	1.14	1.95
0.779	0.872	0.677	0.989	1.14	1.84
0.805	0.888	0.616	1.078	1.14	1.73
0.832	0.904	0.548	1.168	1.13	1.62
0.859	0.920	0.474	1.259	1.13	1.51
0.887	0.936	0.393	1.351	1.13	1.40
0.914	0.952	0.306	1.444	1.13	1.30
0.943	0.968	0.211	1.538	1.12	1.20
0.971	0.984	0.109	1.633	1.12	1.10
1.000	1.000	-0.000	1.729	1.12	1.00

SPALL DYNAMICS
HIGH PRESSURE LIMIT ANALYSIS

WAVELENGTH = 1778.27941 FEET
MAXIMUM SURFACE EXCURSION = -8.94928 FEET PER THOUSAND PSI SQUARED
CLOSURE DEPTH = 231.28994 FEET
CLOSURE TIME = 1.37910 SECONDS PER THOUSAND PSI

TIME	SPALL THICKNESS	SURFACE POSITION	SURFACE VELOCITY	SURFACE ACCELERATION (IN GEES)	LOWER CAVITY BOUNDARY
0.000	0.000	0.000	-2.000		
0.001	0.034	0.006	-1.969	*******	******
0.005	0.068	0.024	-1.930	4.12	26.33
0.012	0.102	0.052	-1.884	2.56	21.03
0.022	0.137	0.091	-1.829	2.04	17.93
0.034	0.171	0.139	-1.767	1.78	15.74
0.048	0.205	0.194	-1.697	1.62	14.05
0.065	0.239	0.257	-1.619	1.52	12.67
0.084	0.273	0.325	-1.535	1.44	11.51
0.105	0.307	0.397	-1.443	1.39	10.50
0.130	0.341	0.471	-1.344	1.34	9.62
0.157	0.375	0.547	-1.239	1.31	8.83
0.186	0.410	0.622	-1.126	1.28	8.12
0.215	0.444	0.696	-1.007	1.26	7.48
0.250	0.478	0.765	-0.882	1.24	6.88
0.285	0.512	0.829	-0.750	1.22	6.34
0.322	0.546	0.885	-0.612	1.21	5.83
0.362	0.580	0.935	-0.468	1.19	5.35
0.403	0.614	0.969	-0.318	1.18	4.91
0.445	0.648	0.992	-0.162	1.17	4.49
0.492	0.683	1.000	-0.000	1.16	4.10
0.514	0.698	0.998	0.077	1.15	3.73
0.535	0.714	0.992	0.156	1.15	3.56
0.559	0.730	0.983	0.235	1.15	3.40
0.581	0.746	0.969	0.316	1.14	3.24
0.603	0.762	0.950	0.398	1.14	3.09
0.628	0.778	0.927	0.481	1.14	2.93
0.652	0.794	0.899	0.565	1.13	2.79
0.677	0.810	0.866	0.651	1.13	2.64
0.702	0.825	0.828	0.737	1.13	2.50
0.727	0.841	0.784	0.825	1.13	2.36
0.753	0.857	0.734	0.914	1.12	2.22
0.779	0.873	0.679	1.004	1.12	2.09
0.805	0.889	0.617	1.095	1.12	1.96
0.832	0.905	0.550	1.187	1.12	1.83
0.859	0.921	0.475	1.280	1.11	1.71
0.887	0.937	0.395	1.374	1.11	1.58
0.914	0.952	0.307	1.469	1.11	1.46
0.943	0.968	0.212	1.565	1.11	1.34
0.971	0.984	0.110	1.663	1.11	1.23
1.000	1.000	-0.000	1.761	1.11	1.11
				1.10	1.00

SPALL DYNAMICS
HIGH PRESSURE LIMIT ANALYSIS

WAVELENGTH = 2371.37371 FEET
MAXIMUM SURFACE EXCURSION = -9.37549 FEET PER THOUSAND PSI SQUARED
CLOSURE DEPTH = 268.64923 FEET
CLOSURE TIME = 1.42616 SECONDS PER THOUSAND PSI

TIME	SPALL THICKNESS	SURFACE POSITION	SURFACE VELOCITY	SURFACE ACCELERATION (IN GEES)	LOWER CAVITY BOUNDARY
0.000	0.000	0.000	-2.000	*******	*******
0.001	0.034	0.006	-1.972	3.47	30.13
0.005	0.069	0.023	-1.937	2.34	24.04
0.012	0.103	0.051	-1.892	1.89	20.48
0.021	0.137	0.089	-1.840	1.67	17.97
0.033	0.171	0.136	-1.780	1.53	16.02
0.048	0.206	0.191	-1.712	1.44	14.43
0.065	0.240	0.253	-1.636	1.38	13.09
0.084	0.274	0.321	-1.552	1.33	11.94
0.105	0.309	0.392	-1.461	1.29	10.92
0.130	0.343	0.467	-1.363	1.27	10.01
0.155	0.377	0.543	-1.257	1.24	9.20
0.185	0.412	0.618	-1.145	1.22	8.45
0.215	0.446	0.692	-1.025	1.20	7.77
0.249	0.480	0.762	-0.898	1.19	7.13
0.284	0.514	0.826	-0.765	1.18	6.55
0.322	0.549	0.884	-0.625	1.16	6.00
0.362	0.583	0.931	-0.478	1.16	5.49
0.403	0.617	0.968	-0.325	1.15	5.01
0.447	0.652	0.992	-0.166	1.14	4.55
0.493	0.686	1.000	-0.000	1.13	4.12
0.515	0.702	0.998	0.078	1.13	3.93
0.537	0.717	0.992	0.157	1.13	3.75
0.559	0.733	0.983	0.238	1.12	3.57
0.582	0.749	0.969	0.319	1.12	3.39
0.605	0.764	0.950	0.402	1.12	3.22
0.629	0.780	0.927	0.485	1.12	3.05
0.653	0.796	0.900	0.572	1.11	2.88
0.677	0.812	0.867	0.659	1.11	2.72
0.702	0.827	0.828	0.746	1.11	2.56
0.727	0.843	0.785	0.835	1.11	2.41
0.753	0.859	0.735	0.926	1.10	2.25
0.779	0.874	0.680	1.017	1.10	2.10
0.805	0.890	0.619	1.110	1.10	1.96
0.832	0.906	0.551	1.203	1.10	1.81
0.859	0.921	0.477	1.298	1.10	1.67
0.887	0.937	0.396	1.394	1.10	1.53
0.914	0.953	0.308	1.491	1.09	1.40
0.943	0.969	0.213	1.590	1.09	1.26
0.971	0.984	0.110	1.689	1.09	1.13
1.000	1.000	-0.000	1.790	1.09	1.00

SPALL DYNAMICS
HIGH PRESSURE LIMIT ANALYSIS

WAVELENGTH = 3162.27766 FEET
MAXIMUM SURFACE EXCURSION = -9.76628 FEET PER THOUSAND PSI SQUARED
CLOSURE DEPTH = 311.80845 FEET
CLOSURE TIME = 1.46867 SECONDS PER THOUSAND PSI

TIME	SPALL THICKNESS	SURFACE POSITION	SURFACE VELOCITY	SURFACE ACCELERATION (IN GEES)	LOWER CAVITY BOUNDARY
0.000	0.000	0.000	-2.000	********	*******
0.001	0.034	0.006	-1.975	3.29	34.53
0.005	0.069	0.023	-1.942	2.15	27.52
0.012	0.103	0.050	-1.900	1.76	23.43
0.021	0.138	0.088	-1.850	1.57	20.54
0.033	0.172	0.134	-1.792	1.46	18.30
0.047	0.207	0.189	-1.725	1.38	16.47
0.064	0.241	0.250	-1.650	1.33	14.93
0.083	0.275	0.317	-1.568	1.29	13.60
0.105	0.310	0.389	-1.478	1.25	12.43
0.129	0.344	0.463	-1.380	1.23	11.38
0.156	0.379	0.539	-1.274	1.21	10.44
0.184	0.413	0.615	-1.161	1.19	9.58
0.215	0.448	0.689	-1.041	1.17	8.79
0.249	0.482	0.759	-0.913	1.16	8.06
0.284	0.517	0.824	-0.778	1.15	7.38
0.322	0.551	0.882	-0.636	1.14	6.75
0.362	0.585	0.930	-0.487	1.13	6.16
0.404	0.620	0.968	-0.332	1.13	5.60
0.448	0.654	0.992	-0.169	1.12	5.08
0.494	0.689	1.000	0.000	1.11	4.58
0.515	0.704	0.998	0.079	1.11	4.36
0.537	0.720	0.993	0.159	1.11	4.15
0.560	0.735	0.985	0.240	1.11	3.94
0.582	0.751	0.969	0.322	1.10	3.74
0.606	0.767	0.951	0.406	1.10	3.54
0.629	0.782	0.928	0.491	1.10	3.35
0.653	0.798	0.900	0.578	1.10	3.16
0.678	0.813	0.867	0.666	1.10	2.97
0.702	0.829	0.829	0.755	1.09	2.79
0.727	0.844	0.786	0.845	1.09	2.61
0.753	0.860	0.736	0.936	1.09	2.44
0.779	0.875	0.681	1.029	1.09	2.27
0.805	0.891	0.620	1.123	1.09	2.10
0.832	0.907	0.552	1.218	1.09	1.93
0.859	0.922	0.478	1.315	1.08	1.77
0.885	0.938	0.397	1.413	1.08	1.61
0.914	0.953	0.309	1.511	1.08	1.45
0.942	0.969	0.213	1.612	1.08	1.30
0.971	0.984	0.110	1.713	1.08	1.15
1.000	1.000	-0.000	1.815	1.08	1.00

SPALL DYNAMICS
HIGH PRESSURE LIMIT ANALYSIS

WAVELENGTH = 4216,96504 FEET
MAXIMUM SURFACE EXCURSION = -10,12204 FEET PER THOUSAND PSI SQUARED
CLOSURE DEPTH = 341,66345 FEET
CLOSURE TIME = 1,50687 SECONDS PER THOUSAND PSI

TIME	SPALL THICKNESS	SURFACE POSITION	SURFACE VELOCITY	SURFACE ACCELERATION (IN GEES)	LOWER CAVITY BOUNDARY
0,000	0,000	0,000	-2,000	*******	*******
0,001	0,035	0,006	-1,978	2,97	39,60
0,005	0,069	0,022	-1,947	1,98	31,54
0,012	0,104	0,050	-1,907	1,66	26,83
0,021	0,138	0,087	-1,859	1,49	23,50
0,033	0,173	0,133	-1,802	1,39	20,92
0,047	0,207	0,187	-1,737	1,33	18,82
0,064	0,242	0,248	-1,663	1,28	17,05
0,083	0,276	0,314	-1,582	1,25	15,51
0,105	0,311	0,386	-1,492	1,22	14,16
0,129	0,346	0,460	-1,395	1,20	12,96
0,155	0,380	0,536	-1,289	1,18	11,87
0,184	0,415	0,612	-1,176	1,16	10,88
0,213	0,449	0,686	-1,055	1,15	9,97
0,245	0,484	0,757	-0,926	1,14	9,13
0,284	0,518	0,822	-0,790	1,13	8,34
0,322	0,553	0,881	-0,646	1,12	7,61
0,362	0,587	0,930	-0,496	1,11	6,93
0,404	0,622	0,967	-0,337	1,11	6,29
0,445	0,657	0,991	-0,172	1,10	5,68
0,495	0,691	1,000	0,000	1,10	5,10
0,515	0,707	0,998	0,079	1,10	4,86
0,539	0,722	0,993	0,160	1,09	4,61
0,560	0,737	0,983	0,242	1,09	4,38
0,583	0,753	0,969	0,325	1,09	4,15
0,605	0,768	0,951	0,410	1,09	3,92
0,630	0,784	0,928	0,496	1,09	3,70
0,653	0,799	0,901	0,583	1,08	3,48
0,678	0,815	0,868	0,672	1,08	3,27
0,702	0,830	0,830	0,762	1,08	3,06
0,729	0,846	0,786	0,853	1,08	2,85
0,753	0,861	0,737	0,946	1,08	2,65
0,779	0,876	0,682	1,040	1,08	2,46
0,805	0,892	0,621	1,135	1,08	2,26
0,832	0,907	0,555	1,232	1,07	2,07
0,859	0,923	0,479	1,330	1,07	1,89
0,986	0,938	0,398	1,429	1,07	1,70
0,914	0,954	0,309	1,529	1,07	1,52
0,942	0,969	0,214	1,631	1,07	1,35
0,971	0,985	0,111	1,734	1,07	1,17
1,000	1,000	-0,000	1,838	1,07	1,00

SPALL DYNAMICS
HIGH PRESSURE LIMIT ANALYSIS

WAVELENGTH = 5623.41326 FEET
MAXIMUM SURFACE EXCURSION = -10.44388 FEET PER THOUSAND PSI SQUARED
CLOSURE DEPTH = 419.24847 FEET
CLOSURE TIME = 1.54104 SECONDS PER THOUSAND PSI

TIME	SPALL THICKNESS	SURFACE POSITION	SURFACE VELOCITY	SURFACE ACCELERATION (IN GEES)	LOWER CAVITY BOUNDARY
0.000	0.000	0.000	-2.000	*******	******
0.001	0.035	0.006	-1.980	2.70	45.46
0.005	0.069	0.022	-1.951	1.85	36.18
0.012	0.104	0.049	-1.913	1.56	30.77
0.021	0.139	0.086	-1.867	1.42	26.93
0.033	0.173	0.131	-1.811	1.34	23.96
0.047	0.208	0.185	-1.747	1.28	21.54
0.063	0.243	0.245	-1.675	1.24	19.49
0.083	0.277	0.312	-1.594	1.21	17.73
0.104	0.312	0.383	-1.505	1.19	16.17
0.129	0.347	0.457	-1.408	1.17	14.78
0.155	0.381	0.533	-1.302	1.15	13.52
0.183	0.416	0.609	-1.189	1.14	12.38
0.214	0.451	0.684	-1.067	1.13	11.33
0.245	0.485	0.755	-0.938	1.12	10.36
0.283	0.520	0.821	-0.800	1.11	9.45
0.321	0.555	0.879	-0.655	1.11	8.61
0.362	0.589	0.929	-0.503	1.10	7.82
0.404	0.624	0.967	-0.343	1.09	7.08
0.449	0.659	0.991	-0.175	1.09	6.38
0.495	0.693	1.000	-0.000	1.08	5.71
0.517	0.709	0.998	0.080	1.08	5.43
0.539	0.724	0.993	0.161	1.08	5.15
0.561	0.739	0.983	0.244	1.08	4.88
0.583	0.755	0.969	0.328	1.08	4.61
0.604	0.770	0.951	0.413	1.08	4.35
0.630	0.785	0.928	0.500	1.07	4.10
0.654	0.801	0.901	0.588	1.07	3.85
0.679	0.816	0.868	0.678	1.07	3.61
0.703	0.831	0.830	0.769	1.07	3.37
0.728	0.847	0.787	0.861	1.07	3.13
0.753	0.862	0.738	0.955	1.07	2.90
0.779	0.877	0.683	1.050	1.07	2.67
0.805	0.893	0.622	1.146	1.06	2.45
0.832	0.908	0.554	1.244	1.06	2.23
0.859	0.923	0.480	1.343	1.06	2.02
0.886	0.939	0.398	1.443	1.06	1.81
0.914	0.954	0.310	1.545	1.06	1.60
0.942	0.969	0.214	1.648	1.06	1.40
0.971	0.985	0.111	1.752	1.06	1.20
1.000	1.000	-0.000	1.858	1.06	1.00

DOCUMENT CONTROL DATA - R & D

(Security classification of title, body of abstract and indexing annotation must be entered when the overall report is classified)

1. ORIGINATING ACTIVITY (Corporate author)	2a. REPORT SECURITY CLASSIFICATION
ENGINEERING-PHYSICS COMPANY 12721 Twinbrook Parkway Rockville, Maryland 20852	UNCLASSIFIED
	2b. GROUP

3. REPORT TITLE

ON THE THEORY OF BULK CAVITATION

4. DESCRIPTIVE NOTES *(Type of report and inclusive dates)*

Final Report

5. AUTHOR(S) *(First name, middle initial, last name)*

Vincent J. Cushing

6. REPORT DATE	7a. TOTAL NO. OF PAGES	7b. NO. OF REFS
December 1969	i45	9

8a. CONTRACT OR GRANT NO. Nonr-3709(00) b. PROJECT NO. EPCO Project No. 106 c. d.	9a. ORIGINATOR'S REPORT NUMBER(S) 9b. OTHER REPORT NO(S) *(Any other numbers that may be assigned this report)*

10. DISTRIBUTION STATEMENT

This document has been approved for public release and sale; its distribution is unlimited.

11. SUPPLEMENTARY NOTES	12. SPONSORING MILITARY ACTIVITY Office of Naval Research Field Projects Programs Washington, D. C. 20360

13. ABSTRACT

When the compressive shock from an underwater explosion intercepts the free water surface, part of the shockwave energy is propagated into the overlying air and part is reflected back into the water. Early acoustic theories failed to describe the transmitted and reflected waves because acoustic theory implies a linear stress/strain relationship for the water--including the ability of water to withstand considerable tension. The analysis provided in this report assumes that the water can withstand no substantial amount of tension, so that an incident shockwave causes a surface layer of the water to rupture and spall upward. The region between the spall and the underlying (relatively) quiescent water has long been termed the cavitated region, and the entire process has been termed bulk cavitation.

The energy contained in the incident compressive shockwave is temporarily stored in the kinetic and gravitational potential energy of the spall. When the spall falls back and impacts (water hammers) the underlying water this stored energy is re-emitted. The spalled interface behavior is essentially different from the earlier acoustic interface picture, and the magnitude and shape of the pressure waves in the overlying air and those generated in the water at the time of spall impact are essentially different from that derived from the acoustic interface assumption.

This report studies the mechanism of water rupture, cavitation, and spall formation; studies the dynamics of this spall and cavitated region; studies the dynamics of spall impact and generation of secondary waves under water. The study concludes with a discussion of the air blast wave shape to be expected when the water surface moves in accord with the spallation and cavitation picture.

14. KEY WORDS	LINK A		LINK B		LINK C	
	ROLE	WT	ROLE	WT	ROLE	WT
Bulk cavitation						
Explosions						
Underwater explosions						
Water surface effects						
Cavitation						
Surface reflections						
Air blast						